GEOLOGY AND PETROLOGY OF THE MAFIC VOLCANIC ROCKS WITHIN THE KARAKAYA COMPLEX FROM CENTRAL (ANKARA) AND NW (GEYVE AND EDREMIT) ANATOLIA

A THESIS SUBMITTED TO
THE GRADUATE SCHOOL OF NATURAL AND APPLIED SCIENCES
OF
MIDDLE EAST TECHNICAL UNIVERSITY

BY

KAAN SAYIT

IN PARTIAL FULFILLMENT OF THE REQUIREMENTS FOR
THE DEGREE OF MASTER OF SCIENCE
IN THE DEPARTMENT OF GEOLOGICAL ENGINEERING

SEPTEMBER 2005

Approval of the Graduate School of Natural and Applied Sciences

Prof. Dr. Canan ÖZGEN
Director

I certify that this thesis satisfies all the requirements as a thesis for the degree of Master of Science.

Prof. Dr. Asuman TÜRKMENOĞLU
Head of Department

This is to certify that we have read this thesis and that in our opinion it is fully adequate, in scope and quality, as a thesis for the degree of Master of Science.

Prof. Dr. M. Cemal GÖNCÜOĞLU
Supervisor

Examining Committee Members

Prof. Dr. Asuman TÜRKMENOĞLU (METU,GEOE) _____

Prof. Dr. M. Cemal GÖNCÜOĞLU (METU,GEOE) _____

Assoc. Prof. Dr. Kenan YALINIZ (Celal Bayar University) _____

Assist. Prof. Dr. Pırıl ÖNEN (METU,GEOE) _____

Dr. Fatma TOKSOY KÖKSAL (METU,GEOE) _____

I hereby declare that all information in this document has been obtained and presented in accordance with academic rules and ethical conduct. I also declare that, as required by these rules and conduct, I have fully cited and referenced all material and results that are not original to this work.

Name, Last name : Kaan Sayıt

Signature:

ABSTRACT

GEOLOGY AND PETROLOGY OF THE MAFIC VOLCANIC ROCKS WITHIN THE KARAKAYA COMPLEX FROM CENTRAL (ANKARA) AND NW (GEYVE AND EDREMIT) ANATOLIA

Sayıt, Kaan
M.Sc., Department of Geological Engineering
Supervisor: Prof. Dr. M. Cemal Göncüoğlu

September 2005, 173 pages

This study aims to reveal the geochemical signatures of the basic igneous rocks with well-determined age within the Karakaya Complex in Central and NW Anatolia and also exhibit the relationships between the studied units in terms of geological and petrographical features.

The Karakaya Complex comprise a number of tectono-stratigraphic units in the studied regions (the Olukman Melange, the Bahçecik Formation, the Ortaoba Unit and the informally named pillow basalt-limestone association) and the pre-Karakaya basement unit (the Eymir Complex).

The basic igneous rocks have been all intensely affected by hydrothermal metamorphism as reflected by the secondary products strongly overprinting the primary mineral phases and most of them exhibit vesicular structures which are filled by mainly calcite.

The primary mineral assemblage dominating the basaltic rocks is clino-pyroxene, plagioclase and olivine, whereas secondary phases are characterized by actinolite, pistacite, zoisite/clinozoisite group and chlorite. Kaersutite, as a late stage magmatic mineral, is distinctive for Ti-augite bearing

İmrahor basalts; on the other hand, the diabase dykes include hornblende as an essential primary phase.

The basic rocks are represented by three groups; sub-alkaline, alkaline and transitional. The alkaline samples from İmrahor, Hasanoğlan, Kadirler and Ortaoba are of Anisian age and akin to oceanic-island basalts (OIB). The sub-alkaline and transitional samples from İmrahor and Ortaoba reflect P-MORB features and are younger than the first group. The diabase dykes cross-cutting the Eymir Complex, on the other hand, are too dissimilar, indicating back-arc basin signatures.

Based on the data obtained from this study, the Karakaya Complex is characterized by a number of tectonic components (seamount, plume-related mid ocean ridge and back-arc basin) with different ages and origins, which were later amalgamated during the “Cimmerian orogeny”.

Keywords: the Karakaya Complex, petrology, mafic volcanics, OIB, P-MORB.

ÖZ

ORTA (ANKARA) VE KB (GEYVE VE EDREMIT) ANADOLU'DA KARAKAYA KOMPLEKSİ İÇERİSİNDEKİ MAFİK VOLKANİK KAYAÇLARIN JEOLOJİSİ VE PETROLOJİSİ

Sayıt, Kaan
Yüksek Lisans, Jeoloji Mühendisliği Bölümü
Tez Yöneticisi: Prof. Dr. M. Cemal Göncüoğlu

Eylül 2005, 173 sayfa

Bu çalışma Orta ve KB Anadolu'da yüzeylenen Karakaya Kompleksi içindeki yaşları paleontolojik olarak bilinen bazik magmatik kayaçların jeokimyasal niteliklerinin ortaya çıkarılmasını ve çalışılan birimler arasındaki ilişkileri jeolojik ve petrografik yönlerden ortaya koymayı amaçlar.

Karakaya Kompleksi çalışma alanlarında birden fazla tektono-stratigrafik birimle (Olukman Melanjı, Bahçecik Formasyonu, Ortaoba Birimi ve resmi olarak adlanmamış yastık yapılı bazalt-kireçtaşı birliği) temsil edilir ve bu birimler bir Karakaya öncesi temel ile (Eymir Kompleksi) ile birarada yeralır.

Mafik magmatik kayaların hepsi yoğun bir şekilde hidrotermal alterasyondan etkilenmiştir. Bu durum birincil mineral fazlarının ikincil ürünlerle ornatılması ile belirgindir ve bu kayaların çoğu ağırlıkla kalsit dolgulu amigdüller içermektedir.

Mafik kayalar başlıca klino-piroksen, plajioklaz ve olivinden oluşan ilksel mineral fazlarını içermekte iken, ikincil fazlar genellikle aktinolit, pistasit, zoyisit/klinozoyisit grup ve klorit ile temsil edilirler. Geç magmatik fazda oluşan Karsutit Ti-ojitli İmrahor bazaltları için tipiktir. Diyabaz daykları ise birincil olarak hornblend içermektedir.

Mafik kayalar jeokimyasal olarak üç grup ile temsil edilirler; sub-alkalen, alkalen ve geçişli bazaltlar. Alkalen karakterli İmrahor, Hasanoğlan, Kadirler ve Ortaoba örnekleri okyanus-adası bazaltı (OIB)'na yakınlık gösterirken, sub-alkalen ve geçişli karakterde olan İmrahor ve Ortaoba örnekleri ise zenginleşmiş okyanus-ortası sırtı bazaltı (P-MORB) özelliği yansıtırlar. Eymir Kompleksini kesen diyabaz daykları diğerlerinden farklı olarak yay-ardı baseni volkanizması niteliği taşırlar.

Bu çalışmada edinilen veriler, Karakaya Kompleksi'nin yaşları ve jeolojik konumları birbirinden farklı birden fazla tektonik birimden meydana geldiğini (okyanus adası, manto sorgucu ile ilişkili okyanus ortası sırt ve yay-ardı baseni) ve bu birimlerin Kimmeryen Orojenezi sırasında biraraya geldiğini gösterir.

Anahtar Kelimeler: Karakaya Kompleksi, petroloji, mafik volkanikler, OIB, P-MORB.

To my mother

ACKNOWLEDGEMENTS

I am greatful to my supervisor Prof. Dr. M. Cemal GÖNCÜOĞLU for his supervision, guidance and enthutiastic approach throughout the research.

I would like to thank especially Dr. Fatma TOKSOY KÖKSAL for her help and encouragement throughout the completion of this study.

I wish to express my thanks to Prof. Dr. Demir Altıner for the determination of micro fossils.

Thanks are also extended to my friends, Sinan Öztürk and Ali İmer for their supports and help during the field study.

Thanks finally go to my family, especially my mother for her patience and encouragements throughout the study.

This study was supported by METU Scientific Research Projects (BAP) grant no: BAP-2004-07-02-00-59.

TABLE OF CONTENTS

LIST OF TABLES

TABLE

LIST OF FIGURES

FIGURE

CHAPTER 1

INTRODUCTION

1.1. Purpose and Scope

During its geological evolution, the Turkish area was not a single geological entity; instead it was composed of several continental and oceanic plates or micro-plates reflecting different Palaeozoic and Mesozoic histories. They were assembled due to the successive collisions of Laurasia and Gondwana or smaller micro-plates that were derived from them. The oceanic plates consumed during these events are related to “Tethyan oceans”, including Proto-, Paleo-, Neo-, and Para-tethys (Şengör and Yılmaz, 1981; Stampfli, 2000). One of the most debated problems in this issue is the Palaeo-tethys together with some continental microplates that surround it. The generally accepted model is that during the Early Mesozoic closure of this ocean by the “Cimmerian orogeny” the oceanic and continental margin units were accreted to form the “Karakaya Complex “(Tekeli, 1981; Şengör et al., 1984). The new tectonic unit is known as the Cimmerian continent (Şengör et al., 1984), Sakarya Zone (Okay, 1984a) or Sakarya Basement Complex of the Sakarya Composite Terrane (Göncüoğlu et al., 1997) that is represented by an east-west trending belt along northern Turkey (Figure 1.1A).

The term “Karakaya Complex” have been a matter of debate for about 30 years, beginning with the term “the Karakaya Formation” first used by Bingöl et al. (1973) to describe the low-grade metamorphic rock assemblage of Lower Triassic age. If it is taken into consideration that some part of the Ankara Melange (Bailey and Mc Callien, 1953) belongs to the Karakaya Complex, then it can be inferred that this problem still remains unsolved since 1950’s.

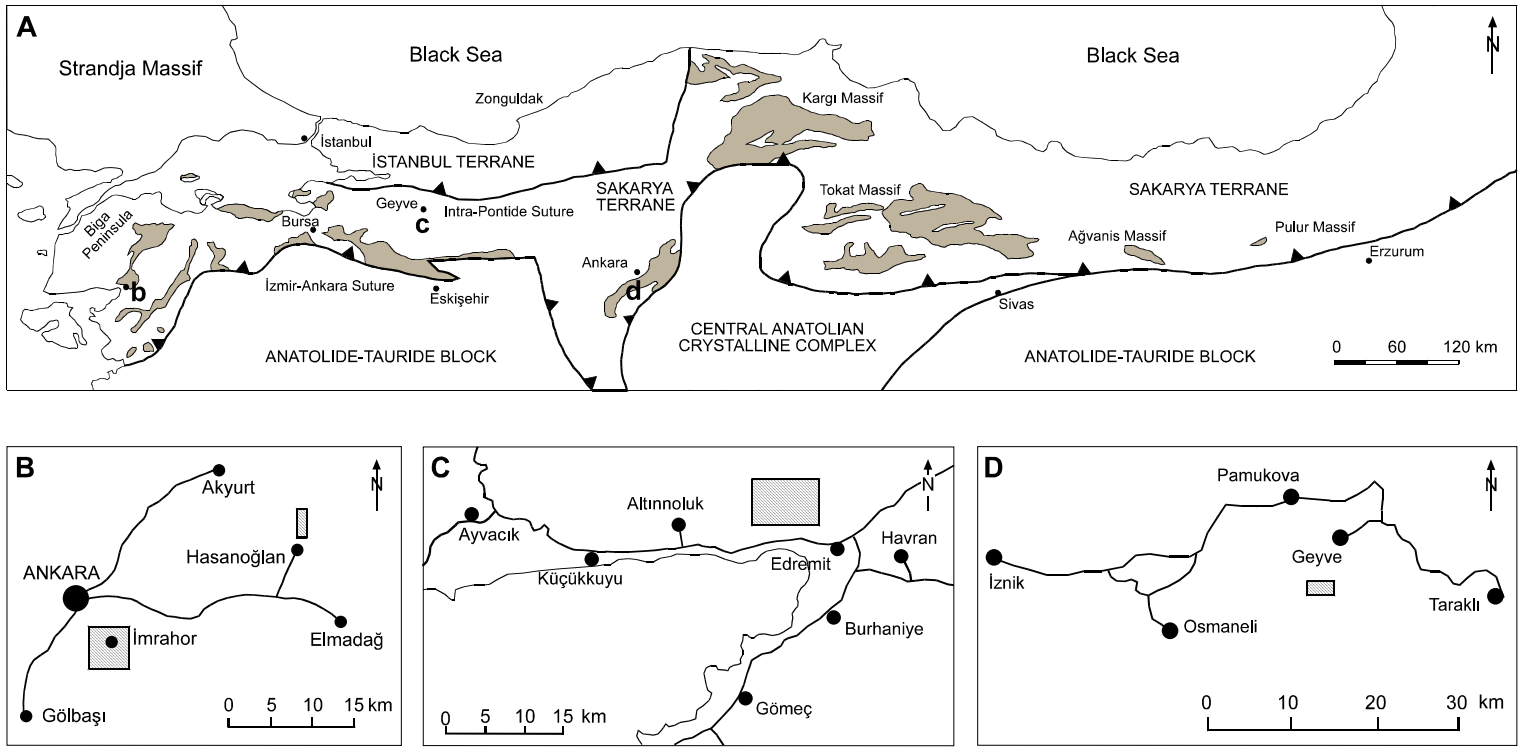

Figure 1.1. Distribution of the Karakaya Complex in northern Turkey (after Okay and Göncüoğlu, 2004) and location maps of the study areas.

Recently, in a brief review, Okay and Göncüoğlu (2004) have discussed the competiting hypotheses regarding the generation of the Karakaya Complex. The models cited by the authors comprise a wide range of interpretations including rifting, accretion etc. In all these models the presence of intensive volcanism has been mentioned but not thoroughly considered to decipher the tectonic evolution.

Several geochemical studies have been carried out, regarding the tectonic evolution of the Karakaya Complex (e.g. Çapan and Floyd, 1985; Floyd, 1993; Ustaömer and Robertson, 1994, 1999; Pickett and Robertson, 1996, 2004; Yalınız and Göncüoğlu 2002; Genç, 2004); on the other hand, they have either examined the units without well-determined age or included insufficient sampling or have not used the rare-earth element data (REE) needed for the geochemical interpretation.

This study aims to examine the basic volcanic rocks with well-determined age within the Karakaya Complex in terms of geochemical aspects together with the geological relationships between the units to reveal their petrology and petrogenesis. As a result of this study, the geochemical features of the Karakaya Complex could be better envisioned, so enabling more accurate interpretation about its tectonic evolution.

1.2. Geographic Setting

This study includes mainly four areas in central and northwestern part of Turkey, covering totally about 26 km^2: a) İmrahor (Ankara), b) Hasanoğlan (Ankara), c) Ortaoba (Edremit-Balıkesir) and d) Kadirler (Geyve-Sakarya).

The first study area is located at İmrahor village, 5 km southeast of Ankara (Figure 1.1B). It covers an area of approximately 20 km^2 and included in the Ankara I29-b2 quadrangles of 1:25 000 scale topographic map of Turkey lying between the coordinates of 39°52’30’’ N - 39°56’00’’ N latitudes and of 32°52’30’’ E - 33°57’00’’ E longitudes. The main hills in the study area are Naldöken Hill in the north, Tepetarla Hill in the south and Büyük Esatbeli Hill in the southwest.

The second area is Hasanoğlan region which is located about 35 km northeast of Ankara (Figure 1.1B). This area comprises approximately 2 km^2 and contained in the Çankırı H30-d3 quadrangles of 1: 25 000 scale topographic map of Turkey lying between the coordinates of 40°00'00'' N - 40°02'00'' N latitudes and of 33°12'00'' E - 33°13'00'' E longitudes. Highest peaks in the area are the Kolcınarkaç Hill to the north and Damlanınsırtı Hill to the northeast.

The third study area is situated in Ortaoba village, 4 km northwest of Edremit (Balıkesir), covering about 2 km^2 (Figure 1.1C). It occurs in the Balıkesir K18-c3 quadrangles of 1:25 000 scale topographic map of Turkey within the coordinates of 39°38'00'' N - 39°39'00'' N latitudes and of 26°59'30'' E - 27°00'00'' E longitudes.

The fourth and last study area is placed to the north of Kadirler village, 10 km southeast of Geyve (Sakarya; Figure 1.1D). It covers 2 km^2 and included in Adapazarı H24-b1 quadrangles of 1: 25 000 scale topographic map of Turkey lying between the coordinates of 40°26'00'' N - 40°27'30'' N latitudes and of 39°52'30'' E - 39°56'00'' E longitudes. The main hills in the study area are Pazarkaya Hill to the east and Karakaya Hill to the south of the study area.

1.3. Methods of Study

This study consists mainly of two stages as field and laboratory studies.

During the fieldwork, sampling was performed for all of the study areas mentioned above during the summer of 2004 and approximately 250 rock samples were collected from those locations. On the other hand, a geological map on the 1:25 000 scale topographic map of Ankara sheet was also prepared for the İmrahor region.

During the laboratory studies, 147 thin-sections were prepared from the collected samples for mineralogical and petrographical examination under polarizing microscope in order to designate the relationships in terms of texture, fabric and mineral assemblages and also to compare the petrographic

features of rock samples from different locations, so unraveling the possible connection of those features with their petrology.

Petrographic examinations were carried out on the Swift and Nikon microscopes and photomicrographs were taken by using the Nikon camera in the Department of Geological Engineering of METU.

For the geochemical identification, a total of 32 relatively less altered basaltic rock samples were analyzed for major, trace by using inductively coupled plasma-emission spectrometer (ICP-ES) and inductively coupled plasma-mass spectrometer (ICP-MS) in ACME Analytical Laboratories, Canada.

1.4. Previous Studies

In this chapter, based on a review of previous studies only the overall features of the different units of “Karakaya Complex” will be evaluated in historical order. The details of the geology of the sampled localities with emphasize on local characteristics will be given in the next chapter.

Bailey and Mc Callien (1953) together with Erol (1956) were the first who identified the melange character of a broken formation in the vicinity of Ankara, which was identified later as a lithostratigraphic unit (Karakaya Formation) by Bingöl et al. (1973) in NW Anatolia around Edremit. Bingöl et al. (1973) described the unit as a low grade metamorphic assemblage, consisting of greywacke, conglomerate, siltstone intercalated with spilitic basalt, radiolarite and mudstone with Permo-Carboniferous limestone blocks. They suggested an intra-continental rift environment for deposition of the Karakaya Formation and proposed a Lower Triassic age. They also suggested that gravity-sliding due to tensional forces that influenced the Tethys immediately after the beginning of the Lower Triassic time lead to the limestone blocks to be incorporated into the Karakaya Formation as olistoliths.

Bingöl (1975) then pointed out that the basement rocks of the Western Anatolia probably were generated during pre-Cambrian time. The overlying shallow marine rocks were formed during the Permo-Carboniferous interval; however an oceanic realm dominated during Upper Permian-Lower Triassic

times. The tensional forces for the opening of this ocean cause the Karakaya Formation to be formed between the Menderes and Kazdağ massifs at the same time-interval. According to him, the basin should have been closed at the end of Lower Triassic based on the data that deformed Lower Triassic rocks are unconformably overlain by transgressive Middle-Upper Triassic, Lower-Middle-Upper Jurassic and Lower Cretaceous successions.

Akyürek et al. (1979a) stated that in the Hacılar region (Ankara), the metaclastic complex, which was regarded previously as Palaeozoic-Carboniferous, is of Lower Triassic (Scythian) age, based on the fossil findings in the sandy limestones of the unit. They also reported that this unit contains Permian limestone blocks and this metaclastic sequence is overlain by Middle-Upper Triassic units by an angular unconformity, starting with conglomerate-sandstone and continuing upwards with limestone beds.

Şengör et al. (1980) stated that the pre-Late Jurassic basement in the eastern Pontides is represented by two distinct rock associations as oceanic and continental assemblages. The oceanic assemblage is characterized by an ophiolite-bearing accretion complex of Permian-Late Jurassic age, representing the remnants of the Palaeo-Tethys. The continental assemblages characterize the northern margin of the Gondwana, represented by a north-facing magmatic arc during the Permian to Early Jurassic times. They reported that the metamorphism of the ophiolitic assemblages in greenschist facies occurred before the deposition of the Late Jurassic sediments. They also suggested a southward-dipping subduction model for the closure of the Palaeo-Tethys and that the continental assemblages correspond to the Cimmerian Continent of Şengör (1979).

Tekeli (1981) documented that an orogenic zone with highly deformed pre-Liassic rocks occurs essentially between the internal Anatolian massifs and the North Anatolian fault, and he named this zone as “the North Anatolian Belt”. Furthermore, he separated the pre-Liassic rock units within the North Anatolian belt into four groups; three metamorphic assemblages characterized by blueschist, greenschist and amphibolite facies and a dynamometamorphic mélange. He suggested that these rock units were developed in a subduction

complex, reflecting the closure of a Late Paleozoic-Early Mesozoic Tethyan ocean, which corresponds to the Palaeo-Tethys of Şengör (1979).

Yılmaz (1981) studied the Central Sakarya region and suggested that the Triassic basin in the Central Sakarya was a short-lived back-arc basin developed above the southward subducting Palaeo-Tethys. According to him, this Triassic basin was closed before Liassic time. On the other hand, the ophiolite belt in the southern part of the Sakarya River is characterized by metamorphics which are composed of metalava, greenschist, metachert and marble blocks, probably of pre-Liassic age developed in this Triassic basin.

Okan (1982) separated the Karakaya units as members of the Elmadağ Formation that include three members; these are from bottom to top Arabıntaş member, Çakıllıdere member and Devecioğlu member, respectively. They are represented mainly by a clastic rock assemblage including flaxoturbiditic conglomerate, arenite (especially quartz-arenite), wackestone (mainly greywacke), siltstone and claystone. The members mentioned also include numerous Carboniferous, Permian and Triassic limestone blocks. He stated that the Elmadağ Formation interfingers with the Döşemedere Formation.

Akyürek and Soysal (1983) defined the Upper Permian Çamoba Formation in the area between the Biga Peninsula and the Menderes Massif as allochthonous shallow-water deposits. They stated that Çamoba Formation represents blocks of various sizes within the Halilağa Group of Lower Triassic age. They also mentioned that the Çamoba Formation can be the equivalent of the Permian blocks in the Karakaya Formation of Bingöl et al. (1973). According to them, the Lower Triassic time in the area is characterized by a shallow-marine environment and they relate the formation of the Permian blocks to the tensional forces prevailing at that time. They also proposed that the graben faults gave way to the incorporation of the basalts into clastic rocks.

Akyürek et al. (1984) reported that the Emir and Elmadağ Formations in Ankara region are composed of volcano-sedimentary rocks that have undergone greenschist facies metamorphism and there is a stratigraphic contact between the Emir and Elmadağ formations. They also named the Emir, Elmadağ, Ortaköy and Keçikaya formations as “Ankara Group” that

corresponds to the Karakaya Complex. They stated that the Ankara Group is the oldest autochtonous unit in the region and allochthonous rocks with Carboniferous-Permian age is observed in the Ankara Group as blocks. A Lower Triassic age was given for the Emir Formation according to fossils found in the transition zone between Emir and Elmadağ Formations. On the other hand, lower parts of the Elmadağ Formation is of Anisian age based on fossil dating from the intercalated limestones, while upper parts is of Middle-Upper Triassic age. According to them, Ankara Group represent the rock assemblage deposited as a result of rifting (block faulting) during the opening of Paleotethys in Triassic. Both Emir and Elmadağ Formations correspond to deposits accumulated in a deep-marine environment in a continental margin. The Ortaköy Formation, which is represented by spilitic and diabase rocks, was formed by extensional volcanism. They related the presence of Carboniferous and Permian neritic limestone blocks to normal faulting at the basin-margins during the Triassic.

Okay (1984b) mentioned that the Karakaya Complex in NW Anatolia is characterized by regionally metamorphosed rocks with strong deformation and it locally displays features of a blocky melange in parts where low grade metamorphic rocks have a semi-brittle character and the basic volcanics intercalated with limestones are boudinaged.

Tankut (1984) stated that the Triassic metamorphic and limestone melange belts in the Ankara Melange consist of basic volcanics only as blocks, clasts and dykes and she reported the absence of ultramafic rocks in these melange belts. Based on geochemical study of the basalt samples collected from the Nenek Village and the Emir Lake area, she suggested that basic volcanics from metamorphic melange belt display both tholeiitic and calc-alkaline characteristics.

Koçyiğit (1987) stated that there are two tectonic units of Triassic age exposed in the Ankara region. The name “Karakaya Nappes” were given to these units and a Norian age is accepted for their formation age. He subdivided the Karakaya Nappes into two; the Lower and Upper Karakaya Nappes. The Lower Karakaya Nappe consists of volcano-sedimentary rock assemblage of

wild flysch character. However, the Upper Karakaya Nappe is represented by low-grade metamorphic rocks of greenschist facies metamorphism. He divided the Lower Karakaya Nappe into six informal litho-stratigraphic units, which are Karacadere Limestone, Çaltepe Limestone, Yazılıkaya Formation, Döşemedere Formation, Bayramdere Formation and Kısıküstü Formation. Among those units, the Karacadere Limestone represents a block which is of Early Permian age. On the other hand, the Upper Karakaya is characterized by the "Tokat Group". He suggested a volcano-sedimentary sequence developed in an active continental margin for the origin of the Tokat Group. He stated that the ultrabasics, the Upper and Lower Karakaya Nappes display features reflecting the opening of the Karakaya Basin (rifting), the development (oceanic basin) and the closure (active continental margin and orogeny). He also suggested that the starting of sea-floor spreading and the opening of the Karakaya oceanic basin took place towards the end of Anisian (?), corresponding to the separation of the Cimmerian continent from the northern part of the Gondwana.

Kaya et al. (1989) suggested that the complicated structure of the Dışkaya Formation in Bergama area, which is composed of pre-Jurassic blocky sedimentary and spilitic mafic volcanic rocks, is not resulted from an accretionary prism- or subduction-related event such as, tectonic melange or ophiolitic melange, instead it is due to layer rupture coeval with the sedimentation. He also documented meta-tuff blocks found at the basement of the formation indicates an unconformity, which is mentioned before by Özkoçak (1969). He proposed a slope apron environment for the deposition of the Dışkaya Formation.

Bozkurt (1990) examined the area including the Beytepe Village (Ankara) which is characterized by the units of the Karakaya Complex. He reported that the calcareceous sandstone in this location is of Visean-Serpukhovian age. He named the limestone and limestone-marn intercalation as the Beytepe Formation and proposed an Asselian-Sakmarian age for that formation. It is important to note that these two units represent blocks within the Karakaya Nappe. He stated that the Beytepe Formation represents a shallow subtidal depositional environment.

Ercan et al. (1990) in their study around Balıkesir and Bandırma regions stated that the Upper Palaeozoic Fazlıkonağı Formation includes metamorphic rocks with marble and serpentinite masses and forms the basement of the area. On the other hand, the calc-alkaline Kapıdağ granite intrudes the Fazlıkonağı Formation. They documented that the Karakaya Formation unconformably overlies both the Kapıdağ pluton and Fazlıkonağı Formation. They also pointed out that the Karakaya Formation is unconformably overlain by the Middle-Upper Triassic Çaltepe Formation. They proposed a Lower Triassic age for the Karakaya Formation on the basis of the unconformable relation with the Çaltepe Formation and the Permian limestone blocks.

Yılmaz (1990) documented that the Sakarya Continent in Bozöyük area is represented by two main subunits. The northern sector is characterized by greenschist facies metamorphic rocks, while the southern sector consists of dominantly sedimentary rocks. Between these units, a metamorphosed ophiolitic melange exposes. The metamorphic rocks in the southern sector include two tectonostratigraphic units. These are metapelites unconformably overlain by Permian sediments and Triassic basic igneous rocks with high-pressure metamorphism. He proposed that the closure of the Karakaya basin occurred at the end of Triassic while the Palaeo-Tethys still existed in the north. He suggested a Dogger age for the closing time of the Palaeo-Tethys and the obduction of ophiolitic slabs.

Kaya (1991) characterized the Dışkaya Formation as a Late Triassic turbidite-olistostrome assemblage. He evaluated the repetition of units as stratigraphic and stated the absence of the metamorphism in the Dışkaya Formation. He also proposed a transgressive deposition for the Dışkaya Formation in a slope-setting above a low-grade metamorphic basement. Unlike the previous studies he strikingly suggested that the Late Triassic formation does not bear the direct evidences of a subduction event.

Okay et al. (1991) stated that the Sakarya Zone is composed of the metamorphic rocks of Kazdağ Group, the Karakaya Complex that tectonically overlie the Kazdağ Metamorphics and post-Triassic clastics. They reported that the Karakaya Complex includes four tectono-stratigraphic units of the

same age but displaying different basinal and tectonic environments. These units are the Nilüfer Unit, the Hodul Unit, the Orhanlar Greywacke, and the Çal Unit. They suggested a fore-arc / intra-arc setting for the Nilüfer Unit, a Late Triassic trench sequence for the Hodul Unit, an accretionary prism setting for the Orhanlar Greywacke, and a back-arc basin setting for the Çal Unit. They also proposed that the ophiolitic melanges incorporated to the Karakaya Complex in the previous studies (e.g. Bingöl et al., 1973; Tekeli 1981; Gözler et al., 1984) are actually of Late Cretaceous-Paleocene age. They suggested that the Biga Peninsula characterize the western boundary of the Karakaya Complex and this boundary represents the Palaeotethyan Suture formed by the collision of a Permo-Triassic passive continental margin which is defined by an ophiolite obduction (Denizgören Ophiolite) and an active continental margin which is described by the units of the Karakaya Complex.

Altıner and Koçyiğit (1993) documented Anisian ages for the carbonate sequence (Bahçecik Formation) in the Hasanoğlan region (Ankara). They proposed that the Bahçecik Formation in the Karakaya Nappe reflects a transitional zone, starting from wildflysch to shallow water carbonates generated during the mature rifting stage of the Karakaya basin (Figure 1.2).

Floyd (1993) studied the low-grade metamorphosed submarine basaltic lavas situated in the east of the Ankara (Karakaya and Anatolian Nappes) which are alkaline, displaying an ocean island affinity (OIB). He also pointed out the chemically resemblance of the alkaline basalts from the Karakaya Nappes of Triassic age and those from the Cretaceous Anatolian Nappe.

Okay and Mostler (1994) studied the limestone blocks in the Karakaya Complex in the Biga Peninsula of northwestern Turkey. They reported Middle Carboniferous (Bashkirian; radiolarian chert block to the northwest of Balya) and Lower Permian (Early Sakmarian-Artinskian; radiolarian chert block, southeast of Çan region) ages. They also proposed that these Upper Palaeozoic blocks reflect the existence of a deep marine basin, unlike the rift basin model indicated by some previous studies (e.g. Altıner and Koçyiğit, 1993; Figure 1.2).

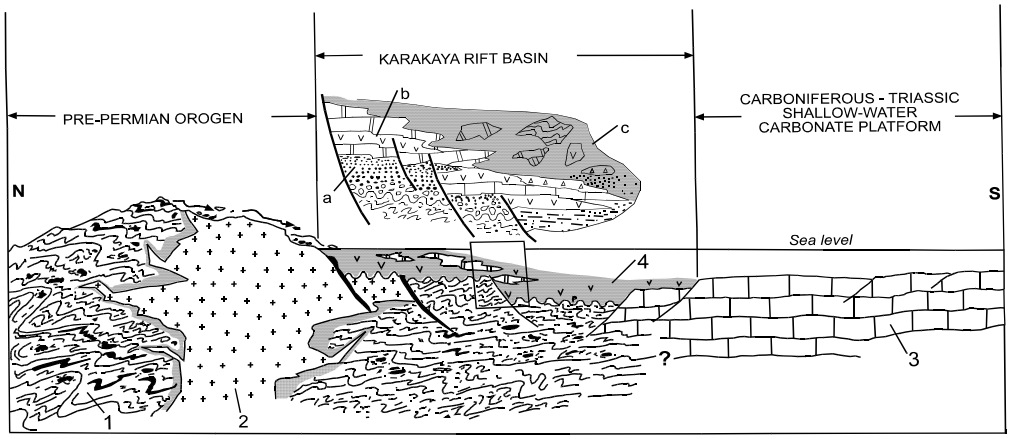

Figure 1.2. Rift model illustrating tectonic evolution of the Karakaya Complex (Altıner and Koçyiğit, 1993; 1. Pre-Permian low-grade metamorphic rocks, 2. Uppermost Carboniferous granitoid, 3. Carboniferous to Triassic shallow-water carbonates, and 4. Permian (?) to Triassic rift basin successions of the Karakaya Group, which includes a) Kendirli Formation, b) Bahçecik Formation, c) Olukman Formation).

Tüysüz and Yiğitbaş (1994) divided the pre-Malm rocks within the Ilgaz-Kargı-Massif into three tectonostratigraphic units: the Karakaya Unit, the Elekdağ Unit and the Küre Unit, all of which is covered unconformably by Late Jurassic or younger cover rocks. They suggested that the Karakaya Unit reflects the occurrence of a Permian carbonate platform associated with volcanism indicating the opening of the Karakaya Basin. They also stated that the Küre Unit is directly related to the events between the Palaeotethys and the Karakaya Basin. The Karakaya Unit comprises three formations which are stratigraphically related to each other. These are the İbi, Aktaş, Gümüşoluğu and Kunduz Formations. They reported that the İbi Formation is characterized by greenschist facies metamorphism and the Upper Carboniferous-Permian fossils within the formation indicates a neritic environment. The Aktaş Formation also displays greenschist metamorphism and contains various blocks. They suggested an extensional regime for the formation of the Aktaş Formation. It is important to note that no geochemical data is available for the formation and the age is also unknown due to lack of fossil data. The Gümüşoluğu Formation is also represented by greenschist facies metamorphism. The geochemical data for the Kunduz Formation are from the

study of Doğan (1990), who interpreted the basic lavas within the formation as alkali and tholeiitic and a marginal basin origin is suggested on the bases of its transitional nature. They finally concluded that the Karakaya Basin represents a small-ocean resulted from back-arc rifting during Late Permian to Triassic.

Akyüz and Okay (1996) studied the Kepsut region in the northwestern Anatolia and stated that the Sakarya Zone includes two formations in this area: the Nilüfer Unit with intensively deformed metabasite-marble-phyllites of Triassic age and the Orhanlar Greywacke which is composed of the Permo-Triassic clastics, tectonically overlying the Nilüfer Unit.

Okay et al. (1996) dated a granodiorite body, known as the Çamlık granodiorite north of Havran in northwestern Turkey. They found a mean Pb/Pb stepwise evaporation age of 399 ± 13 Ma, suggesting Early Devonian crystallization. According to this result they interpreted the Çamlık granodiorite as the oldest known granitoid body within the Sakarya Zone. They also suggested that the Palaeozoic basement of the Sakarya Zone represents a Laurasian affinity in response to the presence of the Lower Palaeozoic granitoids in the Strandja Zone in Bulgaria. Another geochronological study from the gneisses in the northwestern part of the Kazdağ range yielded a mean age of 308 ± 16 Ma. They proposed a Mid-Carboniferous age for the high-grade metamorphism in the Kazdağ range. They suggested again the close relationship between the Sakarya Zone and the Laurasian margin based on the similarity of the isotopic ages obtained from the migmatites of the Serbo-Macedonian massif.

Pickett and Robertson (1996) in their study in Edremit - Kozak area interpreted the Karakaya Complex as a Palaeo-tethyan accretionary complex, including oceanic crust, trench sequences, abyssal sediments and intra-oceanic platforms and proposed a southward-dipping subduction for Late Permian-Triassic time. They suggested a within-plate (WPB) character for the Nilüfer Unit representing a seamount(s), a mid-oceanic ridge type tectonic setting (MORB) for the Ortaoba Unit reflecting trench sequences and WPB origin for the Çal Unit characterizing Permian carbonate platform with intra-oceanic platforms, based on the geochemistry of the basalt samples taken from the

Edremit region in the Western Anatolia. They also interpreted the Kalabak Unit as abyssal plain deposits.

Rojay and Göncüoğlu (1997) stated that the Amasya Metamorphics consist of three tectono-stratigraphic rock-units which differ in protolithology and internal organization. These units are grayish-black schists having quartz boudins and veins, greenschists, and greenschists including marble blocks and/or boudins. They also pointed out that these metamorphics are dissimilar with those of the Karakaya Group in Bilecik region. They suggested that these low-grade metamorphics are pre-Permian in age. They proposed a deep marine environment for the deposition of these rocks.

Akyüz and Okay (1998) studied the area south of Manyas (Balıkesir), where the Karakaya Complex comprises the Nilüfer Unit. It is tectonically overlain by the Hodul Unit and Orhanlar Greywacke. The Nilüfer Unit here is divided into the Kiraz metamorphics at the bottom comprising volcano-sedimentary rocks, and the Çataltepe Marble that unconformably overlie the Kiraz metamorphics. The Kiraz metamorphics represents island-arc tholeiites according to the geochemistry of the metabasites comprising a substantial portion of the Kiraz metamorphics. They also proposed that the unconformity between the Kiraz metamorphics and the Çataltepe marble was formed prior to the regional metamorphism. In addition to that a Late Permian-Triassic age is proposed for the Orhanlar Greywacke, designating trench clastics.

Çapkınoğlu and Bektaş (1998) suggested that the low-grade metamorphic clastics of the Karasenir Formation (Amasya) previously considered as the autochtonous Palaeozoic basement by Tüysüz and Yiğitbaş (1994) is of Triassic age, based on the Devonian and Permian limestone olistoliths within the formation. They proposed that the Karasenir Formation should be included in the Karakaya Complex.

Okay and Tüysüz (1999) stated that the numerous rock-units of the Karakaya Complex in the northwestern part of Turkey and the orogenic units of pre-Jurassic age in the Central Pontides together characterize a Triassic subduction-accretion complex. They stated that there is no indication for existence of a Palaeo-tethyan suture different than the Neo-tethyan İzmir-

Ankara-Erzincan suture, suggesting that the latter characterize the demise of both oceanic lithosphere, for at least the Carboniferous-Paleocene time interval.

Göncüoğlu et al. (2000) stated that in the Central Sakarya area, the Central Sakarya Terrane represents the pre-Jurassic tectonic units, characterized by two tectonic Variscan basement units named as the Söğüt and Tepeköy Metamorphics and an unconformably overlying unit known as the Soğukkuyu Metamorphics. They suggested an island-arc tectonic setting for the Söğüt Metamorphics. On the other hand, they proposed that the Tepeköy Metamorphics, which display similarities in lithological aspects to the Nilüfer Unit of Okay et al. (1991) in the northwestern Anatolia, is characterized by a forearc-trench complex. They interpreted the Soğukkuyu Metamorphics, which is similar to the Hodul and the Çal Unit of Okay et al. (1991), as a rift-basin assemblage, opened possibly on the Söğüt and Tepeköy Metamorphics and their Permian carbonate cover.

Okay (2000) suggested that the Late Triassic deformation and metamorphism known as the Cimmerian Orogeny, was due to the collision between an oceanic plateau of Early-Middle Triassic age and the southern continental margin of Laurasia (Figure 1.3). He also proposed that the Nilüfer Unit, which is a metabasite-marble-phyllite complex of Early-Middle Triassic age, characterizes the upper parts of this Triassic oceanic plateau. In addition to this, he also divided the clastic and mafic volcanic sequence that tectonically overlies the Nilüfer Unit into two parts: the units formed during the subduction-accretion of the Palaeotethys and the ones formed during the collision of the oceanic plateau. While the Orhanlar Greywacke, the Küre Complex and the Kastamonu Granitoids represent the subduction-related units, the Hodul Unit characterizes the collision related one. He stated that the both Palaeo- and Neo-tethyan sutures are indicated by the İzmir-Ankara-Erzincan Suture.

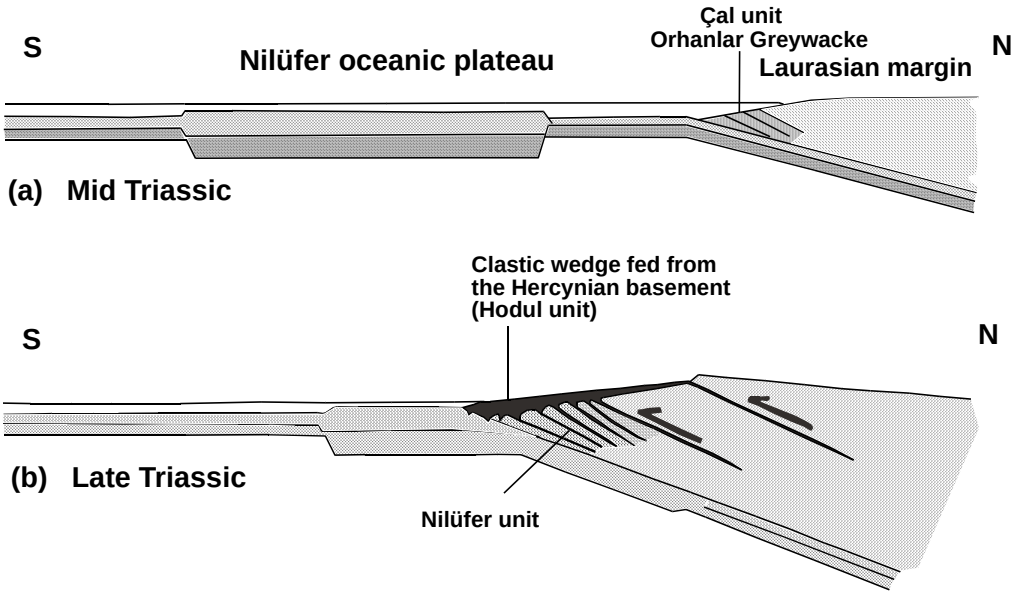

Figure 1.3. Subduction-accretion model depicting tectonic evolution of the Karakaya Complex (Okay, 2000).

Genç (2004) stated that the Nilüfer Unit in N and NW Anatolia, in which the metavolcanic rocks comprise 80% of the sequence, consists mainly of two main mafic rock groups reflecting tholeiitic and alkaline characteristics. He reported that the Nilüfer Unit represents numerous tectonic settings, including within plate, oceanic island and ocean floor, based on the geochemistry of metabasites and that of relict pyroxenes. However, he suggested that there is no signature related to orogeny or subduction and the Nilüfer Unit designates a seamount or seamount chain associated with an oceanic plateau.

Pickett and Robertson (2004) mentioned that the Nilüfer Unit in Edremit region consists mainly of basic massive basalt and pyroclastic deposits and represents one or several oceanic seamounts within Triassic Tethyan ocean. They further suggested that the Nilüfer Unit is of within-plate signatures, representing a non-orogenic setting with no subduction influence, based on the whole-rock geochemistry and clinopyroxene geochemistry. They proposed a northward thrusting for the emplacement of Karakaya Complex over the southern edge of the Eurasian fore-arc before the earliest Jurassic time.

Okay and Altıner (2004) studied the Kaşal Limestone Member within the Hodul Unit, and they offered a Norian-Rhaetian age according to the microfauna in the limestone. They suggested that the Kaşal Limestone characterize in-situ carbonate deposition in the Hodul Unit due to the similar ages of the clastic matrix and the limestone, and presence of muddy lithologies that are transitional with the limestone. Furthermore, they proposed Rhaetian-Hettangian interval for the deformation age of the Hodul Unit and signify the resemblance of this time period to the age of regional metamorphism of the Nilüfer Unit, indicating the occurrence of the Cimmeride orogeny in a short period of time at the end of Triassic.

Göncüoğlu et al. (2004), in their study area to the south of Geyve, divided the Karakaya units informally into two, namely the “arkosic sandstone unit” and the “pillow basalt-limestone association”. They assigned a Changxingian (Late Permian) age for the syn-sedimentary radiolarian chert layer included within the arkosic sandstones. They suggested that these syn-sedimentary radiolarian cherts, which were introduced for the first time in this study, is the evidence of latest Permian rifting of the Karakaya basin within the Midian carbonate platform and its pre-Permian basement in the Sakarya Composite Terrane.

Turhan et al. (2004) stated the presence of autochthonous Upper Permian (Midian) carbonates in the Kadirler area to the south of Geyve, which disconformably overlie a crystalline basement complex. They implied that the Midian transgression and foraminiferal assemblage in the area are similar to those reflected by the northern Tauride-Anatolide platform, indicating that the Sakarya basement represents the northern continuation of the Gondwanan Tauride-Anatolide unit before the opening of İzmir-Ankara oceanic branch of Neotethys. They further suggest that this Permian carbonates represent a platform-margin, upon which the Karakaya basin was opened in latest Permian times.

Yılmaz and Yılmaz (2004) separated the Tokat Group into two units; the Turhal Metamorphics and the Devecidağ Melange. They stated that the Turhal Metamorphics is characterized by a volcano-sedimentary sequence which has

been overprinted by greenschist facies metamorphism, whereas the Devecidağ Melange comprises exotic blocks in a meta-volcanosedimentary matrix. They suggested a fore-arc depositional environment for the Tokat Group, which was later accreted to the mélange prism along the North Anatolian Ophiolite Belt prior to Campanian.

As inferred from the numerous previous studies mentioned above, there are a number of tectonically-related units which have been regarded to represent the Karakaya Complex. However, there is no consensus which of sub-units actually characterizes the Karakaya Complex and it is still a matter of debate in which tectonic environment and time interval these sub-units of the Karakaya Complex have been developed.

1.5. Regional Geology

The Sakarya Zone is a continental fragment extending in east-west direction between the Anatolide-Tauride Block to the south and Istanbul and Strandja zones and the eastern Black Sea to the north (Okay, 1989; Okay and Tüysüz, 1999). It comprises the Sakarya Continent of Şengör and Yılmaz (1981) in addition to the Central and Eastern Pontides that exhibit a similar stratigraphic and tectonic evolution (Okay, 1989). The same region is termed as Sakarya Composite Terrane by Göncüoğlu et al. (1997) with regard to its pre-Alpine history (Figure 1.4 inset map).

The Sakarya Composite Terrane is prominently characterized by a Pre-Jurassic basement and a Jurassic - Late Cretaceous cover. Within the basement, various metamorphic inlayers with pre-Permian (Variscan?) deformation next to rocks with Triassic deformation are separated by Permian platform sequences. Both the Variscan and Cimmerian assemblages include rock units that were formed in different tectonic settings. This very complex mosaic of tectonic units was assembled as the “Karakaya Complex” by Şengör et al. (1984; for details see Okay and Göncüoğlu, 2004).

In the following section the regional geological aspects of the Karakaya Complex in the different areas sampled for the geochemical study of volcanic rocks will be briefly described.

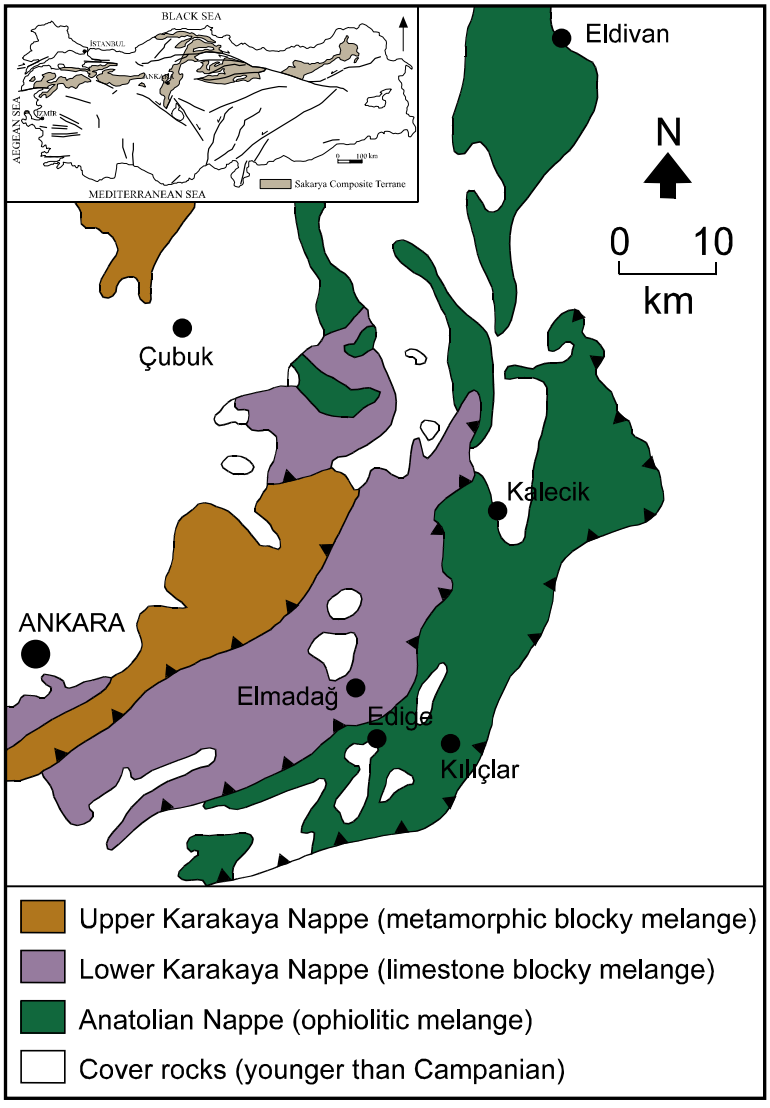

Figure 1.4. Distribution of three major tectonic units in the Ankara region (after Koçyiğit, 1991). Inset map shows the distribution of the Sakarya Composite Terrane in northern Turkey (after Göncüoğlu et al., 1997).

1.5.1. Ankara Region (Central Anatolia)

The rock units that characterize the Ankara region can be classified mainly into 3 units: (from oldest to youngest) the pre-Permian Eymir (Pazarcık) Complex, the Permo-Triassic Karakaya Group and their Jurassic-Tertiary cover rocks. In the Ankara region, the Eymir Complex, Karakaya Group and the Mesozoic rocks all together represent NE-SW trending thrust-bound tectono-stratigraphic units (Figure 1.4; Koçyiğit, 1987).

The Eymir Complex of Koçyiğit (1992) is the oldest rock unit, forming the lowermost part of the sequence in the Ankara region. This unit was first described by Akyürek et al. (1982, 1984) and named as the Emir Formation. It is characterized by a chaotic mixture of volcano-sedimentary rock assemblage which has undergone greenschist facies metamorphism. No paleontological data could have been recognized from the Eymir Complex yet. However, a Lower Triassic age was assigned by Akyürek et al. (1984), depending on the fossil assemblage in the transitional zone assumed to be present between the Emir Formation and the overlying Elmadağ Formation. On the contrary to Akyürek et al. (1984), age of the unit was determined as pre-Permian by Koçyiğit et al. (1991) based on an intruding granitoid body of 271 m.y. in the vicinity of Bozüyük (Yılmaz, 1981) and the unconformably overlying Triassic clastics. In the Ankara region, the Eymir Complex can be regarded as equivalent to the Dikmen Greywackes (Erol, 1956), the Epimetamorphic Schists (Çalgın et al., 1973), the Metamorphic Blocky Melange (Norman, 1973).

The Eymir Complex tectonically overlies the younger Lower Karakaya Nappe, namely the Karakaya Group (Koçyiğit, 1987; Koçyiğit et al., 1991) which is described by a tectonosedimentary mixture with large Permo-Triassic limestone blocks. In the Ankara region, two formations of the Karakaya Group exposes, which are the Olukman Melange and Bahçecik Formation. The Bahçecik Formation is characterized by an alteration of spilitic pillow basalt flows, pyroclastics and shallow-water carbonates, while the Olukman Formation is mainly composed of a sedimentary melange of wildflysch nature (Altıner and Koçyiğit, 1993).

The Bahçecik Formation can be considered equivalent to the Ortaköy Formation (Akyürek et al., 1984) and a part of Limestone Blocky Melange (Norman, 1973). The Olukman Melange, represented by the greywackes series, can be correlated with the Elmadağ Blocky Series (Erol, 1956), a part of Limestone Blocky Melange (Norman, 1973), the Kulm flysch formation (Erk, 1977), the Elmadağ Formation (Okan, 1982; Akyürek et al., 1984) and Hisarlıkaya Formation (Batman, 1978).

The paraautochthonous Ankara Group of Koçyiğit (1987) unconformably overlies the Karakaya Nappes and it is characterized by a thick, discontinous sedimentary sequence of late Hettengian-early Campanian age. This sequence starts with the Hasanoğlan Formation (Akyürek et al., 1982) which is represented by poorly-sorted fluvial conglomerates at the bottom and continues with a trangressive marine sequence. The Hasanoğlan Formation is laterally transitional to the Günalan Formation (Akyürek et al., 1996) which consists of volcanic rocks intercalated with pelagic limestones. The Hasanoğlan Formation passes gradually to the Akbayır Formation (Akyürek et al., 1982) which is dominated by pelagic limestones.

The Jura-Cretaceous Anatolian Complex (Koçyiğit and Lünel, 1987) displays tectonic relationships with both the Karakaya Group and Ankara Group. The Anatolian Complex is tectonically overlain by the Karakaya Group, while it thrusts over the Ankara Group. The Anatolian Complex is divided into three sub-units (Akyürek et al., 1996), which are the Jurassic-Lower Berrasian Eldivan Ophiolitic Complex (Akyürek et al., 1979b), the Lower Cretaceous Dereköy Ophiolitic Melange (Ünalan et al., 1976; Batman, 1977) and the Dereköy ophiolitic Melange, found in the Upper Cretaceous sedimentary units.

In the Ankara region, Upper Cretaceous-Lower Tertiary interval is characterized by a thick flyshoidal sequence, which conformably lies over the ophiolitic melange at the bottom. This unit is unconformably overlain by younger volcano-sedimentary units.

1.5.2. Biga Peninsula

The Biga Peninsula forming the western portion of the Sakarya Composite Terrane (Figure 1.4, inset map) is confined by Rhodope and Serbo-Macedonian Massifs in Greece to the west and the Thrace Basin to the north. The Biga Peninsula is one of the type-areas of the Karakaya Complex, as it was first described in this region by Bingöl et al. (1973) and studied in detail by various authors.

There are four major NE-SW trending tectonic belts that characterize the Biga Peninsula (Okay et al., 1991). These are the Gelibolu, Ezine, Ayvacık-Karabiga and Sakarya zones (Figure 1.5).

The pre-Jurassic basement of the Sakarya Composite Terrane here comprises two units as the pre-Karakaya units, and the Karakaya units (Bingöl et al., 1973; Okay et al. 1991).

The Kalabak Formation and the Çamlık Metagranodiorite both compose the pre-Karakaya units in the Biga Peninsula. The Kalabak Formation is characterized by low-grade metasediments. It is intruded by the Devonian Çamlık metagranodiorite and overlain unconformably by the Upper Triassic clastics of the Hodul Unit about the Çamlık village where its name come from (Okay et al., 1991).

The Kazdağ Group, which is largely composed of gneiss, migmatite, amphibolite and marble (Bingöl et al., 1973), constitutes the oldest rock assemblage in the Biga Peninsula. The gneisses from this unit have provided a mean age of 308 ± 16 Ma (Moscovian), which indicates the time of high-grade metamorphism and migmatization in the Kazdağ range (Okay et al., 1996). The Kazdağ Group is tectonically overlain by the Nilüfer and Hodul Units of the Karakaya Complex in the east (Okay et al., 1991).

The pre-Jurassic Karakaya Complex is represented by four tectono-stratigraphic units in the Biga Peninsula: the Nilüfer, Çal, Orhanlar Greywacke and Hodul units (Okay et al., 1991).

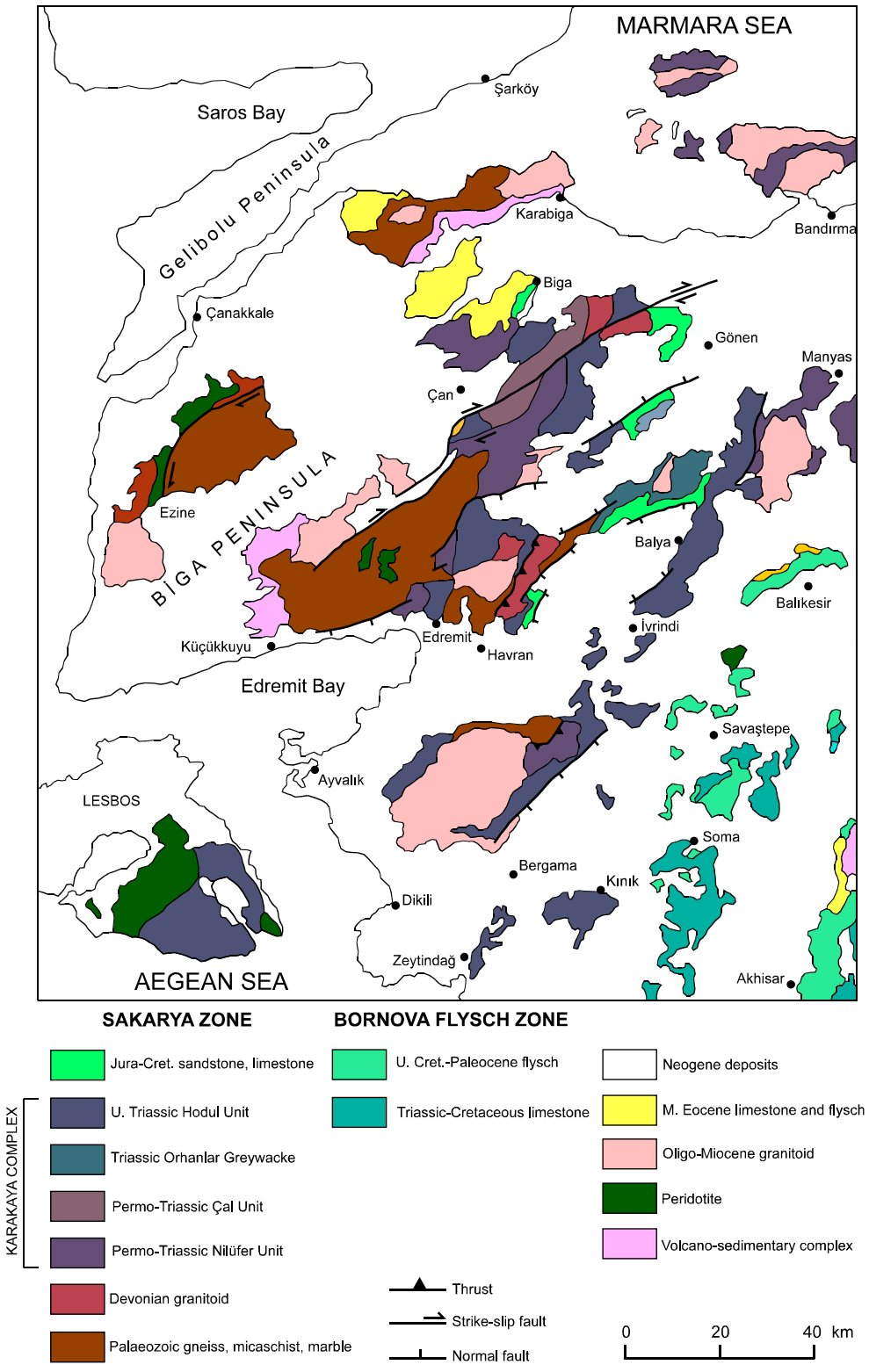

Figure 1.5. Distribution of major tectono-stratigraphic units of the Karakaya Complex and the other units in the northwestern Anatolia (after Okay et al., 1996).

The Nilüfer Unit is characterized by a strongly deformed sequence of dominating metabasic rocks intercalated with marble and phyllite (Okay et al., 1991). The Nilüfer Unit generally reflects low-grade greenschist facies metamorphism, however in some parts high-pressure greenschist facies also occur. The contact between the Nilüfer Unit and other pre-Liassic ones is a matter of debate (stratigraphic in Akyürek and Soysal, 1983; tectonic in Okay et al., 1991, 1996). An Early Triassic age is assigned based on the conodont fauna from marbles intercalated with metabasites in the section south of Bursa (Kozur et al., 2000), while Middle Triassic (Anisian-Ladinian boundary) conodonts are reported from the north of Bergama (Kaya and Mostler, 1992). In the NW Anatolia, the Nilüfer Unit can be correlated with the Çavdartepe Formation (Akyürek and Soysal, 1983), the İznik Metamorphics (Göncüoğlu et al., 1987) and the Yenişehir Metamorphic Group (Genç and Yılmaz, 1995).

The Çal Unit (the Çal Köy Series of Blanc, 1965; 1969), comprises mainly debris and grain flows as well as basalt and Upper Permian limestone clasts (Okay et al., 1991, 1996). The unit has been dated as Upper Permian from the radiolarian cherts in the Biga Peninsula (Kozur and Kaya, 1994; Kozur, 1997; Göncüoğlu et al., 2004). On the other hand, a Lower Triassic age is ascribed to the pelagic limestones (Kozur et al., 2000), whereas, Middle Triassic (Anisian) limestones (Camialan Limestone) are also reported (Okay et al., 1991). In Inegöl region, the equivalent of the Çal Unit has been mapped as the Abadiye Formation (Genç and Yılmaz, 1995).

The Hodul Unit is characterized by thick sequences of arkosic sandstones intercalated with shale and siltstone (Okay et al., 1991). In the Havran region it rests unconformably over the Çamlık Metagranodiorite. The macrofauna, consisting mainly of Halobia, indicates a Late Triassic age (Norian; e.g. Kaya et al., 1986; Wiedmann et al., 1992; Leven and Okay, 1996; Okay and Altıner, 2004). In NW Anatolia, the Hodul unit can be regarded as equivalent to the Ortaoba Unit (Pickett and Robertson, 1996), the Dışkaya Formation (Kaya et al., 1986), the Kınık Formation (Akyürek and Soysal, 1983) and the Kendirli Formation (Altıner and Koçyiğit, 1993).

The Orhanlar Greywacke comprises homogeneous clastic sequence of greywackes with a clay rich matrix (Brinkmann, 1971; Okay et al., 1991, 1996). The Orhanlar Greywacke represents a tectonic relationship with the Hodul Unit in the east, between İvrindi and Manyas (Okay et al., 1991). In the Ankara region, the foraminifera from the limestones of the Elmadağ Formation displays Middle to Late Triassic age for this unit (Akyürek et al., 1984). A similar age is also assigned from the Kısıküstü Formation (Koçyiğit, 1987).

In the Biga Peninsula, The Karakaya Complex is unconformably overlain by undeformed Jurassic and younger sedimentary rocks (e.g. Altınlı, 1975; Genç et al., 1986). The Mezosoic succession is composed of three formations namely, the Bakırköy Formation, the Bilecik Limestone and the Vezirhan Formation (Okay et al., 1991).

CHAPTER 2

LOCAL GEOLOGICAL FEATURES OF THE STUDIED ROCK UNITS

This study, which covers the volcanic rocks of all different sub-units of the Karakaya Complex, contains four study areas, which are İmrahor (Ankara), Hasanoğlan (Ankara), Ortaoba (Edremit-Balıkesir) and Kadirler (Geyve-Sakarya) areas.

In the following, field observations in four different areas, from where the geochemical samples were derived will be summarized in detail.

2.1. İmrahor Area

The İmrahor area consists of three main units; the (?) Palaeozoic Eymir Metamorphic Complex, the Triassic Karakaya Group including the Bahçecik and Olukman formations, and the unconformably overlying Tertiary Gölbaşı Formation.

2.1.1. Eymir Complex

The Eymir Complex, which is the oldest rock unit exposed in the Ankara region (Akyürek et al., 1980, 1982, 1984), comprises a regionally metamorphosed chaotic mixture of clastic and basic volcanic rocks, which are intruded by diabase dykes and it occupies an area about 6 km^2 in the region studied.

This metamorphic unit, in the area, outcrops in the region to the south of Aşağı İmrahor village (Figure 2.1). Between Aşağı and Orta İmrahor villages, its upper boundary is a tectonic contact with the Olukman Formation. In the other places, it is unconformably overlain by the Tertiary Gölbaşı Formation. However, no contact relationship could be observed between the Eymir complex and Bahçecik Formation.

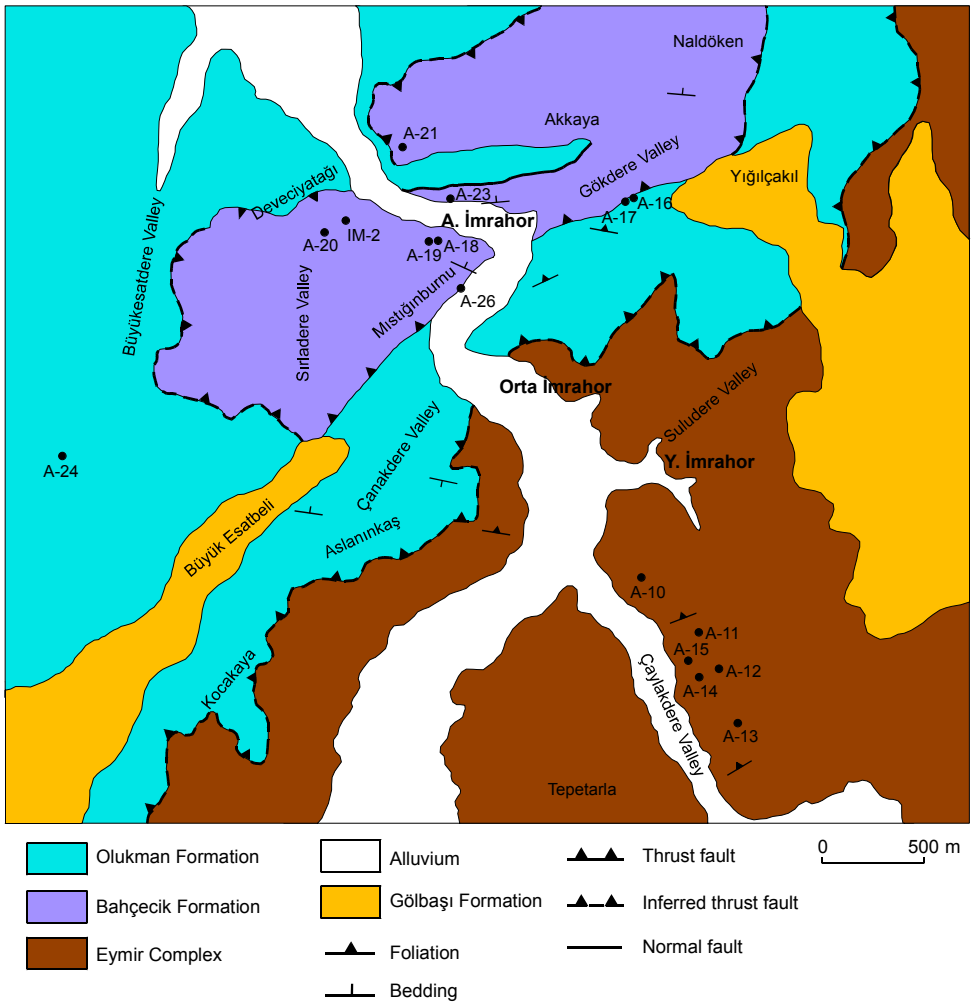

Figure 2.1. Geological map of the İmrahor area (only geochemically analyzed samples are indicated on the map).

In contrast to the Karakaya Group, it constitutes no limestone blocks, so that no palaentological data could be obtained on its age of deposition. In its outcrop-scale, it is very similar to the Olukman Melange of the Karakaya Group (disregarding the character of the basic rocks), which is also composed of deformed turbiditic clastics. Although, the dynamo-thermal metamorphism and a well developed foliation are distinctive for the the Eymir Complex, sometimes the non-cleaved occurrence of the coarser grained greywackes on the outcrop makes the differentiation of the two unit nearly impossible. Indeed, if the petrographic observations are taken into account, it is revealed that the Eymir Complex comprise both well-foliated and poorly-foliated parts in itself.

The basic igneous rocks within the complex are actually recognized as two types;

a) The diabase dykes cutting across the complex and
b) The metavolcanic rocks interlayered with the clastic rocks of the metamorphic complex.

The diabases, which are of approximately 10 m thickness, outcrop mostly to the south and to the southwest of Yukarı İmrahor village. Less frequently, they are encountered to the south of Kocakaya Hill, but in these parts it is very hard to observe their distribution, since their outcrops are so scarce. They are intensely affected by surface weathering and alteration, so they generally appear as reddish and brownish colored rocks (Figure 2.2). However, their fresh parts are dark green-colored, displaying the influence of hydrothermal alteration. In some places, these altered diabases may be overlooked due to similarity with the sheared and deformed meta-clastics into which they intruded, if not examined carefully.

The metavolcanics are actually composed of two types, as reflected by their color and appearance. The first type is characterized by green to light green colored basaltic volcanics. It is clear that they are hydrothermally altered basalts, evidenced by amygdaloidal structure and greenish colors. However, the other type is apparently different such that the foliation and presence of larger grains can be noticed at the first glance. They are of dark purplish and greenish colors and very probably of pyroclastic origin. Although the first type is confined to one locality, the second type can be traced as a SW-NE trending body, where it is surrounded by meta-clastics. It is noteworthy that this meta-volcanic unit does not appear in the locality other than Kocakaya Hill and Aslanınkaş Hill surroundings.

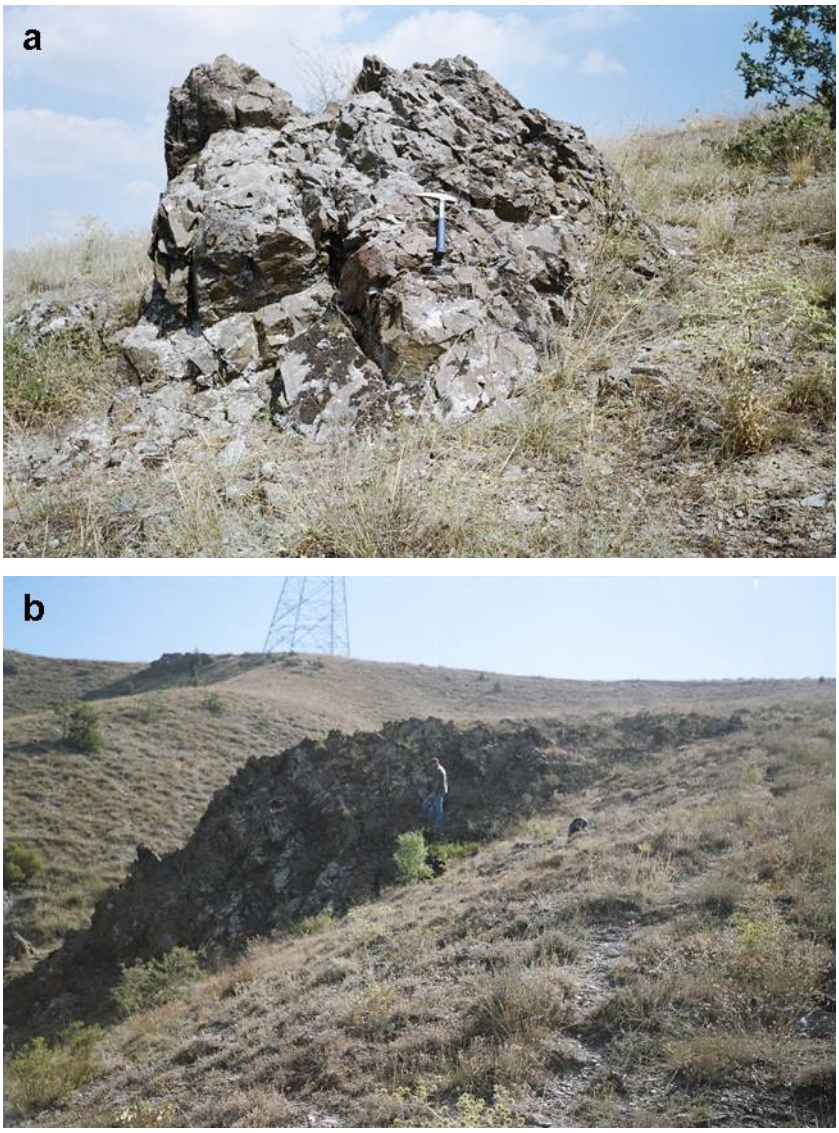

Figure 2.2. Diabase dykes within the Eymir Complex (a, b: east of Çaylakdere Valley).

The clastic rocks, which constitute the substantial part of the Eymir Complex, include several types of grain sizes, namely, conglomerate, greywacke, siltstone and pelites. They could be observed in every part of the complex. It should be noted that intense deformation and partial metamorphism makes difficult to understand primary relationships.

Conglomerates are represented by grayish, thick-bedded clastic rocks, surrounded by finer-grained clastics. They have phyllitic appearance with shiny

surfaces. The very low-grade metamorphism characterizing these clastics is also evident by elongated clasts. Furthermore, they reflect a polygenetic origin as indicated by clasts of different rock types. These coarse-grained rocks are especially well-observed to the south Yukarı İmrahor village.

Greywackes, similar to the conglomerates, are generally found as thin- to medium-bedded and less commonly thick-bedded rocks. Metagreywackes have silvery phyllitic appearance with oriented grains. These rocks are also cut by several thin quartz and calcite veins. It can be observed the presence of numerous small-scale faults as indicated by discontinuous veins.

In contrast to the coarser clastics mentioned above, finer-grained silt- and clay-sized clastics are found as thin-bedded rocks. The fine-grained nature makes them easy to identify their metamorphic features, as displayed by the presence of slates and phyllites. Slates in the study area are characterized by black color together with apparent slaty cleavage, whereas phyllites are composed of grains that can be distinguished by naked eye with silvery shiny surfaces. In some parts, greenish gray colored phyllites are also present within the complex. The inconsistency in the degree of deformation can be better inferred from these fine-grained clastics such that due to intense deformation some parts are characterized by highly folded phyllitic levels in both micro- and macro-scale, while some places are dominated by undeformed equivalents (Figure 2.3). Furthermore, in some parts crenulation cleavages were also recognized, especially to the eastern parts of the complex.

The contact between the Eymir Complex and Olukman Formation is recognized as a thrust fault between Aşağı and Yukarı İmrahor villages (Figure 2.1). It must be noted these relationship is not well-observable owing to the similarity of rock types within the units. However, such a tectonic boundary should be certainly present. Because, the metamorphic complex markedly display higher degree of metamorphism (especially reflected by Na-amphibole-bearing assemblages as discussed in Chapter 3) and presence of variable types of schists which are of both clastic and igneous origin, which are not included in the Olukman Formation. Therefore, these two rock assemblages could not be stratigraphically related.

Figure 2.3. Intense folding on the phyllitic levels within the Eymir Complex (Suludere Valley).

As mentioned at the beginning, no fossils have been found within the Eymir Complex in the study area yet. Thus, the age of the complex is not known. However, it may be older than the Karakaya Complex itself, as the latter include vast amounts of metamorphic clasts (slates, phyllites, etc) that can be derived from the Eymir Complex. On the other hand, it is obvious that the doleritic dykes, the main topic of this study, cut across this unit, thus making them younger than the deposition of the Eymir Complex. It is very important to note that in the study area, there are not any dykes that intrude the Karakaya Group which tectonically overlies the metamorphic complex. The other metabasic rocks, however, most probably represent products of syn-depositional volcanism.

In the previous studies, there are also no fossil data conforming the age of the Eymir Complex. Akyürek et al. (1984), according to whom the Emir (equivalent of the Eymir Complex) and the Elmadağ (equivalent of the part of the Karakaya Group) formations are transitional, proposed a Lower Triassic age for this unit based on the fossil findings within the Elmadağ Formation in the transition zone between Emir and Elmadağ Formations near Hacılar village (Akyürek et al., 1979a,b, 1980; Akyürek, 1981). However, there is no

stratigraphic contact between the Eymir Complex and the Olukman Formation in the study area, thus any relative age data about the complex have not been acquired.

Depending on the geological features in the study area, it can be deduced that the Eymir Complex represents a huge clastic sequence associated with volcanic activity which have been later intensely deformed, intruded by doleritic dykes and affected by regional metamorphism.

2.1.2. Bahçecik Formation of the Karakaya Complex

The Bahçecik Formation is mainly characterized by a mixture of spilitic lavas, shallow and deep (pelagic) marine limestones, radiolarian cherts as well as volcaniclastic sandstones. It exposes in a relatively small area when compared with the Eymir Complex, covering approximately 3 km^2.

In the study area, the Bahçecik Formation outcrops to the northwest of Orta İmrahor. Its contact with the Olukman Formation is best observed along Mıstığınburnu Hill and Gökdere Valley (Figure 2.1), and to the north of Deveciyatağı Hill where it thrusts over the Olukman Formation.

The Bahçecik Formation can be easily distinguished from the Olukman Formation and the Eymir Complex, as it consists mainly of spilitic basalts alternating with the limestones. There are also limestone blocks of various sizes within this unit. Furthermore, it includes both shallow- and deep-water carbonates, radiolarian cherts, volcanoclastics as well as mudstones.

It is possible to recognize both massive and pillowed basalts within the Bahçecik Formation. The massive lavas mostly have dark greenish appearance, indicating low-grade hydrothermal alteration. On the other hand, pillowed basalts have been also influenced by metamorphic alteration, gaining dark-greenish and reddish colors. Both types of spilitic basalts are best exposed in the Aşağı İmrahor village, to the west of Gökdere valley where the pillow basalts occurs at the bottom of sequence, then overlain by pinkish to pinkish grey pelagic limestones with volcanoclastic and mudstone interlayers, which in turn are followed by massive basalt flows alternating with pinkish

pelagic limestones (Figures 2.4 to 2.6). This relationship is better observed in Gökdere valley, where the sequence again starts with pillow basalts, then covered by pelagic limestones, which are followed by an alternation of thin pelagic limestone and mudstone layers, and finally green colored volcanoclastics occurs at the top. Furthermore, there are also red colored thin chert layers associated with both basalt and volcanoclastics in the mentioned sequence and it may be confused with the oxidation surface of basalts at the first look on the outcrop. In the reddish colored lavas, the pillow structures are relatively well-preserved compared to the greenish ones. In the western section of the study area, especially to the west of Büyük Esatbeli Hill, the intra-pillow structures within reddish spilitic lavas can be clearly recognized in a small lens of the Bahçecik Formation (Figure 2.7). Most of the metabasalts in the study area consist of spherical degassing structures which are largely filled with calcite.

Figure 2.4. Alternation of basalts and pelagic limestones within the Bahçecik Formation (Aşağı İmrahor).

Figure 2.5. Pelagic limestones with volcanoclastic and mudstone interlayers within the Bahçecik Formation in Aşağı İmrahor.

Figure 2.6. Alternation of pelagic limestone with massive lavas associated with cherts (Aşağı İmrahor).

Figure 2.7. The relationships of basalts, micritic limestones and cherts within the Bahçecik Formation indicating syn-depositional features (west of Büyük Esatbeli Hill).

As emphasized at the beginning, the most distinctive feature of the formation is the alternating sequences of basaltic lavas and carbonates (Figures 2.8 and 2.9). It is evident that the basalts and the limestones reflect syn-depositional characteristics such that while basalt clasts can be found within limestones, in a similar way, the clasts of limestones are also encountered inside the basalts (Figure 2.8). In Mıstığınburnu Hill, this relationship is recognized in relatively large scale compared to the other parts of the study area such that after a thick pile of pillow basalts, the sequence gradually followed by carbonate levels alternating with volcaniclastics, and then followed by thick bedded (oolitic) shallow-water limestones. In the northeastern parts of Mıstığınburnu Hill, this situation is clearly reflected by the abrupt changes between volcanics and carbonates (Figure 2.8b). It is observed that the sequence starts with the massive lava flows associated with thin chert layers, then carbonates participates the deposition and this is followed by simultaneous lava and carbonate alternation. The syn-depositional contact relationships are also evident on the road-cuttings in Naldöken Hill, however in this locality both

limestones and basalts are intensely affected by numerous folds and faults (Figure 2.9).

Figure 2.8. Syn-depositional nature of basalt and limestone within the Bahçecik Formation (a: Deveciyatağı Hill, b: west of Mıstığınburnu Hill).

Figure 2.9. the contact relation of the basaltic lavas and the recrystallized limestones deposited between and on top of them. The normal fault in the center is a late feature (road-cuttings at Naldöken Hill).

Both shallow- and deep-water carbonates exist within the Bahçecik Formation. The limestones representing shallow-marine environment are whitish to grayish colored in their outer surfaces, but they appear as black colored in the fresh parts. They occur as thin- to thick-bedded and in some parts highly recrystallized with abundant secondary calcite veins. Thick-bedded neritic limestones can be well-observed in Mıstığınburnu Hill. In some localities, the alternation in thickness of limestone beds is very obvious, especially in Naldöken Hill. On the other hand, pelagic limestones have pinkish to light-greenish appearances and are accompanied by radiolarian mudstones and cherts. In some parts, folding and bending on shallow-water limestones unravel the effect of deformation, especially around Deveciyatağı and Akkaya Hills (Figure 2.10).

It is important to note that the pelagic limestones dominate the eastern sector of the Bahçecik Formation, whereas shallow limestones are mostly present in the western part.

Figure 2.10. Intense deformation on limestones of the Bahçecik Formation (Sırladere Valley).

There are also olistostromal conglomerates which are composed of limestone fragments cemented by a clastic material (Figure 2.11a). It is observed that they are poorly-sorted rocks as indicated by variable size of clasts. These grayish-brownish colored olistostromes are confined to the western sector of the study area to the south of Büyükesatdere valley where they occur next to pillow lavas. Another type of olistostrome is observed to the east of Büyükesatdere Valley. This type is represented by moderately rounded clasts, which is composed of volcanic material (Figure 2.11b). These olistostromes have greenish to brownish surface colors, while the fresh inner parts display dark reddish colors.

The large outcrop of olistostromes is associated with thin-bedded shallow marine limestones. These limestones are characterized by grey surface colors but fresh parts appear black. In lower parts, they are intercalated with shaly-sandy levels, while upper parts of the sequence comprise some rounded parts.

Figure 2.11. Olistostromal conglomerates observed in the Bahçecik Formation on the road-cutting at Büyükesatdere Valley. The pebbles are dominantly of limestone in the upper and of basalt in the lower photograph.

The volcaniclastics are mostly silt- and sand-sized sedimentary rocks. They are characterized by greenish to brownish appearance and thin- to medium-bedding. The Deveciyatağı Hill and the southern sections are the places, where these volcaniclastics are intercalated with limestones (Figure 2.12).

Figure 2.12. Volcanoclastics alternating with limestones within the Bahçecik Formation (north of Büyükesatbeli Hill).

Along the thrust zone, where the Bahçecik Formation tectonically overlies the metamorphic complex, the spilitic basalts and limestones blocks of the Bahçecik Formation are exposed in the Mıstığınburnu Hill. It is very interesting that there are also serpentinized gabbros and ultramafic rocks exposed along the thrust zone and this is the only place where they are recognized. The influences of thrusting on the igneous rocks are evidenced by their highly sheared and deformed structures. Along the fault zone, the rocks are characterized by fractured natures and in some parts mylonitic zones are also observed (Figure 2.13). Development of foliation in basalts shown in Figure 2.14 is another feature resulted from this tectonic event. If the rock types included in the Bahçecik Formation is considered, the presence of such basic and ultrabasic rocks that represent oceanic crust seems unusual.

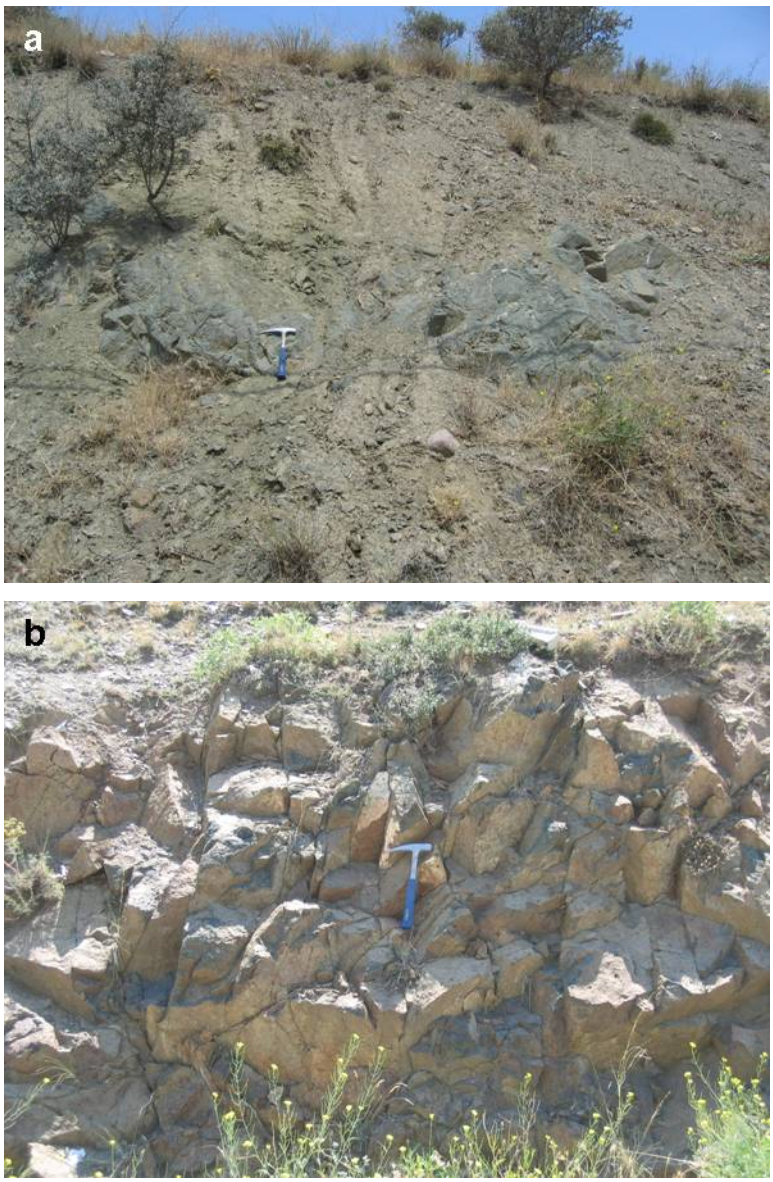

Figure 2.13. Gabbros exposed in the thrust zone between the Bahçecik Formation and Eymir Complex. Note that the gabbro is included in a mylonitic matrix (above). Fractured appearance of gabbro owing to tectonic effects (below) (a: Mıstığınburnu Hill, b: Gökdere Valley).

Figure 2.14. Development of foliation in basalts of the Bahçecik Formation within the thrust zone in Gökdere Valley.

The slightly recrystallized limestones that show syn-depositional features with the basic volcanic rocks around Mıstığınburnu Hill include foraminifers (*Glomospira densa*, *Glomospirella grandis* (?), *Endothrid* sp., *Meandrospira dinarica* (?)) that were assigned to Anisian (Özgül, 1993). In the present study, the gray and black limestones around Mıstığınburnu Hill had been once more investigated in detail. From several samples taken from limestone and turbiditic limestone with volcanic clasts, Prof. D. Altıner (METU) identified the following fossils (see Appendix A): *Pliammina densa* (PANTIC, 1965), *Meandrospira dinarica* (KOCHANSKY-DEVIDE and PANTIC, 1965), *Meandrospira deformata* (SALAJ, 1967), *Endoteba* sp., *Aulotortus* (?) sp., *Aulotortus* (?) *eotriasicus* (ZANINETTI, RETTORI and MARTINI, 1994) and *Paulbronnimannella whittakeri* RETTORI. This fossil content is characteristic for Middle Anisian (Prof. D. Altıner, oral communication) and is an evidence for the age of the basaltic volcanism studied in detail.

2.1.3. Olukman Formation of the Karakaya Complex

The Olukman Formation is represented by intensely deformed and sheared mixture of clastic rocks with variable thickness and sizes. In the study area, it is exposed in the western sector, surrounding both sides of Büyükesatdere Valley, whereas in the eastern part, it appears to the north of Orta İmrahor village (Figure 2.1). It occupies an area of approximately 6 km^2.

The Olukman Formation resembles the Eymir Metamorphic Complex in terms of both lithological and deformational features. This make sometimes difficult to differentiate these units from each other.

The clastics within the formation generally appear as brownish colored rocks, although greenish tones are also observed in the study area. The greenish ones may be deceptive if not carefully examined, since they look like hydrothermally altered basalts at the first glance. As mentioned above, rock assemblage of the Olukman Formation is similar to that of the Eymir Metamorphic Complex. Variably foliated and metamorphosed black shales, siltstones, greywackes and conglomerates are also included in the Olukman Formation. In addition, this unit is of incipiently metamorphic nature and it also comprises both non-foliated and poorly-foliated parts within itself. However, the Olukman Formation does not include any basic volcanic rocks or schists, which is distinctive for the metamorphic unit.

It is observed that the effects of deformation are not the same in every part of the formation. In this respect, clastic sequences in road-cuttings in Çanakdere valley and Mıstığınburnu Hill represents relatively less deformed parts, whereas, the west of Büyük Esatbeli Hill are characterized by higher degree of deformation (Figure 2.15). This variability is also recognized in micro-scale such that both deformed and non-deformed parts can be identified even in a single hand specimen. Similar to that observed in the metamorphic unit, fine-grained clastics reflect slaty appearances (Figures 2.15a and 2.16) since they are more vulnerable to dynamic effects. Intense folding is especially evident in Büyükesatdere Valley (Figure 2.15b). The alternation of variably sized clastic rocks can be well-observed especially in the Çanakdere Valley in both side of the road (Figure 2.17), where relatively thick-bedded parts are characterized

by greywackes, while slaty and silty parts alternate between them. Note that this assemblage has been relatively less affected by deformation.

Figure 2.15. Intense shearing and deformation observed in clastic rocks of the Olukman Formation (a,b: Büyük Esatdere valley).

Figure 2.16. The fine-grained clastics (slates) of the Olukman Formation. Note the very well-developed cleavage (Gökdere valley).

Figure 2.17. Clastic units of the Olukman Formation including alternation of variably sized incipiently metamorphosed rocks (Çanakdere Valley).

In the study area, the Olukman Formation is largely dominated by fine- and medium-grained clastics, whereas conglomerates are rarely found and especially confined to the southeast of Çanakdere Valley. Similar to

metamorphic equivalents in the Eymir Complex they are also of polygenetic origin, however elongated clasts and phyllitic appearance could not be recognized in the conglomerates of Olukman Formation.

Greywackes, on the other hand, are characterized by various types and grain sizes within itself. The medium-grained ones are predominant in the study area, whereas fine- and coarse-grained are less commonly encountered. In some parts, blackish colored sandstones with high quartz content can be observed. Furthermore, the greywackes are of variable mica content and micaceous ones can be characterized by shiny surfaces. On the contrary to the metamorphic complex, the Olukman Formation does not include any sandstone which is composed of apparent mafic component as indicated by dark greenish fragments.

Another feature that discriminate the Olukman Formation from the metamorphic complex is the absence of diabase dykes which cut across the latter unit. There are also no volcanic rocks included within the former unit in the study area. Thus, although the lithological and structural features are alike at the first glance, there are actually important differences between the two units. Thus, the Olukman Formation is of clearly different origin relative to the Eymir Complex.

In Aşağı İmrahor locality, the Olukman Formation is tectonically overlain by the Bahçecik Formation of Karakaya Group along a NE-SW trending thrust-zone of approximately 2 km. This tectonic contact is best observed in the Mıstığınburnu Hill and along Gökdere Valley. Along the tectonic contact, the rock units that belong to the Olukman Formation are represented by brownish colored slates displaying well-developed cleavages and non-foliated greywackes, which are tectonically overlain by the pillow basalts, gabbros and limestones of the Bahçecik Formation. The tectonic relationship can not be followed to the southwestern part of the complex due to the unconformably overlying Gölbaşı Formation. On the other hand, to the northwest of Aşağı İmrahor, the tectonic contact is again recognized, where basic volcanics of the Bahçecik Formation have been partly foliated and deformed (Figure 2.18).

In the study area, no paleontological data could be obtained regarding the age of the Olukman Formation. However, the unit was assigned to Carnian-Rhaetian based on the fossil fauna within limestones of the unit (Özgül, 1993). However, a Lower-Upper Triassic age was ascribed to the unit depending on the fossil findings within the Elmadağ Formation (Akyürek et al. 1984).

Figure 2.18. The thrust zone between the Olukman and Bahçecik Formation. The former unit tectonically underlies the latter along the valley (Büyükesatdere Valley; the white dashed line indicates thrust contact).

2.2. Hasanoğlan Area (Ankara)

The study area in the Hasanoğlan area includes the Bahçecik Formation and it covers a small area, about 2 km^2 (Figure 2.19). This formation is represented by a volcano-sedimentary assemblage that includes the informally defined "Yazılıkaya Formation" and "Döşemedere Formation" together with a huge limestone block, called "Çaltepe limestone" (Koçyiğit, 1987; Altıner and Koçyiğit, 1993). However, it must be noted that the geochemical sampling were performed on the pillow basalts of the formation, so the lithological features other than basalts will not explained here (for details see the references above).

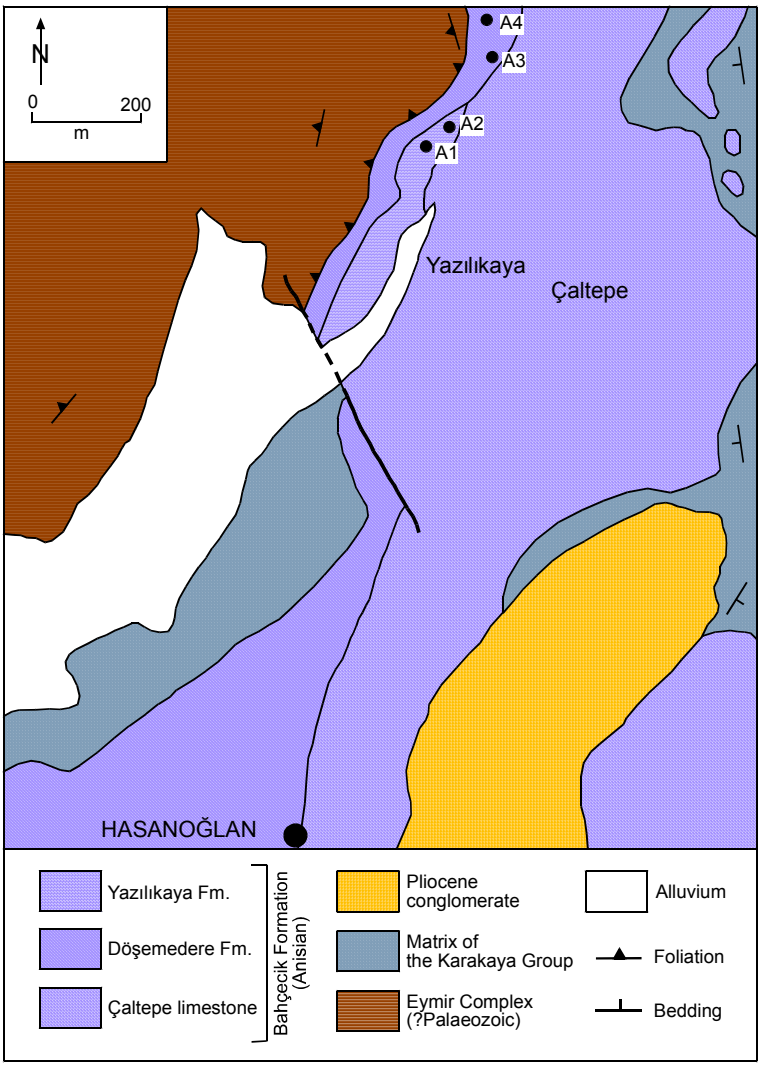

Figure 2.19. The geological map of the Hasanoğlan region (after Altıner and Koçyiğit, 1993; only geochemically analyzed samples are indicated on the map).

The basic volcanic rocks are surrounded by the Çaltepe limestone which is characterized by white, gray colored recrystallized limestone in the eastern sector of the area, whereas they are in contact with the Eymir Complex. Both contacts are represented by thrust relationship (Koçyiğit, 1987).

In the study area, olistostromal breccias are associated with pillow basalts. These olistostromes are composed of limestone fragments which are binded by reddish mudstone cement. In some parts, it is observed that the pillow

basalts are interlayered with light green colored volcanoclastics which are generally of silt-size and reddish, greenish cherty levels.

The volcanic rocks within the formation are characterized by hydrothermally altered pillow basalts. They are reddish and dark blue colored and exhibit a highly vesicular nature. The pillows together with intra-pillow structures are well-observed, especially inside the Hasanoğlandere Valley. In some parts, reddish colored volcanics, which represents outer parts of the lava flow, can be observed as well.

The age of unit was determined as Anisian according to fossil assemblage within the carbonates of informally named “Yazılıkaya Formation” (Koçyiğit, 1987; Altıner and Koçyiğit, 1993). This data is also conformable with Middle-Upper Triassic age which was assigned to the Ortaköy Formation (Akyürek et al., 1984).

2.3. Ortaoba Area (Balıkesir)

Since only sampling of basic volcanic rocks were carried out from the Ortaoba Unit, just the contact relations related to this unit were given below. The geological framework and the geological map provided (Figure 2.20) is modified from Pickett and Robertson (1996).

This unit covers approximately 5 km^2 in the study area and tectonically overlies the Nilüfer Unit of Okay et al. (1991). It is represented by a disrupted sequence, consisting mainly of clastic rocks. The basement of the unit comprises locally pillow lavas and hyaloclastite, which are overlain by siliceous mudstone. This sequence continues with bedded grey cherts and sandstones. The significant tectonic repetition and disrupted nature are distinctive features of the Ortaoba Unit.

The basalts within the unit are green colored and displays no vesicular structures in contrast to the İmrahor lavas. The influence of hydrothermal metamorphism is clearly evidenced by their greenish appearance.

A Ladinian?-Carnian age is assigned for the Ortaoba Unit, based on the conodont finding (*Gladigondolella tethydis)* in the radiolarian cherts (determination by Dr. H. Kozur, unpublished data). The dominance of turbiditic sequences with no carbonate content indicates that the Ortaoba Unit represents a deep-marine depositional environment (a slope or basin) below CCD-level.

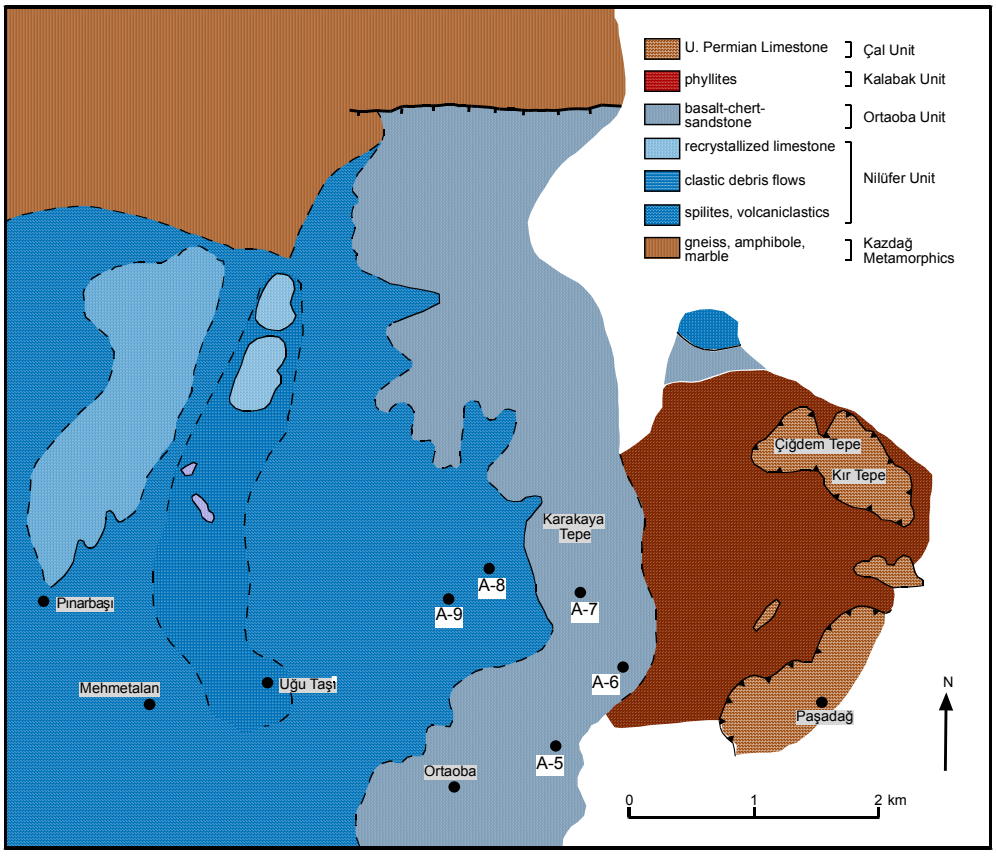

Figure 2.20. Geological map of the Ortaoba area (after Pickett and Robertson, 1996; only geochemically analyzed samples are indicated on the map).

2.4. Kadirler Area (Geyve)

In the Geyve region, the rock units characterizing the Karakaya Complex is divided into two informal sub-units, namely, the “arkosic sandstone unit” corresponding to the Olukman Formation and “pillow basalt-limestone

association" resembling the Bahçecik Formation in Ankara region (Göncüoğlu et al., 2004). The basaltic volcanics were collected from the latter unit for the geochemical purposes, so the geological features of former unit will not be explained here.

The pillow basalt-limestone association tectonically overlies the arkosic sandstone unit to the south of E-W trending Yenişehir-Geyve ridge around Pazarkaya and Karaoluk Hills (Figure 2.21).

This association is represented by a separate thrust slice which exposes around the Pazarkaya, Karaoluk and Asarkaya Hills. On the other hand, around Çinetaşı Hill it appears as a klippen. At the tectonic contact, where this unit rests on the arkosic sandstones, it is recognized that the arkoses are converted to clastites (Göncüoğlu et al., 2004).

The pillow basalts are represented by blackish colors and substantial amount of amygdules which are filled by mostly calcite. The blackish appearance of these pillow basalts displays that the effect of hydrothermal metamorphism is relatively low compared to those observed in the basalts from other localities. In the study area, while the basalts are sometimes incorporated into the limestones as small lenses, in some parts it is observed that the volcanic clasts are associated within the limestones (Figure 2.22). This scene is obviously evidence of the syn-depositional nature of the pillow basalts and limestones. An Anisian age is suggested for the unit, regarding the correlation with the Ankara and Middle Sakarya regions (Göncüoğlu et al. 2004). The conodont (Genç et al., 1986) and foraminifer (Altıner and Koçyiğit, 1993) findings also support the Middle Triassic age for the unit.

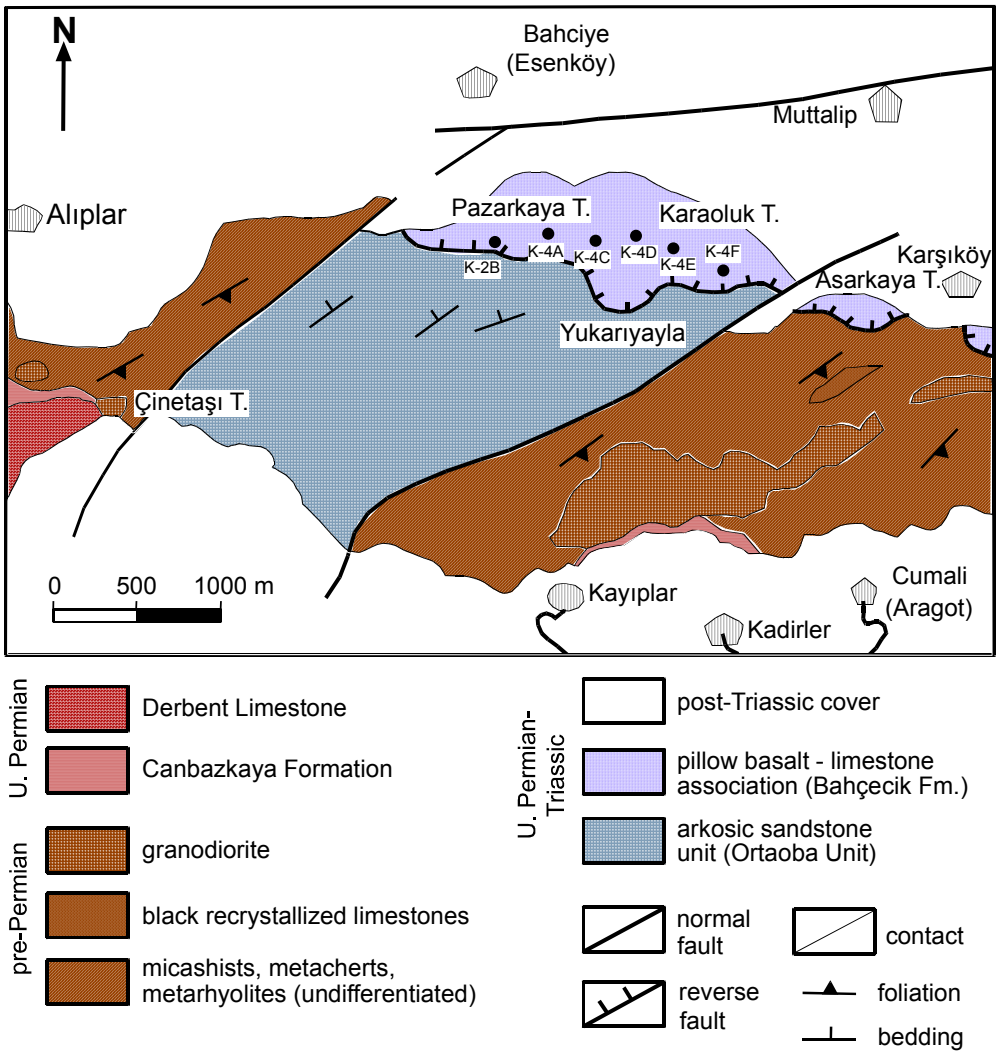

Figure 2.21. Geological map of the Kadirler area (after Göncüoğlu et al., 2004; only geochemically analyzed samples are indicated on the map).

Figure 2.22. Association of pillow basalts with limestones, indicating their contemporaneous formation (south of Asarkaya Hill).

CHAPTER 3

PETROGRAPHY

3.1. Introduction

For petrographical purposes, a total of 147 rock samples from four localities within the Karakaya Complex were examined under polarizing microscope. Among them, 120 samples are from İmrahor (Ankara), 10 samples from Hasanoğlan (Ankara), 7 samples from Ortaoba (Edremit) and 10 samples from Kadirler (Geyve) region. These samples comprise all main rock types, namely sedimentary, igneous and metamorphic. The sedimentary ones are mainly concentrated on greywackes and limestones, while igneous samples are represented by hydrothermally altered basalts, diabases and ultramafics. On the other hand, metamorphic samples consist of meta-greywackes, slates, phyllites and schists. It must be noted that limestone samples were examined only for paleontological age determination and they were not included in this chapter.

The mineralogical and textural features, such as crystallinity, granularity, fabric and degree of alteration were studied in detail. Since the basalt samples are highly altered, modal analysis could not be carried out, even by visual estimation.

3.2. İmrahor Area

3.2.1. Basalts

Based on the petrographical examination, it is deduced that the basalts in İmrahor region are not of single type. Instead, it comprises two types of basalt units whose mineralogical and textural features are very unlike from each other. In this respect, the first type is named as Ti-augite bearing basalts and

the other as diopside-bearing basalts. The second one will not be described in this chapter, as its petrographical features are identical with the Kadirler basalts which will be explained in the later parts.

3.2.1.1. Ti augite-bearing basalts

These basalts, in hand specimen, display blackish to dark-greenish colors and they are of aphanitic texture. However, the presence of relatively large crystals is very distinctive, even in hand specimen. While some of these high-Ti basalts have degassing structures filled by secondary minerals, in the others such structures are absent. Therefore, this may signify their relative position during their generation such that the ones with vesicles should have formed at relatively higher levels than those without vesicles.

Thin-section examination interestingly unravels that these basalts also consist of two different types. One of them is represented by higher Ti-content as indicated by deeper-colored Ti-augites and the other is characterized by relatively larger Ti-augite crystals with lower Ti-content and small plagioclase laths, resembling diabasic texture. However, they are both holocrystalline, microcrystalline and porphyritic. It is somewhat outstanding that at the first glance they are very similar to hypabyssal rocks (dykes) in terms of crystallinity and size of crystals.

The primary minerals characterizing the first type of these lavas are clinopyroxene (Ti-augite), plagioclase, olivine, opaque minerals, and brown amphibole (probably kaersutite) is present as a late stage magmatic phase, whereas the secondary assemblage consists of, chlorite, serpentine, pistacite, zoisite/clinozoisite and sericite. The second type is also dominated by a similar primary mineral assemblage, but differs in secondary products with the absence of brown amphibole.

The essential mineral of these basalts are Ti-rich clinopyroxene (Figures 3.1 to 3.3). It is very abundant in the samples and easily identified by the pinkish to pinkish-brown colors with slight pleochroism, indicating its high-Ti content. It appears mostly as prismatic crystals with subhedral and euhedral outlines and

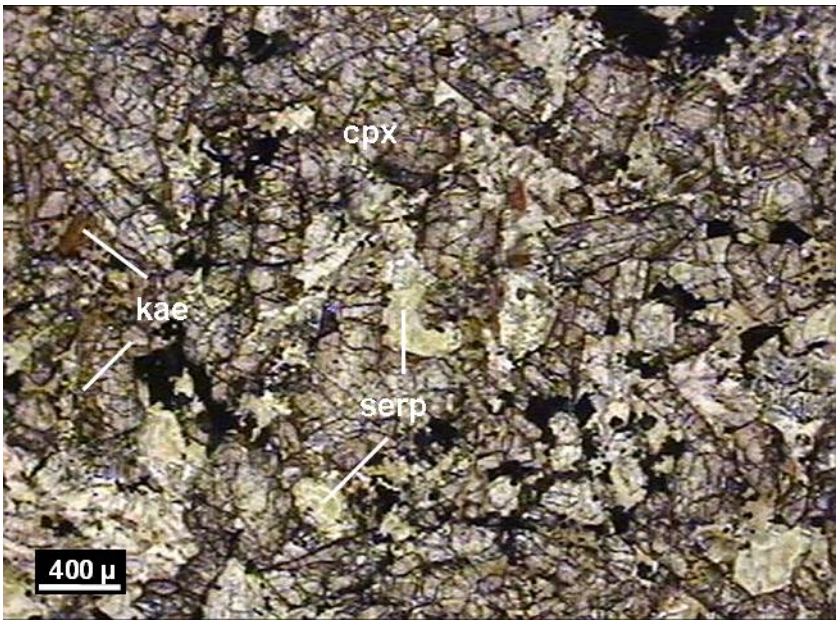

Figure 3.1. Photomicrograph illustrating Ti-augites with characteristic pinkish-brown colors in the Ortaoba basalts (Sample B1; 4x PPL, cpx: Ti-augite, kae: kaersutite, serp: serpentinized parts).

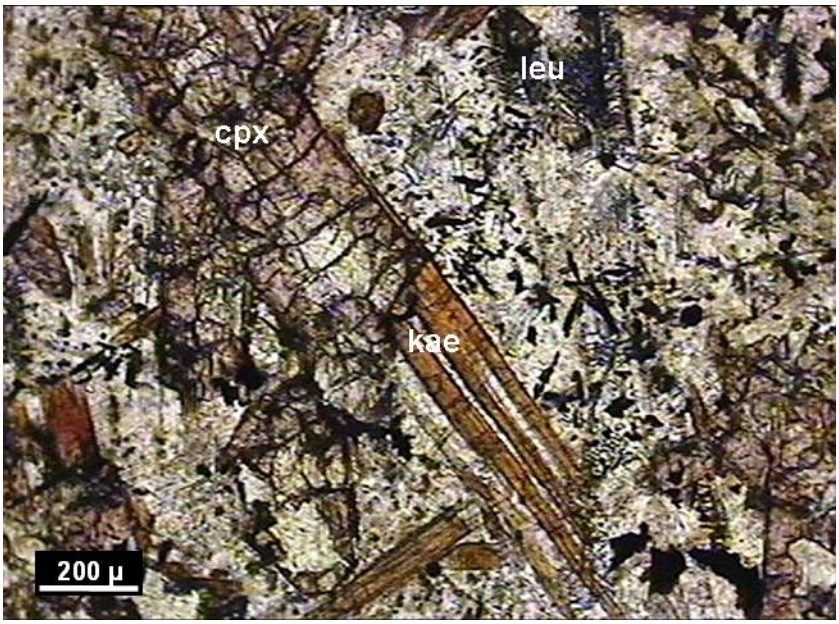

Figure 3.2. Photomicrograph showing partial alteration of Ti-augite by kaersutite in the İmrahor basalts (Sample B1; 10x PPL, cpx: Ti-augite, kae: kaersutite, leu: leucoxene).

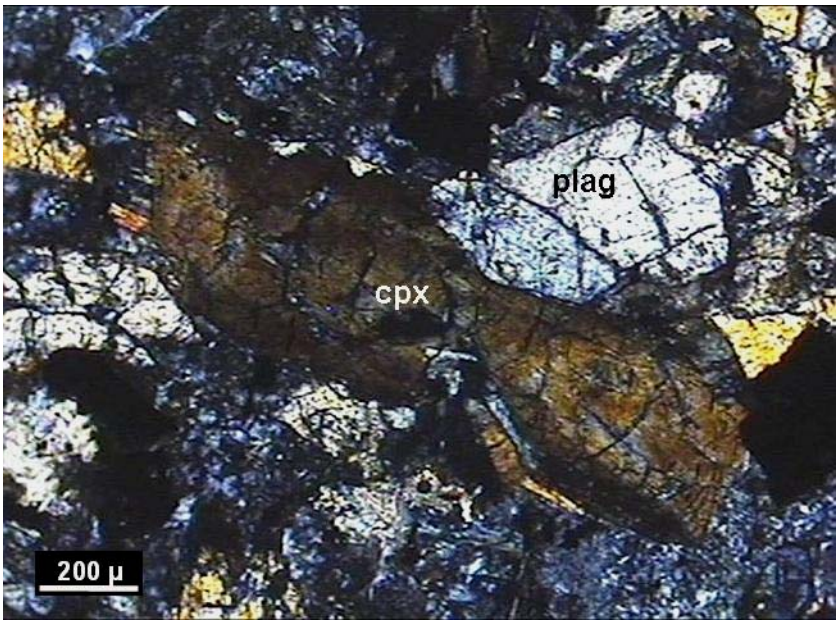

Figure 3.3. Photomicrograph illustrating hour-glass zoning on a Ti-augite phenocryst (Sample B1; 10x XPL, cpx: Ti-augite, plag: plagioclase).

well-developed cleavages. It is present both as phenocrysts and microcrysts in the groundmass. It is characterized by an extinction angle of 43-50°. The compositional variation in invidual Ti-augites can be recognized by color variation in the crystals such that the rims are deeper colored, while central parts are represented by pale colors (Figure 3.2). Indeed, under crossed polars this scenario can be more clearly understood by the compositional zoning, especially sector zoning typical of these type pyroxenes (Figure 3.3). Based on their location in the study area, at times Ti-augites seem relatively fresh, but in some places they are extremely altered and fragmented (Figure 3.4). The euhedral form of Ti-augite can be recognized in the relatively unaltered samples, whereas in highly altered ones, they appear as fragmented crystals replaced by secondary products. In the latter case, it is usually seen that the outlines of Ti-augites are preserved.

Plagioclase is the second common mineral phase, occurring mostly as subhedral crystals. Similar to Ti-augite, it occurs both as phenocryts and lath-shaped microcrysts in the groundmass. The imprints of alteration on plagioclases are so clear that they are partly or completely sericitized. In some

parts, sericite minerals growing up to muscovite flakes is observed. It is possible to see usually polysynthetic and less commonly simple twinning in relatively less altered plagioclases. Very rarely, combined albite and simple twinning is also noticeable in some plagioclases.

Olivine, similar to that of previous samples, is completely altered to serpentines, so no preserved olivine crystal is available (Figures 3.5 and 3.6). Some psedomorphs of olivine includes replacement by both calcite and serpentine, where calcite occupies the center, while serpentine occurs towards the rims.

Seriate texture, displayed by various sized clinopyroxene and plagioclase crystals, can be recognized at the first glance. Furthermore, sub-ophitic relation of plagioclases embedded in Ti-augites is another feature observed in these basalts.

As a late stage magmatic phase, kaersutite, also known as titan-hornblende is most distinctive one in the first type with brownish tones of pleochroism and small extinction angles ranging between 5-18° (Figures 3.1, 3.2 and 3.7). It is generally characterized by low 2^{nd} order interference colors and euhedral to subhedral forms. It occurs mostly as acicular or long prismatic crystals, replacing Ti-augites. These replacements can be recognized in many parts of the thin-sections where Ti-augite crystals are partly rimmed by prismatic kaersutites. In occasional cases, the complete replacement of Ti-augite by kaersutite is also visible. In highly altered samples, biotite also occurs as distinguished by strong brown to reddish-brown pleochroism and characteristic mottled extinction. As epidote group minerals, zoisite/clinozoisite group and pistacite are the alteration products that are encountered in these basalts. Serpentine minerals are observed replacing both clinopyroxene and olivine. Fibrous form and development in veins through the fractures are well-defined, particularly in altered olivines (Figure 3.6). In the vesicular types, the gas cavities are filled largely by calcite. Chlorite sometimes appears in the outer margin, surrounding the inner calcite. As denoted previously, sericite replaces partly or entirely plagioclases (Figures 3.6 and 3.8). It must be noted, however,

that prehnite in some parts reflect similar interference colors, but it differs from sericite in exhibiting fan shaped form with absence of mottled extinction.

Leucoxene yet again occurs among opaque minerals as discriminated by well-developed skeletal and dentritic forms (Figures 3.2 and 3.7). On the other hand, it is not easy to determine the other opaque crystals that have not skeletal outlines, since ilmenite and magnetite cannot be differentiated under polarized light unless leuxocene forms. However, the presence of ilmenite is probable due to its alteration to leucoxene in the samples. In some parts, there are opaque crystals with cubic, hexagonal and rhombohedral forms. Thus, it is likely for these basalts to constitute magnetite as well.

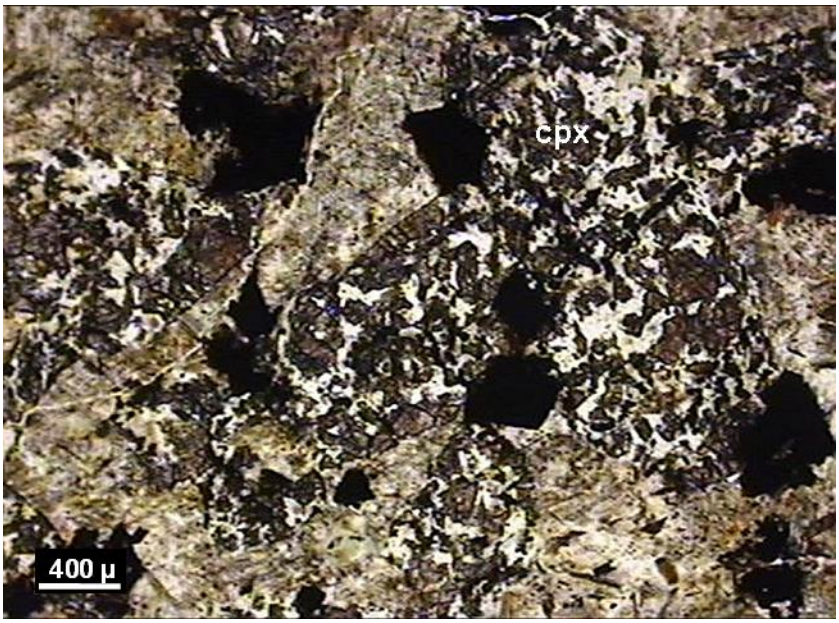

Figure 3.4. Photomicrograph of fragmented Ti-augite phenocrysts in the highly altered İmrahor basalts (Sample C4; 4x PPL, cpx: Ti-augite).

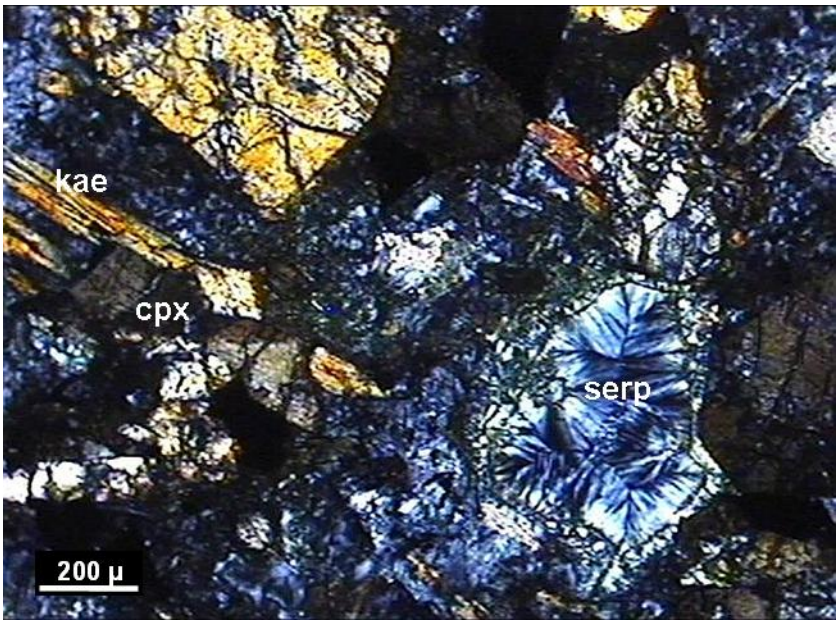

Figure 3.5. Photomicrograph of olivine pseudomorph, entirely replaced by serpentine minerals (Sample B1; 10x XPL, cpx: clinopyroxene, kae: kaersutite, serp: serpentine).

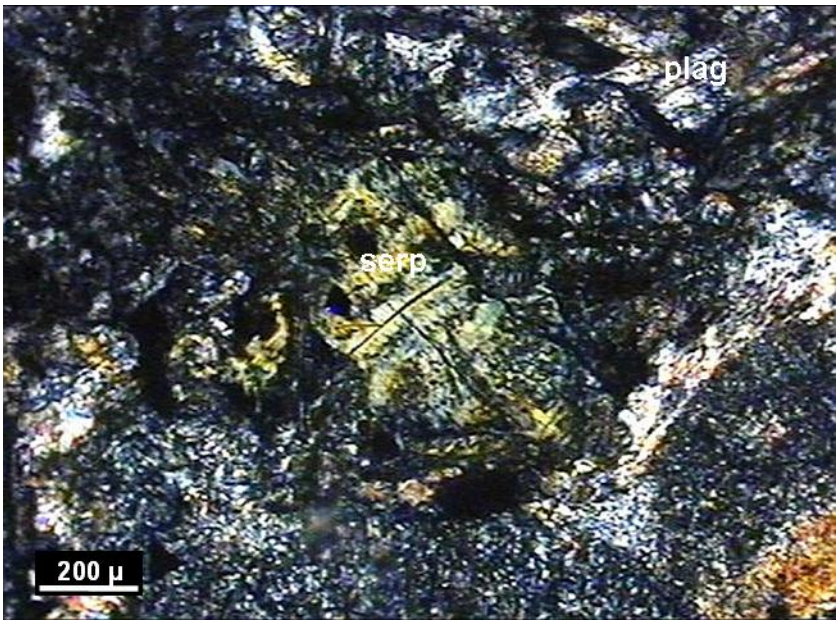

Figure 3.6. Photomicrograph illustrating an olivine psedomorph and sericitized plagioclases (Sample D1; 10x XPL, serp: serpentinized olivine, plag: plagioclase).

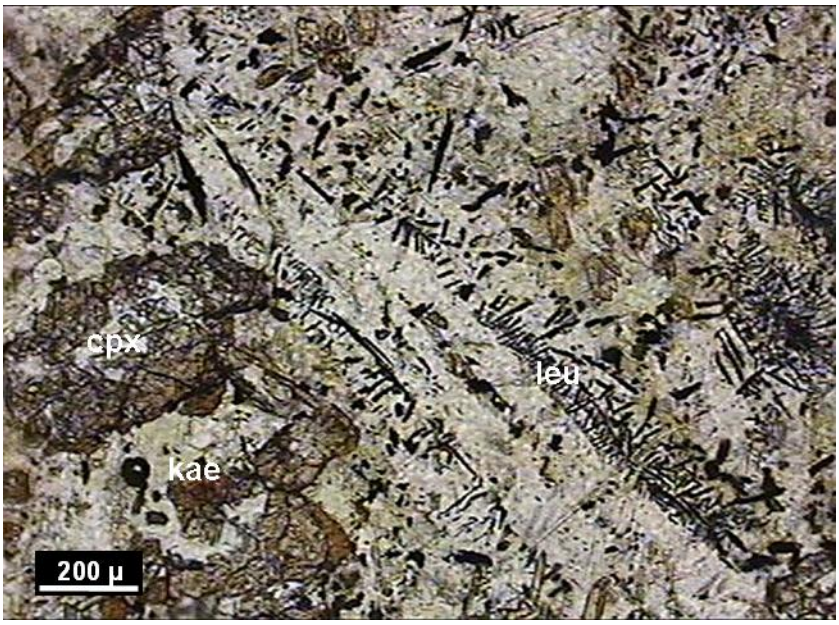

Figure 3.7. Photomicrograph of dendritic leucoxene formations after ilmenite (Sample B1; 10x PPL, cpx: Ti-augite, kae: kaersutite, leu: leucoxene).

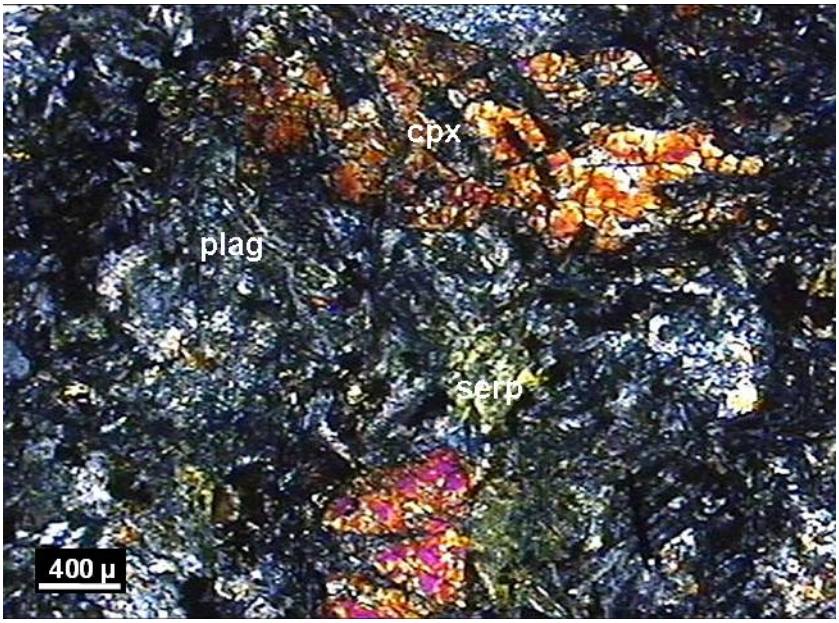

Figure 3.8. Photomicrograph illustrating intense alteration on the İmrahor basalts (Sample B1; 4x XPL, cpx: clinopyroxene, plag: plagioclase, serp: serpentine).

3.2.2. Ultramafic Rocks

In the Imrahor area, an ultramafic block is obtained from only one locality. This sample has dark greenish-blackish colors in hand specimen and is characterized by phaneritic texture. The ultramafic sample is clearly distinct from the basalts with its crystals observable with naked eye and very dark color.

Under microscope, it exhibits holocrystalline and equigranular textures. The most distinctive feature of the sample is the existence of very intense serpentinization such that all olivine crystals are entirely serpentinized, thus it is not possible to encounter a preserved olivine crystal (Figures 3.9 to 3.11). It is clearly observed that serpentine minerals have developed along fractures, forming vein-like structures and dominated every part of the olivine crystals.

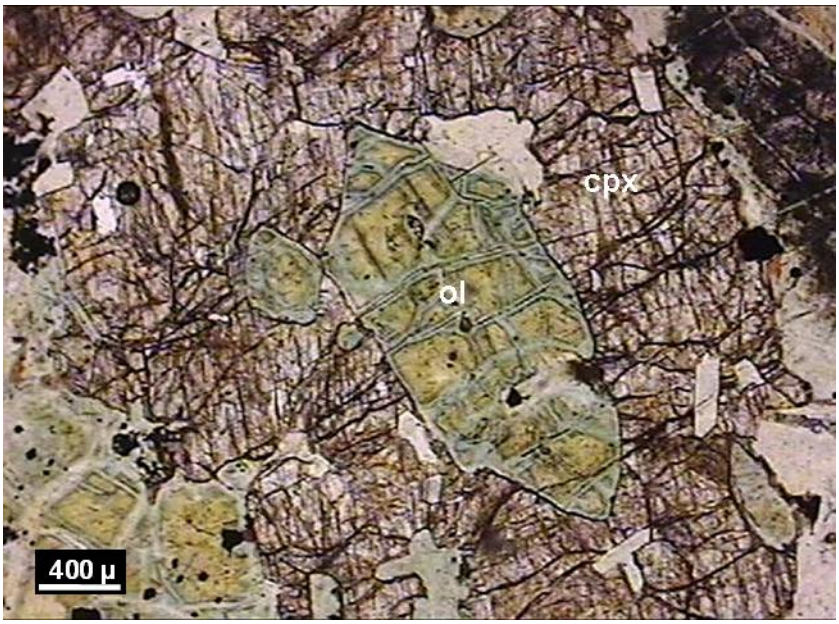

Figure 3.9. Photomicrograph showing poikilitic enclosure of euhedral olivine crystal by a large Ti-augite crystal (Sample S18a; 4x PPL, ol: olivine, cpx: Ti-augite).

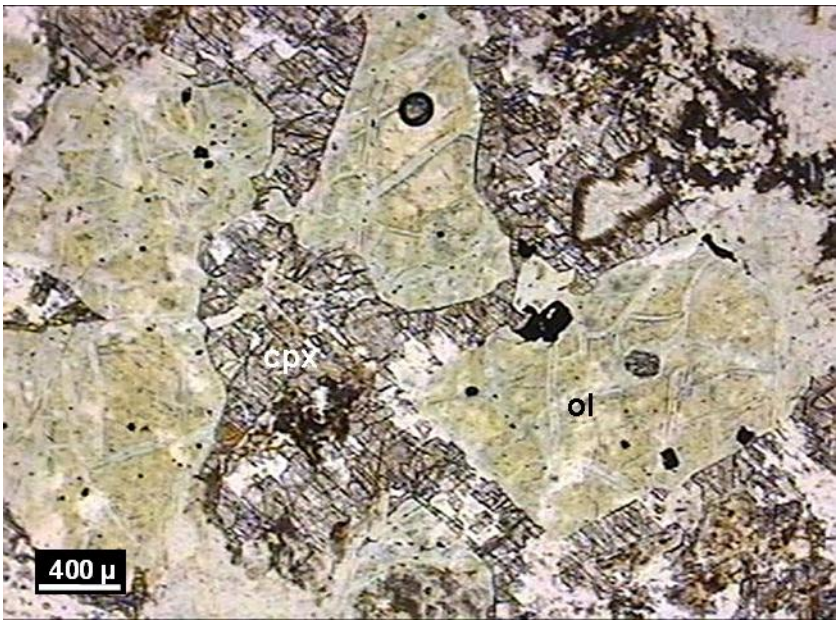

Figure 3.10. Photomicrograph displaying a large Ti-augite enclosing numerous olivine crystals (Sample S18a; 4x PPL, ol: olivine, cpx: Ti-augite).

The ultramafic rock sample primarily constitutes olivine and clinopyroxene minerals. There is no orthopyroxene crystal identified in the section. Although intense serpentinization, it can be deduced that olivine crystals comprise at least approximately 70% of the section and the remaining part is largely composed of clinopyroxene and the other minerals, including opaque and the secondary minerals. In this respect, the sample can be regarded to have a "wherlitic" composition due to the absence of orthopyroxene.

Olivine appear as subhedral to anhedral crystals in the sample. In one part of the section, on the other hand, an olivine crystal of euhedral shape can be observed. As previously mentioned, olivine crystals are totally serpentinized throughout the section. Because of the complete serpentinization, well-developed mesh texture could be recognized (Figures 3.9 to 3.11).

Clinopyroxene occurs as large anhedral crystals and comprises a small amount of the section relative to olivine. It is characterized by brownish color (PPL) and 2nd order interference colors (XPL), reflecting an extinction angle of

appx. 45°. Therefore, these features suggest that the clinopyroxene is of Ti-augite composition (Figures 3.9 to 3.11).

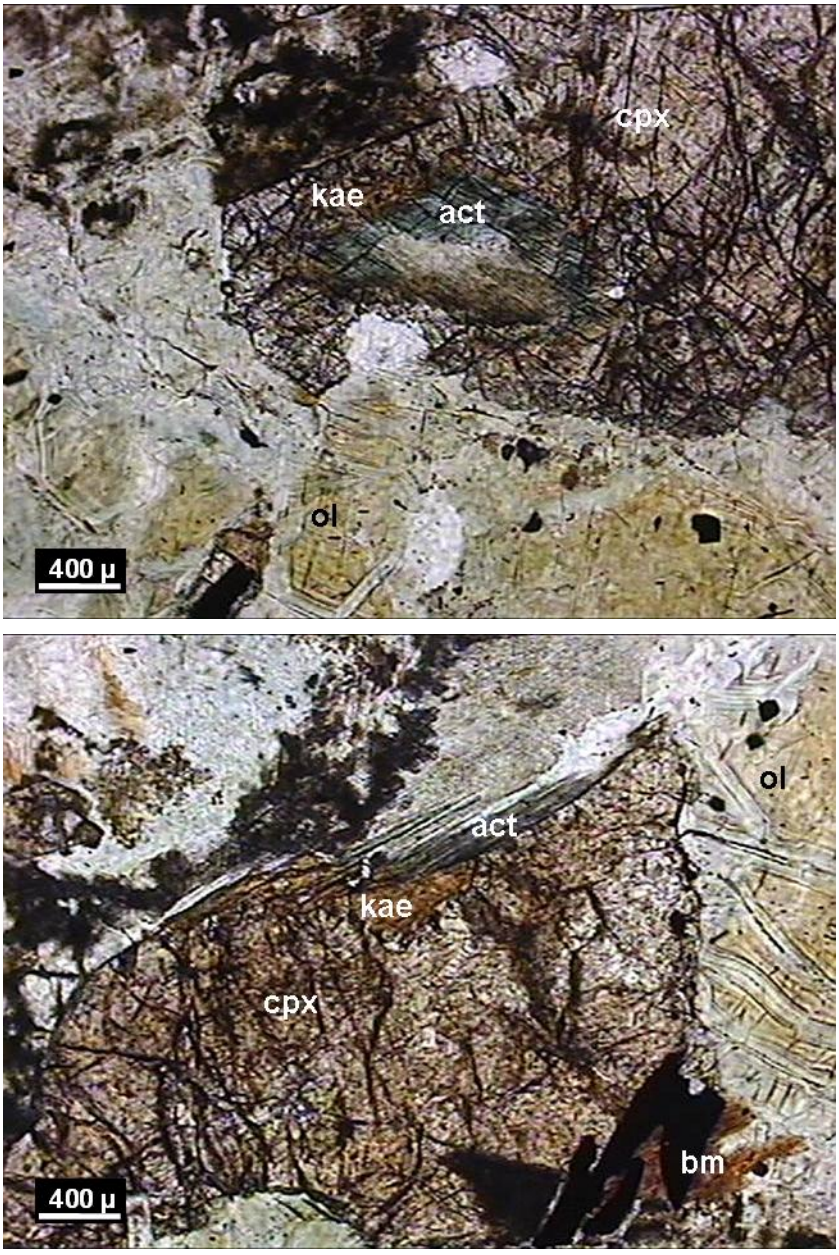

Figure 3.11. Photomicrographs displaying replacement of Ti-augite by actinolite and kaersutite). (Sample S18a; 4x PPL, cpx: Ti-augite, act: actinolite, kae: kaersutite, bm: brown mica, ol: serpentinized olivine).

As a secondary mineral, serpentine is the most important one in the sample. It is distinguished by fibrous and flaky forms and display pale greenish colors in PPL and 1st order grey-green anomalous interference colors in the XPL. The development of vein-type serpentines can also be observed within the olivine. The other secondary minerals include mica and amphibole minerals. The mica minerals in the sample are brown colored and pleochroic and they are characterized by straight extinction and distinctive mottled appearance. At this point, it is not certain whether the micas are biotite or another type of phyllosilicates. However, it is observed that they generally develop around the opaque minerals and also along the rims of both olivine and Ti-augite (Figure 3.11). Another secondary mineral, namely actinolite, occurs nearly in all cases associated with another amphibole group mineral, namely kaersutite (Figure 3.11). The needle-like appearance of actinolite with pale greenish-bluish colors in polarized light and low 2nd order interference colors helps distinguish from the other minerals. It is also important to mention that the actinolite mostly occurs with kaersutite, replacing the primary phases. It sometimes appears in the center surrounded by the latter, or in some cases the situation is the opposite; kaersutite is rimmed by actinolite. However, it is interesting in some cases that under crossed polars both of them extinct at the same time, but obeying the extinction nature of actinolite in the case where it is the central mineral.

3.2.3. Gabbros

The gabbro samples are of dark green colors in hand specimen like the ultramafic one, and similarly they are phaneritic. Their dark-greenish color is evidence of that they have been suffered a degree of hydrothermal alteration.

Although they look like similar to the ultramafic sample, under microscope it is revealed that they are very different in terms of both mineralogy and alteration features. Thin-section examination reflects that they are medium-grained rocks, displaying holocrystalline and porphyritic textures. Furthermore, the influence of hydrothermal alteration is supported by the existence of secondary alteration products.

The primary minerals included in them are clinopyroxene, plagioclase, olivine (probably) and opaque minerals, while the secondary mineral assemblage is composed of chlorite, serpentine, actinolite, prehnite and sericite. In all samples, intense alteration has affected the all primary phases, thus destroying most of the relict features.

The most common constituent in the gabbros is clinopyroxene. It has anhedral and subhedral crystal outlines and recognized by pinkish-brown body color and 2nd order interference colors. Its typical pinkish-brown to brown colors with high degree of extinction angles show that they are Ti-rich augites. However, it can be deduced that they are more diopsidic in composition relative to those of high-Ti basalts, as indicated by the predominant brownish colors rather than pinkish tones. Perfect cleavages can be observed in most of the crystals. Furthermore, sub-ophitic textures seen associated with lath-shaped plagioclases are common (Figure 3.12). Olivine, on the hand, is presumably included in these rocks, since there are intensely serpentinized parts.

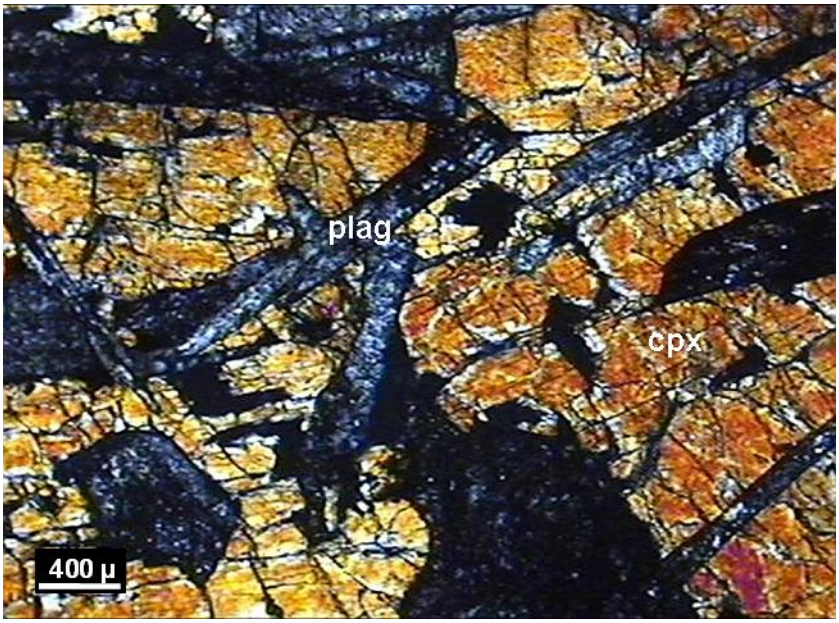

Figure 3.12. Photomicrograph displaying sub-ophitic texture in the gabbros (Sample E4; 4x XPL, cpx: clinopyroxene, plag: plagioclase).

Plagioclase, as being another primary phase, occurs as highly altered crystals with generally subhedral and rarely euhedral outlines. Polysynthetic twinning is commonly observed in partly fresh crystals. It appears that the affect of alteration is relatively higher on plagioclases compared with the Ti-augites such that sericitization is dominant in all plagioclases, sometimes making impossible to observe even their crystal shapes and twinning planes. In addition, there are some parts where replacement of plagioclase by prehnite can be recognized as well.

As mentioned in the beginning, the imprints of low-grade metamorphism on the gabbros are evident by the secondary mineral assemblage. The chlorites are mostly of Fe-rich composition as indicated by anomalous 1st order grayish-blue interference color, however Mg-rich chlorites are also encountered in some places. Prehnite, on the other hand, occur as relatively large crystals and they are distinguished by sheaf-like appearance and 1st order interference colors (Figure 3.13). Sericite is the most common mineral among the alteration products, observed altering the plagioclase. In some parts, sericites which have developed into coarse muscovite flakes can be recognized.

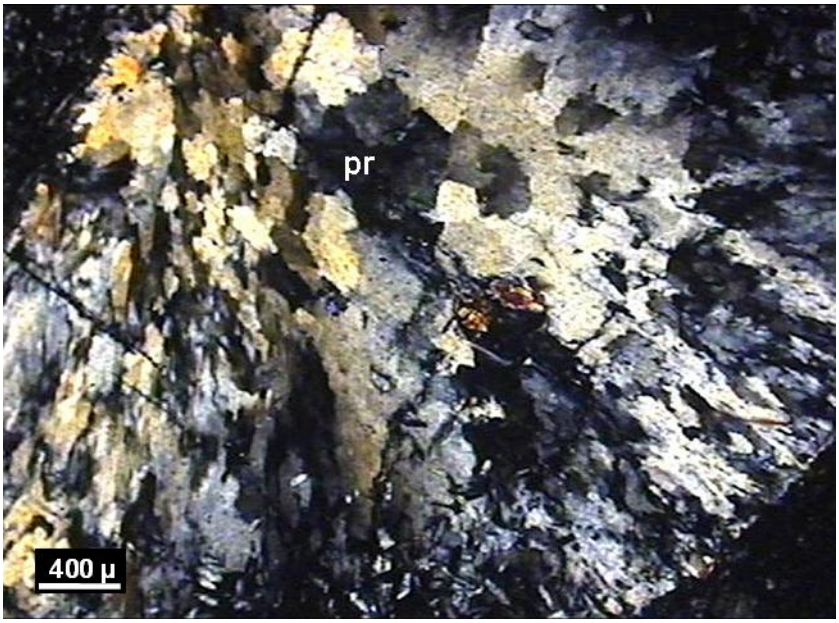

Figure 3.13. Photomicrograph of prehnite in the İmrahor gabbros, indicating presence of metamorphism (Sample E4; 4x XPL, pr: prehnite).

3.2.4. Dyke Rocks (Diabases)

The İmrahor dykes are fine-grained igneous rocks with colors changing between brownish, grayish to dark grayish-green tones in hand specimen. They are micro-phaneritic as indicated fine-grained crystals which can be differentiated by naked eye. Although one of the reason for this variable color content is the affect of surface alteration, the samples reflecting greenish tones indicates that the low-grade alteration is also effective these samples like the previous ones. Due to the fine-grained nature and the effect of hydrothermal alteration, these rocks can be called “diabase” or “dolerite”, respectively depending on U.S. or U.K. terminology.

Microscopically, the diabases are of holocrystalline and equigranular texture. Once again, most of the samples are intensely altered, thus leading to primary phases replaced by secondary ones. The primary mineral assemblage is composed of hornblende, plagioclase, quartz and opaque minerals, while the secondary products are composed of chlorite, actinolite, prehnite, pistacite, zoisite/clinozoisite, sericite and calcite.

Hornblende is the essential mineral phase characterizing these diabases (Figures 3.14 and 3.15). They are distinguished by typical strong green body colors and also 2^{nd} order interference colors. It is observed that they are intensely altered by chlorites. Their oblique extinction varying between 15-20° and the interference colors help differentiate hornblende from chlorite. They occur largely as subhedral prismatic crystals. Rarely, basal sections of hornblende are also observable with well-developed cleavages intersecting at angles of 124-56°.

Plagioclases are the second important constituent in the diabases, occurring generally as subhedral tabular crystals. Polysynthetic twinning is usually observed, whereas Carlsbad and combined types rarely occur. It is observed that the most common alteration recognized on plagioclase is epidotization, where tiny crystals of zoisite/clinozoisite group and pistacite that replace plagioclase are associated together (Figure 3.16). Furthermore, some plagioclases of albitic composition are also found.

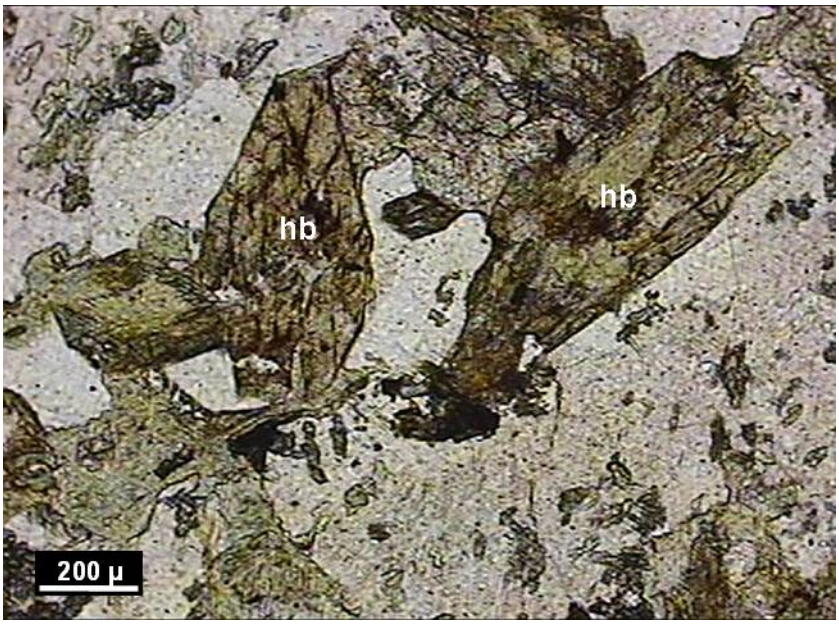

Figure 3.14. Photomicrograph of hornblendes, constituting a substantial part of the diabases (Sample F10; 10x PPL, hb: hornblende).

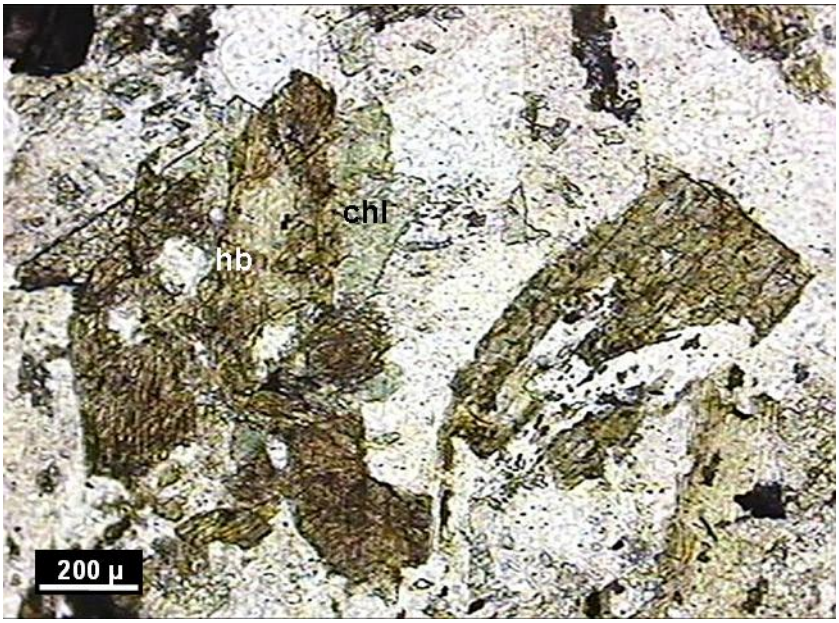

Figure 3.15. Photomicrograph showing replacement of hornblende by secondary chlorite (Sample G5; 10x PPL, hb: hornblende, chl: chlorite).

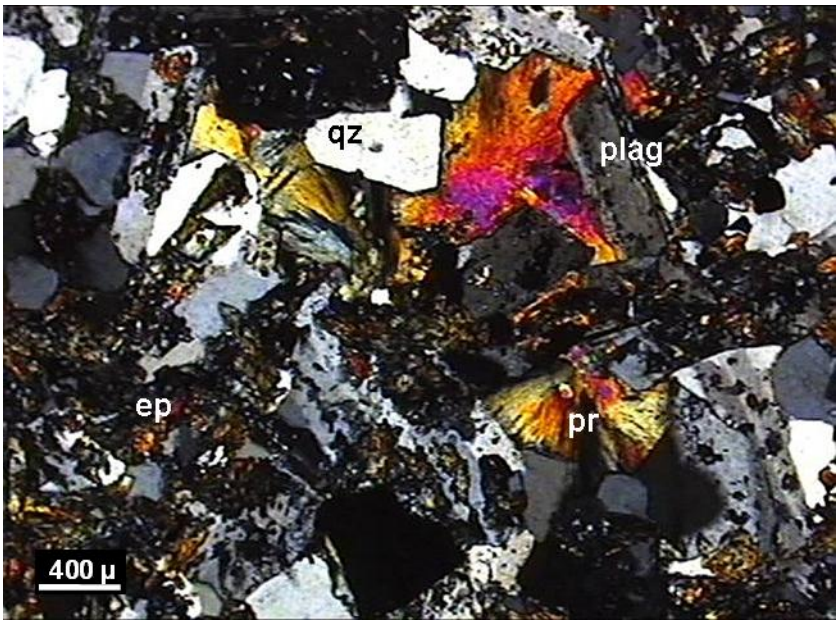

Figure 3.16. Photomicrograph displaying influence of low-grade metamorphism on the diabases (Sample F10; 4x XPL, plag: plagioclase, pr: prehnite, qz: quartz, ep: epidote group).

The most widespread secondary mineral in the diabases is chlorite, replacing nearly most of the hornblende (Figures 3.15 and 3.16). Although most of the chloritization includes partial replacement of hornblende, complete replacements can also be observed (Figure 3.17). In these cases, hornblende appears only as psedomorph of chlorite with anomalous interference colors. Actinolite is not a common secondary phase in the İmrahor diabases. The needle-like development of actinolite, beginning on the margins of hornblende can be identified. Actinolite, in those cases, is distinguished from hornblende by typical relatively low extinction angles (~17°) and slight pleochroism with pale green colors. Epidote group minerals, on the other hand, extensively occur in these rocks. The members, namely zoisite-clinozoisite and pistacite, all intensively replace the plagioclases and generally occur as small anhedral crystals. Prehnite is another alteration product that alters plagioclase. Although, it resembles zoisite/clinozoisite at the first glance, fan-shaped, radiating forms and higher interference colors help differentiate between those minerals (Figures 3.16 and 3.18).

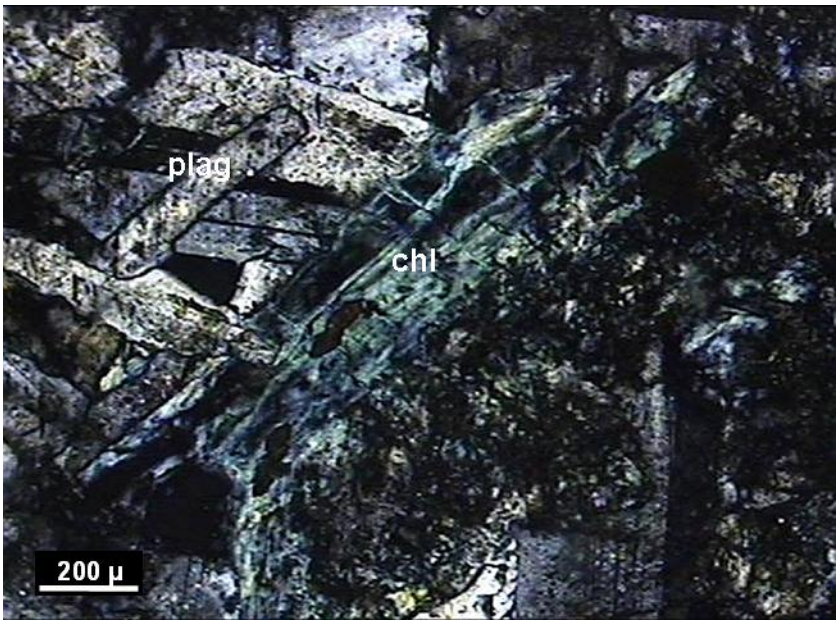

Figure 3.17. Photomicrograph displaying a hornblende pseudomorph after total replacement by chlorite (Sample J5; 10x XPL, chl: chlorite, plag: plagioclase).

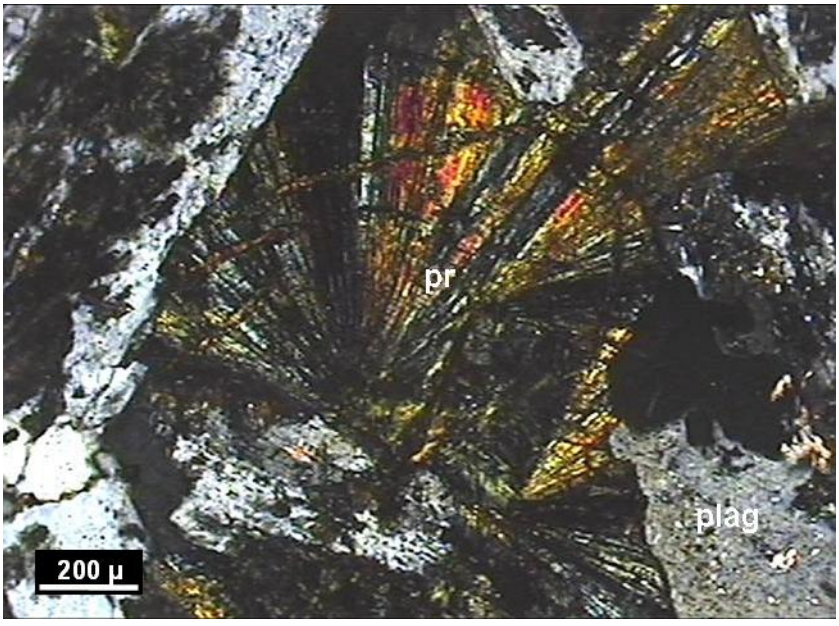

Figure 3.18. Photomicrograph of prehnite, formed after replacing Ca-component of plagioclase (Sample F11; 10x XPL, pr: prehnite, plag: plagioclase).

3.2.5. Clastics

In the İmrahor area, there are also clastic rocks which are of widely varying size and type. Petrographic examination also reveals that these clastics actually comprise both metamorphic and incipiently metamorphic ones. It is sometimes hard to say in hand specimen whether the clastic rock sample have undergone metamorphism or not, but under microscope they are clearly differentiated. As mentioned above, the grain size is highly variable, ranging from clay- to gravel-size.

3.2.5.1. Incipiently metamorphic clastic rocks

They usually appear in light-brown colors due to surface alteration, however in relatively fresh samples grayish tones are also recognizable. Blackish colors, although rarely, is possible depending on mineral content.

Sandstones are the most common rock type among the clastic rocks in the study area. They also display uneven grain-size distribution, as reflected by the presence of silty-sandstones to even conglomeratic sandstones. On the other hand, the common type can be regarded as medium-grained size. Sorting is also changeable such that although well sorted sandstones occur, poorly-sorted ones are present as well. In contrast to the textural features explained up to now, the roundness of grains is not widely variable as they consist mostly of angular grains.

These clastics are represented by both mineral and rock fragments. Their matrix similarly includes both components. It should be noted that rock fragments constitutes a substantial part of the sandstones, therefore they can be called “greywackes”. However, some samples comprise considerable amount of feldspar and thus such arkosic sandstones also occurs within these clastics.

Mineral fragments include quartz, plagioclase, K-feldspar and muscovite. Quartz is the most common constituent among them and it distinctively displays undulatory extinction, indicating the effect of strain on the quartz crystals. In some parts, it exhibits evidences of incomplete recrystallization

where it is divided into many domains with sutured grain boundaries. Plagioclase is the other essential mineral fragment in the sandstones, occurring generally as subhedral crystals (Figure 3.19). Mostly polysynthetic twinning, and less commonly Carlsbad and combination of the two are observable. K-feldspar rarely contains exsolution lamellae of plagioclase, forming perthitic texture. It is recognized that both plagioclase and K-feldspar are largely affected by sericitization. Muscovite, on the other hand, is infrequently present as a mineral fragment.

In terms of rock fragment content, various types of rock can be identified. Clastic and metamorphic rock fragment are the most encountered ones, whereas volcanic fragments less commonly exist. Among metamorphic types, quartzites are easily recognizable, including lots of recrystallized quartz grains with extending crystal outlines. Schist fragments are seldom present; however it is observed that they are of pelitic origin as indicated by extensive quartz crystals alternating with muscovites. Furthermore, chert is frequently identified as a rock fragment and can be distinguished by the microcrystalline quartz crystals it contains. Sandstone and shale are also another rock fragments recognized in these greywackes (Figure 3.19).

3.2.5.2. Metaclastic rocks

Metagreywackes, unlike their incipiently metamorphosed equivalents, are variably colored. They appear as black, brownish, dark grey and greenish rocks in hand specimen. Since, they display similar textural features to earlier ones; they will not be repeated here. It can be identified that the effect of metamorphism and deformation is more apparent (Figures 3.20 to 3.22); especially in the fine-grained members where the clasts are elongated displaying an ellipsoidal shape and foliation is very lucid (Figure 3.20).

Under microscope, the influence of metamorphism can be more clearly understood. Widespread mica (white mica) development is very apparent at the first glance such that there are lots of mica flakes that forms parallel or sub-parallel to the direction of foliation. Pressure shadows, developing around the clasts, is another feature that indicates the presence of metamorphism.

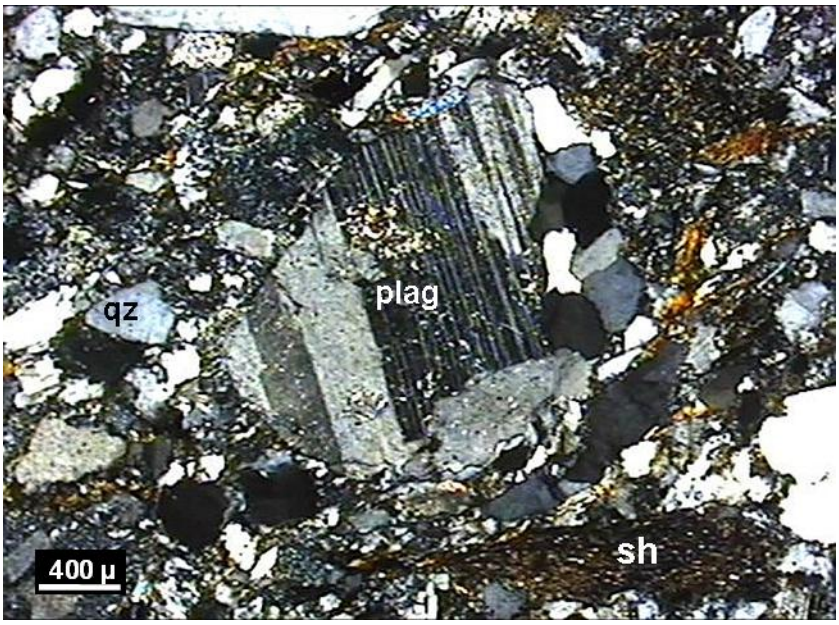

Figure 3.19. Photomicrograph of plagioclase and shale fragment in the İmrahor clastics (Sample H20; 4x XPL, plag: plagioclase, qz: quartz, sh: shale).

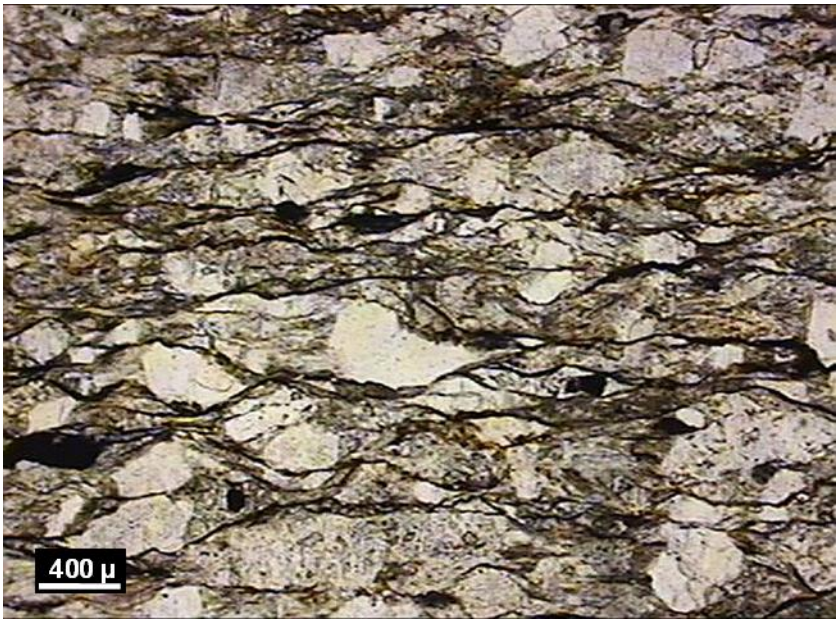

Figure 3.20. Photomicrograph illustrating elongated clasts in the metagreywacke in response to dynamo-thermal metamorphism (Sample I14; 4x PPL).

Figure 3.21. Photomicrograph displaying deformation as reflected by bending in mineral grains. Note also undulose extinction and recrystallization on quartz (Sample J46; 4x XPL, qz: quartz, cc: calcite).

Figure 3.22. Photomicrograph showing imprints of dynamo-thermal metamorphism on the metagreywacke. Notice the sutured boundaries between quartz grains, indicating intermediate stages of recrystallization (Sample K1c; 10x XPL, qz: quartz).

In terms of mineral and rock fragment content, metagreywackes reflect similar assemblages with the non-metamorphic ones. Quartz is the dominant mineral fragment, whereas feldspars (largely plagioclase) occur in fewer amounts. However, in contrast to incipiently metamorphic rocks, in one sample, epidote - clinozoisite neoformations were identified. Some metaclastic samples are very distinct owing to the considerable existence of clinopyroxene crystals which are probably of diopsidic composition (Figure 3.23). This may indicate that the source area for which the clinopyroxene-bearing meta-clastics have been derived should be different than those without pyroxene. Infrequently, the granular development of quartz crystals having polygonal grain boundaries is also observable, indicating again a later stage of metamorphism. Rock fragments, as mentioned above, are of similar types, including cherts, volcanic and metamorphic rocks and clastics (Figure 3.24).

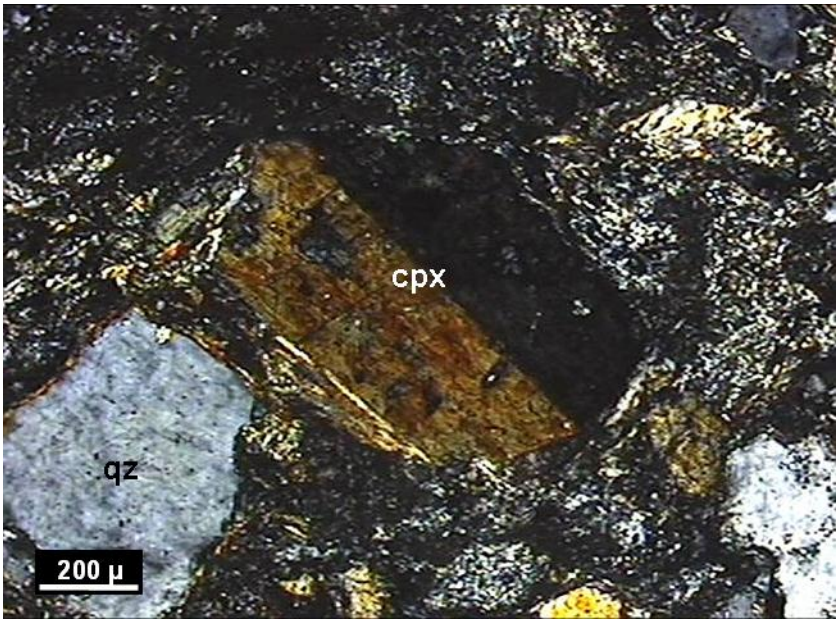

Figure 3.23. Photomicrograph displaying twinning on a clinopyroxene phenocryst in metagreywackes (Sample J44; 10x XPL, cpx: clinopyroxene, qz: quartz).

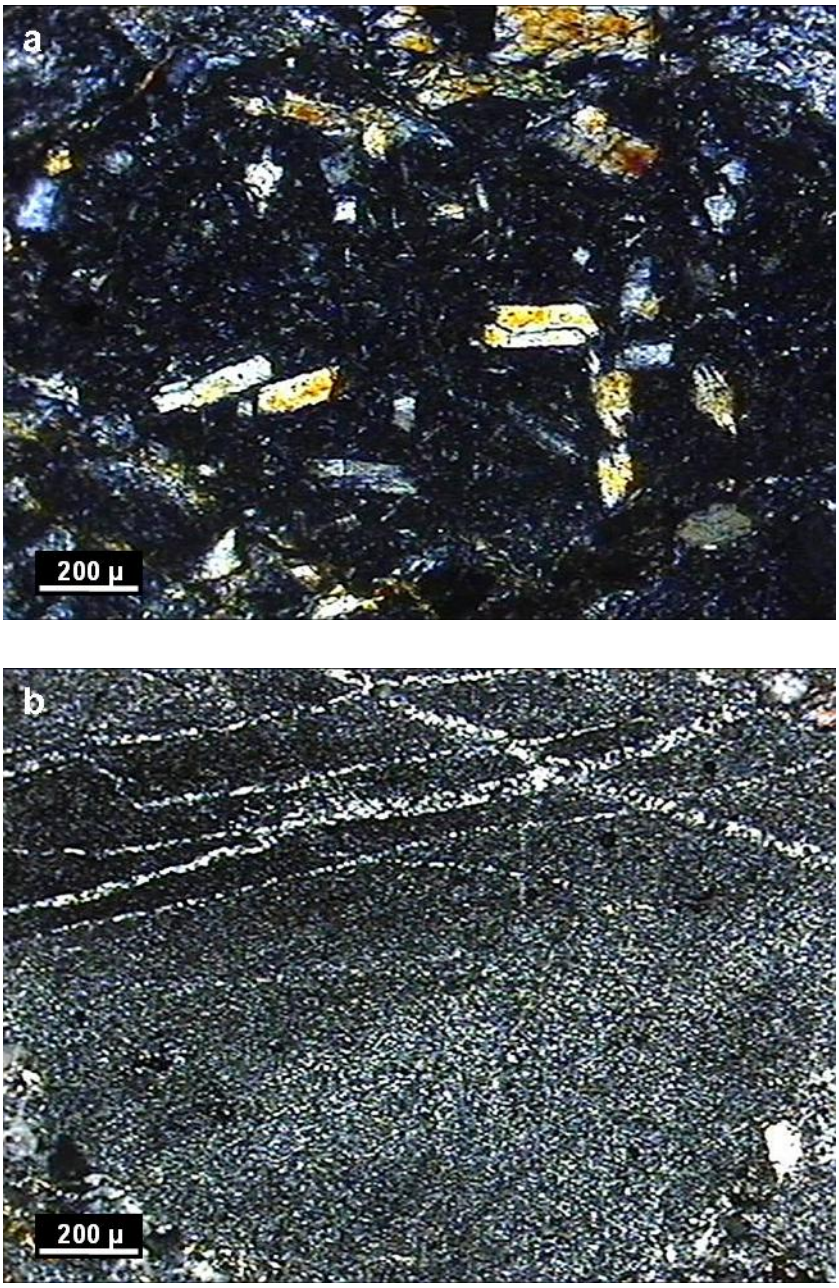

Figure 3.24. Photomicrograph of rock fragments in the metagreywackes; volcanic rock fragment (a, Sample J44; 10x XPL), chert fragment (b, Sample K1d; 10x XPL).

As the fine-grained constituent of the meta-clastics, slates are greenish-grey colored on their alteration surfaces, while the fresh parts reflect black colors. The slaty cleavages can be clearly observed in hand specimen. In relatively less deformed parts, it is recognized that only S_1 cleavage has developed on

the slates, however those found in parts with higher deformation display both S_1 and S_2 cleavage planes. It is observed that S2 cleavage intersects the previous one (S1) at relatively right angles (Figure 3.25).

Muscovite is the most common constituent in the slates, developing along the cleavages. The other minerals observed are quartz, chlorite, clay minerals, epidote (pistacite) and opaque minerals.

3.2.6. Metabasic Rocks with HP/LT Minerals

In the study area, metabasic rocks other than hydrothermally altered basalts also occur with imprints of high-pressure metamorphism. These metabasics are very distinctive in terms of both mineralogy and texture. They have dark-purplish colors in hand specimen, showing well-developed schistosity planes.

Thin-section examination indicates that they should have been derived from a volcanic rock due to the presence of amygdaloidal parts. These metabasics includes a mineral assemblage of Na-amphibole, chlorite, epidote (pistacite), calcite, quartz and opaque minerals. The presence of Na-amphibole is the evidence of elevated pressure during their formation.

Chlorite is the most abundant mineral characterizing these high-pressure rocks. They appear as flaky minerals in the samples and they are of Mg-rich composition as reflected by brownish anomalous interference colors. Na-amphibole, on the other hand, is not common as chlorite. It is easily distinguished by characteristic lilac to deep blue colors with strong pleochroism (Figure 3.26). It is observed that the interference colors are masked by strong body color and characterized by very small extinction angles of about 5°. It occurs usually as tiny prismatic crystals with euhedral crystal outlines, displaying a nematoblastic relationship as indicated by their near sub-parallel arrangement with respect to foliation planes. Calcite is present in substantial amounts, filling the vesicles and veins. Quartz is the least abundant and it occurs together with calcite. Opaque minerals, however, are very commonly recognized, usually appearing around the vesicles filling the spaces among them.

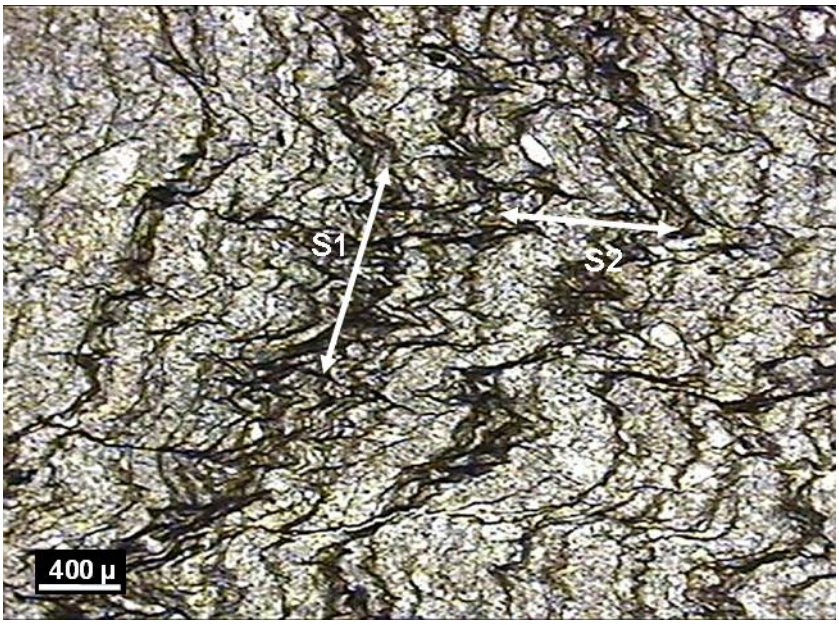

Figure 3.25. Photomicrograph displaying crenulation cleavages in the slaty rocks of İmrahor (Sample J3; 4x PPL, S1: primary foliation plane, S2: secondary foliation plane which intersects the former nearly at right angles).

Figure 3.26. Photomicrograph displaying development of Na-amphibole, indicating high pressure metamorphism (Sample J9; 10x XPL, Na-amp: Na-amphibole, chl: chlorite, cc: calcite).

3.3. Hasanoğlan Area

The Hasanoğlan lavas are recognized by their blackish, dark blue and dark reddish colors in hand specimen, displaying aphanitic textures. The Hasanoğlan extrusives, like the other samples, have been variably altered due to low-grade metamorphism, as indicated by their metamorphic minerals. Amygdaloidal texture is very distinctive for these basalts. Intense presence of vesicles, which are of variable sizes, can be easily identified and they are filled by several secondary minerals.

The Hasanoğlan basalts display microcrystalline and porphyritic textures under microscope, resembling those of Ortaoba and Kadirler. If the metamorphism is considered, these basalts are more akin to the Kadirler extrusives, since actinolite could not be observed amongst the secondary mineral phases.

The Hasanoğlan extrusives primarily include plagioclase, clinopyroxene, olivine and opaque minerals. The secondary phases, on the other hand, are chlorite, pistacite, zoisite/clinozoisite, calcite, serpentine, iddingsite and quartz.

Plagioclases, once again the most common mineral phase, occur both as phenocrysts and microlites in groundmass. They are generally characterized by subhedral crystal outlines. It can be recognized that nearly all plagioclases are replaced by secondary albite, and polysynthetic twinning is sometimes recognizable. Plagioclase minerals form intergranular texture with interstitial clinopyroxene and opaque crystals. In relatively less-altered samples, subophitic texture can be observed. Furthermore, seriate texture is obviously identifiable in these basalts as well.

Clinopyroxene, as the second important primary phase, displays subhedral to anhedral outlines and it is present both as phenocrysts and microcrysts (Figure 3.27). It is observed in some samples that pyroxenes form clusters, reflecting glomeroporphyritic texture (Figures 3.27 and 3.28). The brownish colors and extinction angles changing around 40° indicates that they are of augitic composition. This is also supported by the presence of augite crystals that exhibits well-defined sector zoning (Figure 3.29).

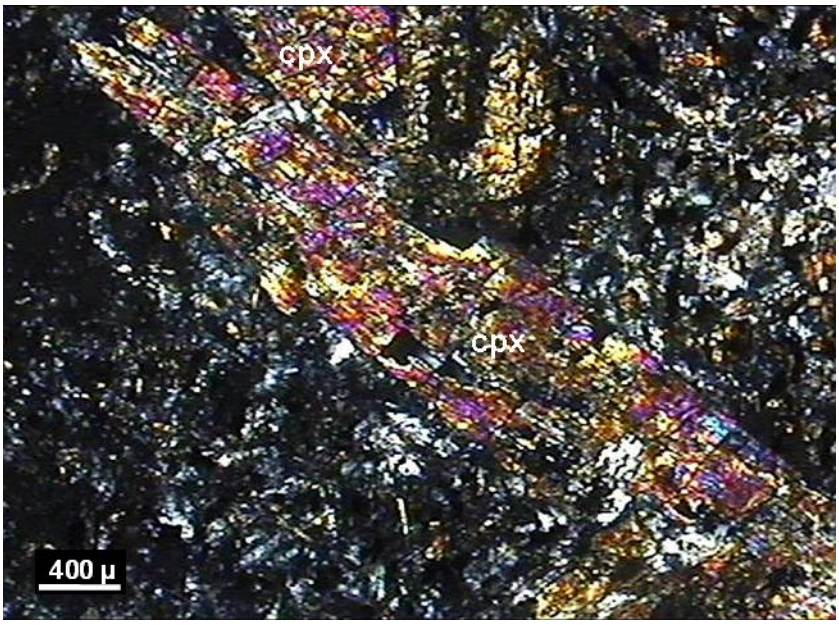

Figure 3.27. Photomicrograph showing cluster of large clinopyroxene phenocrysts included in a highly altered groundmass (Sample HS10; 4x XPL, cpx: clinopyroxene).

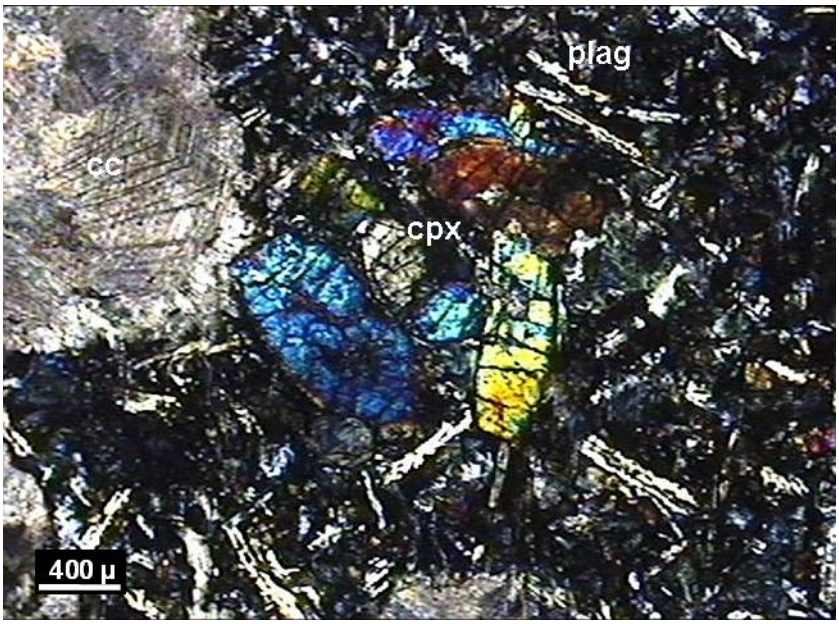

Figure 3.28. Photomicrograph illustrating glomeroporphyritic texture in the Hasanoğlan basalts (Sample H23; 4x XPL, cpx: clinopyroxene, plag: plagioclase, cc: calcite).

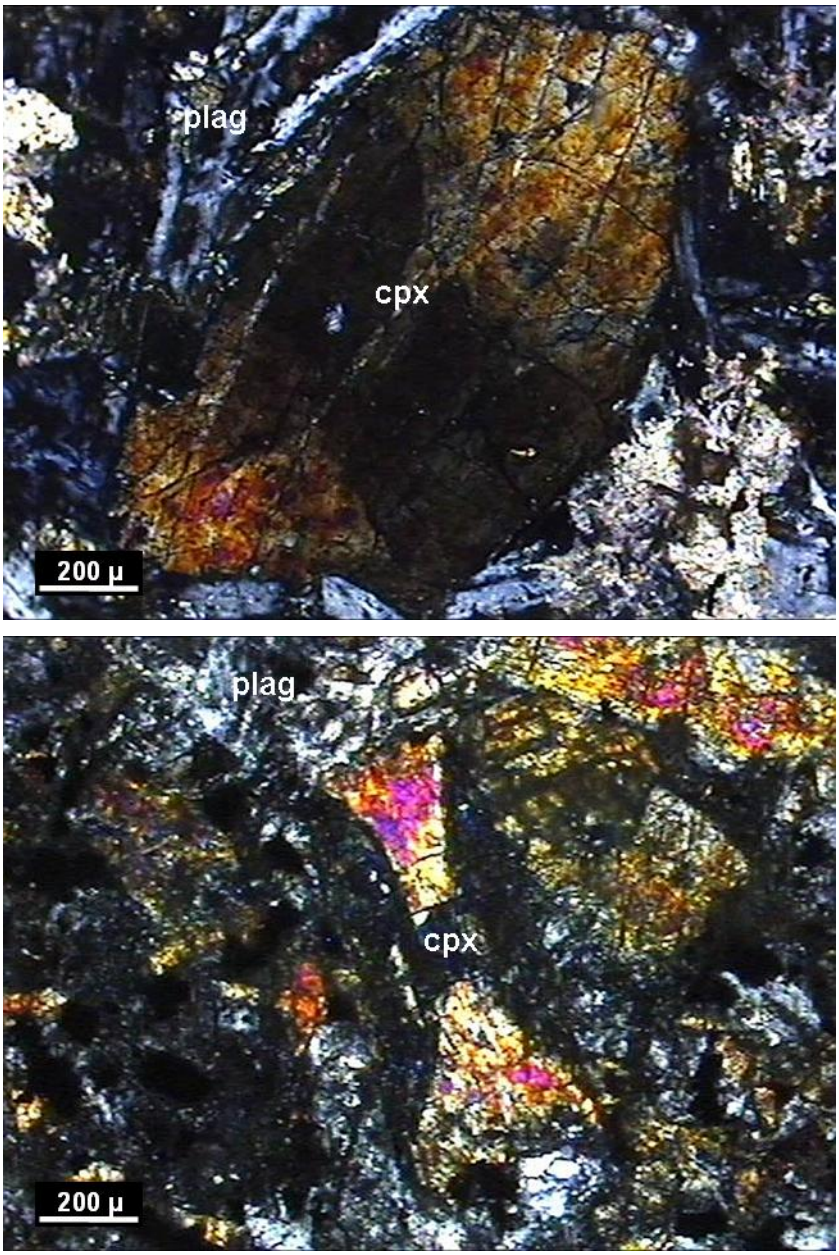

Figure 3.29. Photomicrographs of clinopyroxene phenocrysts displaying sector zoning (hour-glass texture) (Samples HS23 and HS10, respectively; 10x XPL, cpx: clinopyroxene, plag: plagioclase).

Olivine, on the other hand, only occurs as entirely altered phenocrysts. In some parts olivine phenocrysts with euhedral outlines totally replaced by serpentines can be observed.

The secondary phases within the Hasanoğlan lavas are epidote, chlorite, calcite, serpentine and quartz. Epidote group minerals could be regarded as common alteration products characterizing these basalts. Among them pistacite is most encountered one, although zoisite/clinozoisite is also recognizable in substantial amounts in some samples. Chlorite is another alteration product as distinguished by its green color in PPL and anomalous 1st order interference colors. It should be noticed that both Mg- and Fe-rich chlorite occurs in the Hasanoğlan lavas. The Fe-rich chlorites appear as anomalous blue colors, while the Mg-rich can be distinguished by their dark brownish colors. Calcite, on the other hand, mostly fills the vesicles and veins. Chlorite can also be observed as a vesicle filling mineral as well. The vesicles are mainly filled by calcite, however, in some cases Fe-oxides and calcite are observed together as the vesicle filling minerals.

Some of the Hasanoğlan samples reflect intense opaque mineral formation, covering substantial area of the sample. Similar to the Kadirler basalts, many leuxocenes are present in these extrusives as identified by their well-developed skeletal and dentiritic forms. Thus, the Hasanoğlan basalts comprise ilmenites replaced later by leucoxene.

It should be noted that some of the Hasanoğlan basalts is very similar to those of Kadirler in the terms of high degree of calcitization such that it is sometimes not possible to find any preserved primary mineral phases both as phenocrysts and in groundmass. The presence of lots of vesicles filled by secondary minerals is another common point between these two basalts.

3.4. Ortaoba Area

The rock units in the Ortaoba Unit are dominated by metamorphosed basic volcanic rocks that are characterized in the handspecimen by their dark greenish color and aphanitic textures. As indicated by their greenish colors, the Ortaoba basalts were hydrothermally altered. These metabasalts; on the other hand, do not display any vesicular or amygdaloidal texture, thus indicating their generation in relatively inner parts of the lava flow.

Under microscope, the Ortaoba basalts are holocrystalline, microcrystalline and porphyritic. The presence of low-grade metamorphism could be better understood in the thin-sections, such that primary mineral phases and textures are strongly overprinted by secondary minerals (Figures 3.30 to 3.34) and in some of the sections, only secondary phases are present and no relict texture is recognized.

The Ortaoba volcanics primarily consist of clinopyroxene, plagioclase and opaque minerals, while secondary phases include actinolite, chlorite, pistacite, zoisite/clinozoisite group, calcite and quartz. Based on this mineralogical assemblage, these spilitic basalts could be characterized by low-grade metamorphism. In addition, the considerable presence of quartz and calcite may indicate the influence of late-stage low temperature fluids.

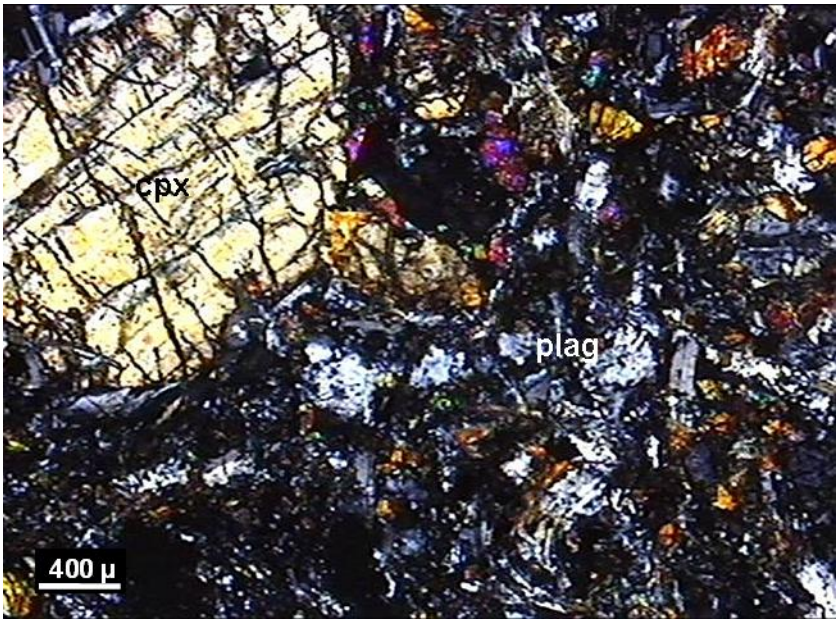

Figure 3.30. Photomicrograph showing highly altered nature of the Ortaoba extrusives (Sample OO19; 4x XPL, cpx: clinopyroxene, plag: plagioclase).

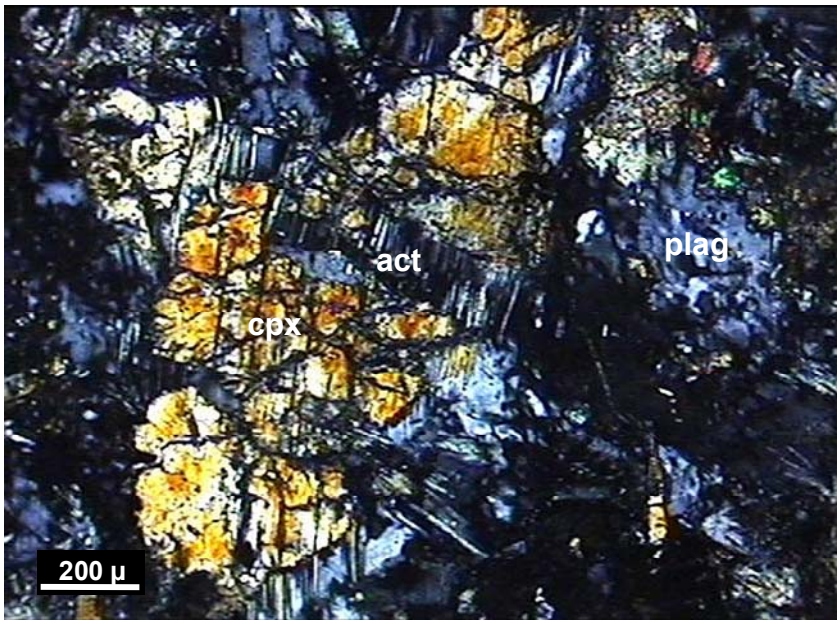

Figure 3.31. Photomicrograph showing the replacement of clinopyroxene by needle-like actinolite crystals (Sample OO19; 10x XPL, cpx: clinopyroxene, plag: plagioclase, act: actinolite).

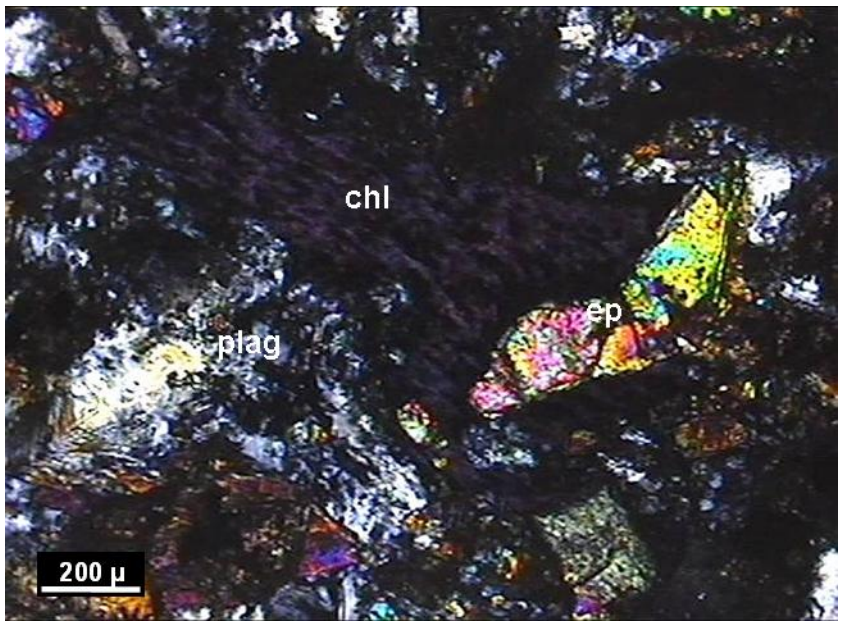

Figure 3.32. Photomicrograph displaying effects of low-grade metamorphism on the Ortaoba basalts (Sample OO19; 10x XPL, chl: chlorite, plag: plagioclase, ep: epidote).

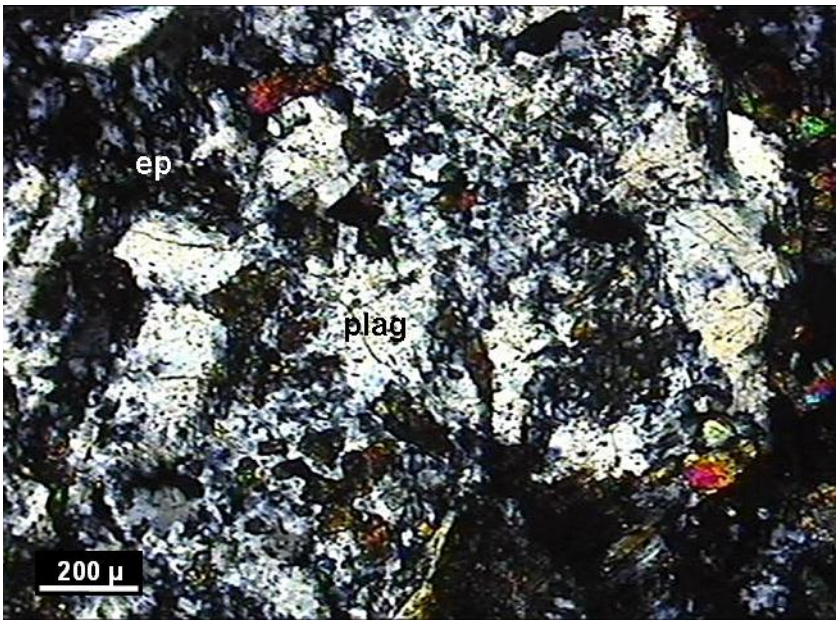

Figure 3.33. Photomicrograph of plagioclase phenocryst which is strongly overprinted by alteration products due to low-grade metamorphism (Sample OO19; 10x XPL, plag: plagioclase, ep: epidote group).

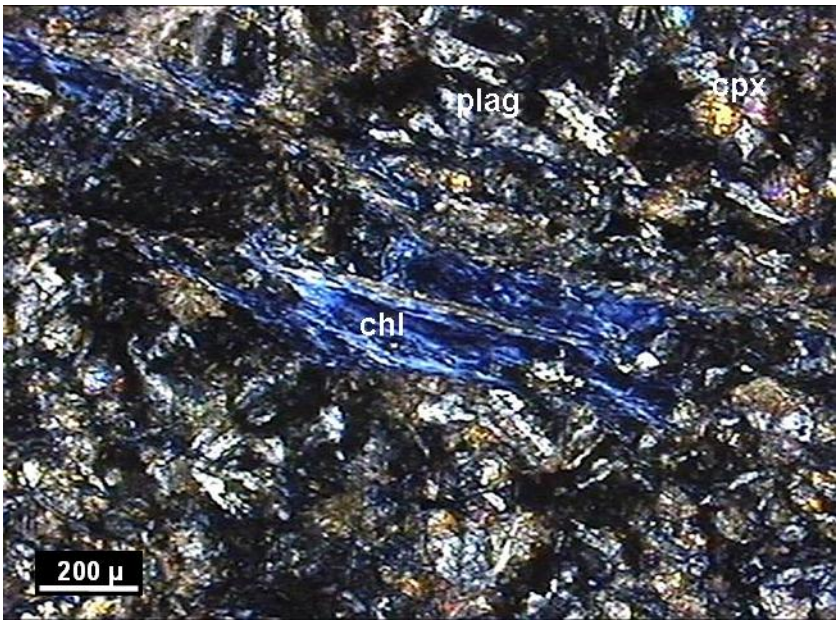

Figure 3.34. Photomicrograph illustrating vein-filling Fe-rich chlorite in the Ortaoba basalts (Sample OO12; 10x XPL, cpx: clinopyroxene, plag: plagioclase, chl: chlorite).

Plagioclases are present in relatively fresh samples as phenocrysts, micro-phenocrysts and lath-shaped microlites in the groundmass and they generally exhibit subhedral to anhedral crystal outlines. Due to hydrothermal alteration, nearly all primary plagioclase phases are replaced mainly by secondary albite, leading to the identification of plagioclase phenocrysts unlikely (Figures 3.30 to 3.33). It is also possible to observe rare polysynthetic twinning and weak zoning displayed by relatively well-preserved plagioclase laths in some of the thin-sections. Unfortunately, intense alteration made the Michel-Levy method inapplicable for the Ortaoba basalts, so compositions of the primary plagioclases could not be determined. Relatively preserved sections unravel that plagioclases display mostly intergranular and seriate texture; on the other hand, sub-ophitic texture characterized by lath-shaped plagioclase crystals partly enclosed by clinopyroxene crystal could be regarded as another texture observed in these metabasalts (Figure 3.34 and 3.35). Albitization is the most common alteration feature recognized on the plagioclases. Furthermore, calcitization and epidotization can be considered as the other alteration events.

Pyroxene, another primary mineral phase in the Ortaoba lavas, is mostly observed in subhedral and anhedral forms and occurs both as phenocrysts and microcrysts in the groundmass. They exhibit a fractured appearance due to alteration and generally the cleavages are hardly identifiable or not recognized (Figures 3.30, 3.31 and 3.35). In partly fresh samples, it can be noticed that clinopyroxene phenocrysts forms clusters, displaying glomeroporphyritic texture. On the other hand, small crystals constitute intergranular texture together with plagioclase laths in the groundmass. Optical identification reveals that there are two types of pyroxene in these metabasalts. The first one is Ti-augite, which is characterized by pinkish-brown color in the plane-polarized light (PPL) and extinction angles of approximately 44°. However, the other type, diopsidic augite is colorless to pale-greenish in PPL and gives extinction angles of about 35-40°. It is observed that pyroxenes are usually altered to actinolite, chlorite and calcite.

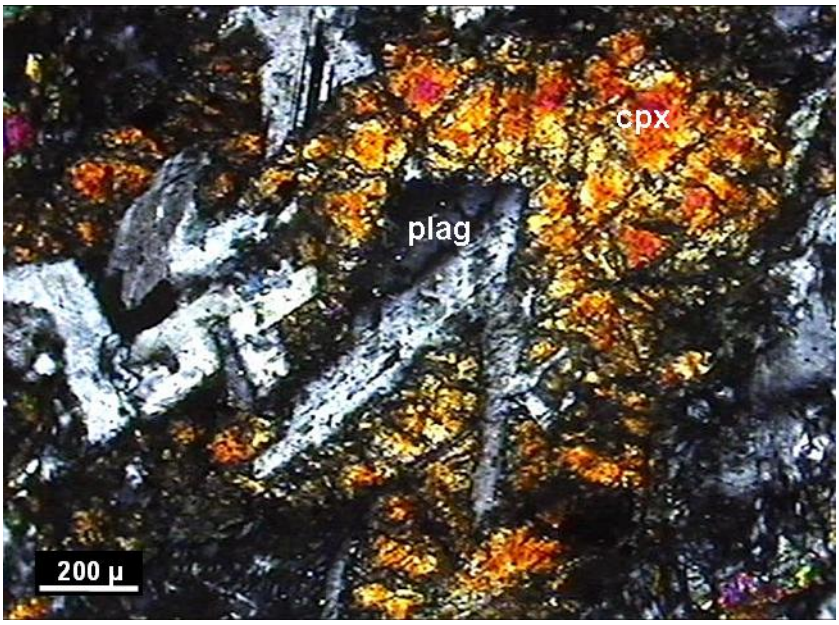

Figure 3.35. Photomicrograph displaying sub-ophitic texture in the Ortaoba basalts (Sample OO-19; 10x XPL, cpx: clinopyroxene, plag: plagioclase).

As a secondary mineral, actinolite appears as needle-like crystals surrounding pyroxene (Figure 3.31) and also inside plagioclases as tiny crystals. They are identified by their greenish color in plane polarized light (PPL) and 2nd order birefringence under crossed polarized light (XPL) as well as typical oblique extinction with approximately 15°. As epidote group minerals, pistacite is observed replacing plagioclase in most cases (Figure 3.33); on the other hand zoisite/clinozoisite group is also identified. The latter can be easily differentiated from pistacite by their anomalous 1st order extinction colors. Calcite is present as both replacing primary mineral phases and also infilling material in many veins. It must be noted that calcitization in some samples is of considerable degree such that primary phases are entirely replaced by calcite and no phenocrysts are observable. Chlorite like calcite occurs in veins and replaces sometimes pyroxenes. The anomalous grayish to bluish (Berlin blue) colors in XPL reveals that it is of Fe-rich composition (Figure 3.34). However, Mg-rich chlorite is also very common in some of the sections as indicated by the very dark purple and brownish interference colors (Figure 3.32).

Numerous actinolite needles together with anhedral epidote crystals developing within plagioclases recognized in the certain Ortaoba samples is a good example for replacement relationships resulted from low-grade metamorphism. Such relationships are also identified on Ti-augites such that they are sometimes totally rimmed by actinolite crystals or the alteration on the augite crystal is very intense that the actinolites develops through weak planes, surrounding the entire structure of augite (Figure 3.31). There are also signatures that display more advanced stages of alteration where only a small part of augite crystal survives and it is entirely confined by alteration products, including needle-like actinolites, Mg-rich chlorite and calcite. Note that the calcite represents a later stage event related to low temperature fluids.

The dominant presence of veins is another prominent feature of the Ortaoba basalts. It is observed that they are filled by various secondary minerals, including calcite, Fe-rich chlorite and quartz. Calcite appears as the predominant mineral among them and usually constitutes substantial part of the veins, occurring with minor amount of Fe-rich chlorite and quartz. It could be observed that calcite is present in the innermost part of the vein, while chlorite and quartz forms the outer parts. Furthermore, it is also possible to see some veins where the predominant mineral is chlorite, and it is associated with minor amount of calcite.

3.5. Kadirler Area

The petrographically studied basic volcanic rocks of Kadirler are nearly black-colored (dark tones of grey) in hand specimen. These are pillow lavas, characterized by aphanitic textures and dominant presence of degassing structures (amygdales) filled by mainly calcite (Figure 3.36). Their blackish appearances indicate that the Kadirler basalts were not largely affected by low-grade hydrothermal alteration compared to the Ortaoba volcanics. Based on the intense existence of amygdales may display that they characterize rather outer parts of the pillow lavas during their generation.

Figure 3.36. Photomicrograph illustrating amygdaloidal texture in the Kadirler lavas (Sample K2a; 4x PPL).

In thin-section, these basalts exhibit porphyritic, holocrystalline and microcrystalline textures. The influence of alteration on the Kadirler volcanics is certainly very intense such that sometimes it would not be possible to observe any phenocrysts. Olivine is recognized only as pseudomorphs, replaced entirely by serpentine and calcite. Alteration is largely due to secondary calcite which occurs both replacing primary mineral phases and also filling vesicles (Figures 3.37 and 3.38).

Primary mineral phases characterizing the Kadirler basalts can be considered as plagioclase, clinopyroxene and olivine as well as opaque minerals. The secondary minerals; on the other hand, include calcite, epidote, chlorite, sericite, serpentine and quartz. According to this mineral assemblage, these basalts could be interpreted as the products of low-grade metamorphism.

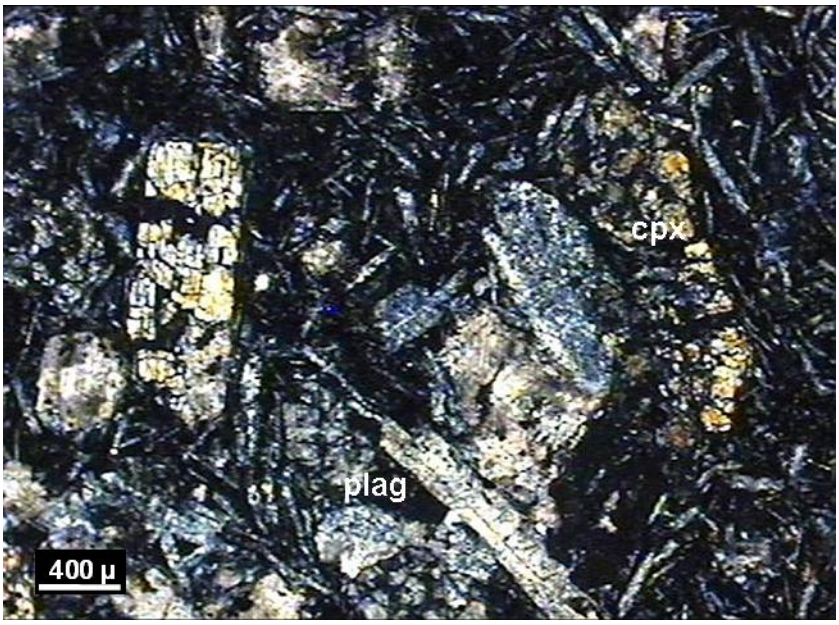

Figure 3.37. Photomicrograph showing the effects of severe calcitization on both phenocrysts and groundmass (Sample K4b; 4x XPL, cpx: clinopyroxene, plag: plagioclase).

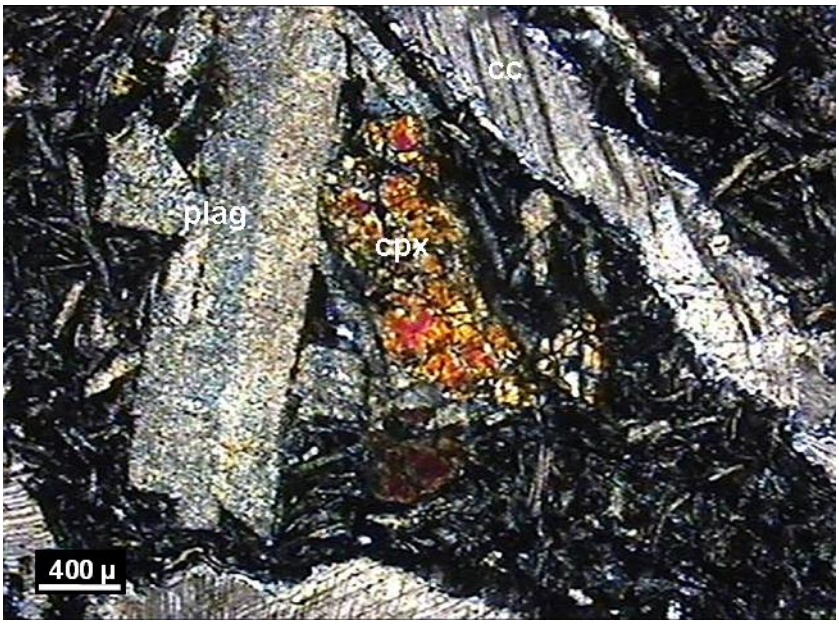

Figure 3.38. Photomicrograph displaying entire replacement of plagioclase phenocrysts by sericite and calcite. Also included a relatively preserved clinopyroxene and a thin vein filled by calcite (Sample K4b; 4x XPL, cpx: clinopyroxene, plag: plagioclase, cc: vein-filling calcite).

Plagioclase is generally observed as microlites in the groundmass and more rarely as phenocrysts. They are mostly of subhedral crystal shapes. As mentioned above, intense alteration has influenced nearly entire primary assemblage, leading Na-rich plagioclase (albite) to be formed by losing their Ca-rich compositions. Thus, the determination of primary plagioclases could not be performed. It can be uncommonly recognized weak polysynthetic twinning and zoning due to strong calcitization and sericitization. Plagioclase minerals mostly exhibit intergranular texture in which the spaces between them are filled with clinopyroxene microcrysts and skeletal-dentritic opaque minerals (probably leucoxene after ilmenite). Less commonly seriate texture including variable sizes of plagioclase and clinopyroxene crystals, and sub-ophitic texture were identified in some of the thin-sections. Notice that intense sericitization leads to plagioclase minerals exhibit a spongy appearance. Furthermore, it is possible in some samples to notice plagioclases entirely replaced by sericite minerals.

The other primary phase characterizing these basalts is clinopyroxene, which appear as subhedral to anhedral crystals, occuring both as phenocrysts and microcrysts in the groundmass. However, pyroxene crystals in the groundmass are sometimes weakly perceptible owing to considerable influence of alteration. Since pyroxene is more resistant to alteration, some unaltered clinopyroxene crystals with well-developed cleavages could be identified. Their slightly-brown appearances with extinction angles ranging around 40° reveal that they are diopsidic augites. Rarely, it is recognized piles of clinopyroxenes which represent glomeroporphyritic texture (Figure 3.39). Clinopyroxenes like plagioclase crystals are largely affected by calcitization, so it is possible to observe pyroxene pseudomorphs replaced entirely by calcite.

Olivine is the least abundant amongst the primary phases. It occurs as phenocrysts, usually with euhedral shapes. However, their entire replacement by serpentine and calcite leads only olivine pseudomorphs to be observed. They are sometimes replaced by totally by serpentine, or in some cases serpentine and calcite both replaces the structure of olivine.

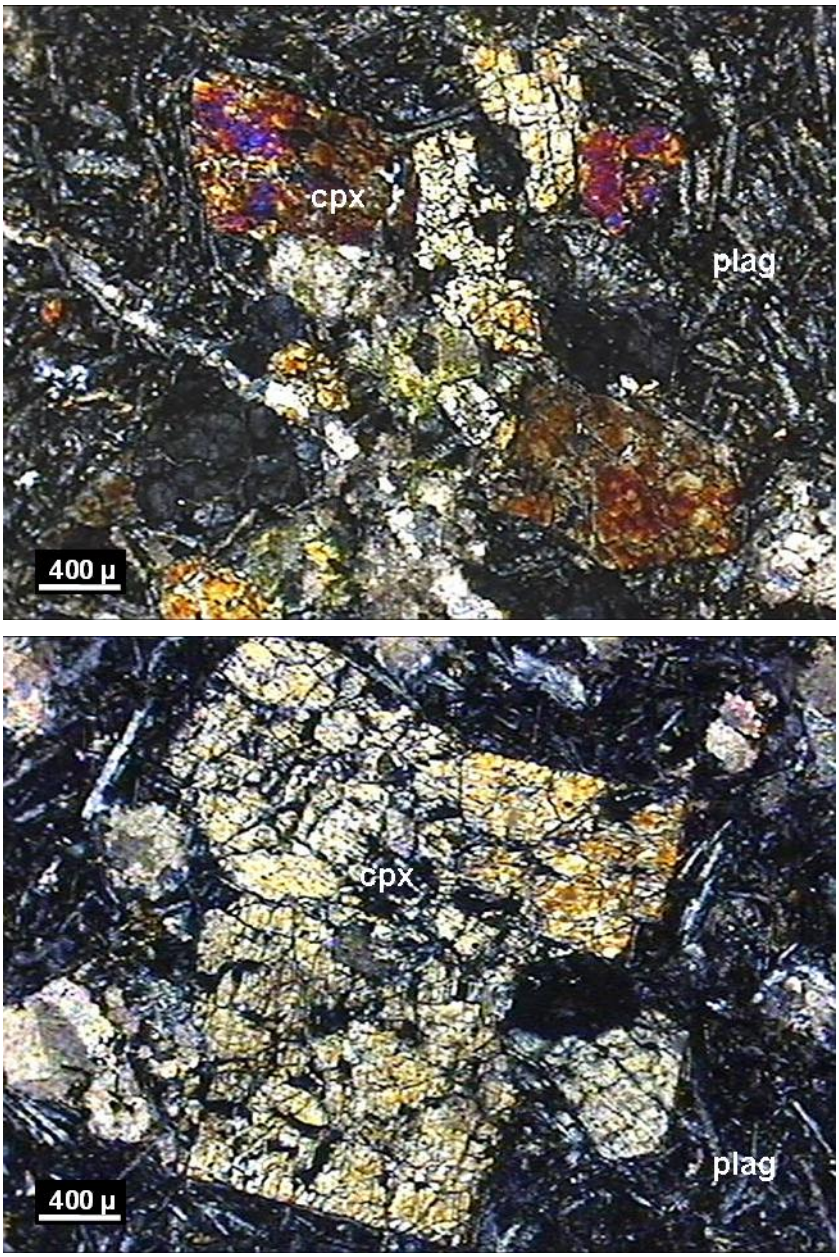

Figure 3.39. Photomicrographs displaying glomeroporphyritic texture in the Kadirler basalts (Samples K4c and K4h, respectively; 4x XPL, cpx: clinopyroxene, plag: plagioclase).

As denoted in the beginning, the Kadirler basalts comprise substantial amount of vesicles all filled by various secondary minerals, including calcite, chlorite and less amount of quartz. Calcite is the predominant secondary mineral among them, filling the vesicles and also veins. They can be easily distinguished by their very high interference colors. They exhibit usually typical rhombohedral twinning and cleavage. Chlorite, on the contrary to calcite, is not encountered inside the veins. Instead, it is present in the vesicles and also in groundmass. When chlorite occurs in the vesicles, it takes place in the outer margin, surrounding calcite which occurs at the center. In the groundmass, however, chlorite commonly replaces mafic minerals. Their greenish-blue anomalous interference colors in XPL signify that these are most probably of Fe-rich composition. Serpentine is less commonly observed, replacing olivine crystals and identified by its fibrous, radial forms and greenish to grayish-blue anomalous interference colors. As epidote group minerals, the Kadirler lavas only comprise pistacite, occurring largely as small crystals in the groundmass. Sericite is observed as numerous tiny crystals, replacing the plagioclases. In some cases, due to intense calcitization sericite crystals can be overlooked. It should be noticed that the groundmass comprise lots of needle-like, skeletal and dentritic opaque minerals. Such crystal shapes displayed by these opaque minerals indicates that they are leucoxenes formed after ilmenite.

CHAPTER 4

GEOCHEMISTRY OF BASIC IGNEOUS ROCKS

4.1. Introduction

In this chapter, 32 representative basic rock samples from the studied areas within the ‘’Karakaya Complex’’ were examined and their geochemical characteristics were interpreted by evaluating inter-element relationships and multi-element variations, using various diagrams based on major and trace elements as well as REE abundances. Consequently, different types of basaltic rocks from different sub-units of the ‘’Karakaya Complex’’ were characterized and identified in the light of the petrogenetic relationships unraveled by this comparative geochemical study in order to determine possible tectonic environments from which they were generated.

4.2. Method

In order to examine the geochemical characteristics of the basic rocks collected from four study areas, 32 relatively less altered rock samples were chosen under microscope and analyzed by ICP-ES for major elements and ICP-MS for trace elements, using powdered samples of 200 mesh-size in ACME Analytical Laboratories (Canada).

The location and distribution of the samples to be interpreted in this part can be summarized as follows:

- 17 samples from İmrahor, among which 7 basalt samples, 2 gabbro samples and one ultramafic rock sample, representing the Bahçecik Formation (Koçyiğit et al., 1991); and 7 diabase dyke samples cutting across the Eymir Metamorphic Complex (Koçyiğit, 1992).

- 4 samples from Hasanoğlan area, characterizing pillow basalts of the Bahçecik Formation.

- 5 samples from Edremit region, representing massive basalts of the Ortaoba Unit (Pickett and Robertson, 1996).

- 6 samples from Kadirler, including pillow basalts from informally named "pillow basalts-limestone association" (Göncüoğlu et al., 2004) resembling those in the Bahçecik Formation in Ankara area.

4.3. Major Element Composition of the Investigated Rocks

As denoted in the former part, the studied rock samples can be grouped by their geological occurrence into three as a) basalts, b) diabase dykes, c) gabbro and ultramafics.

The basalts together with gabbro and ultramafic samples are described by SiO_2 (wt.%) contents ranging from 37.42 to 49.40, while the diabase dykes are represented by higher SiO_2 (wt.%) with the contents ranging from 50.35 to 53.91 (geochemical data is given in Appendix B). On the other hand, the investigated rocks display wide variations in "loss on ignition" (LOI) values, changing between 3.0 and 13.7 (wt.%). Such unusually low and variable SiO_2 contents in addition to very high LOI values can be interpreted as the consequence of chemical mobility of elements during low-grade hydrothermal metamorphism (e.g. Hart et al., 1974; Humpris and Thompson, 1978).

The İmrahor basalts have SiO_2 (wt.%) contents between 40.64 and 47.37, while MgO (wt.%) values ranges in the interval 5.40-10.84. Their TiO_2 (wt.%) contents changes from 1.53 to 3.78. On the other hand, composition of the diabase dykes appears to be more felsic relative to the basalts. They are characterized by SiO_2 (wt.%) contents ranging from 50.35 to 53.91 and MgO (wt.%) values within 3.46 and 5.14. Their TiO_2 (wt.%) contents ranges from 1.50 and 1.75. It should not be overlooked that the basalt samples exhibit a wide range in major element compositions mentioned, whereas the dyke samples are being more felsic than the former, and display limited major element values. The variability of SiO_2 and alkali values is probably caused by

the alteration, however widely varying TiO_2 values may indicate that the İmrahor basalts comprise samples which were possibly derived from different sources. However, the restricted compositions of diabases may reveal their generation from single source.

Gabbro samples have major element compositions similar to the basalts rather than the dykes such that their SiO_2 (wt.%) contents are 44.82 and 44.24, respectively. They have MgO (wt.%) contents of 6.69 and 9.17, whereas their TiO_2 (wt.%) values are 1.84 and 1.24, correspondingly. The ultramafic sample is of unusual elemental abundances relative to the rest as can be expected. It is represented by very low SiO_2 (38.74 wt.%), but very high MgO (23.66 wt.%) contents. Indeed, as mentioned in Chapter 3 this sample is petrographically different than the others; as reflected by its mineralogical composition, including highly serpentinized olivine and clinopyroxene crystals. Such a basic chemical composition together with the petrographical features indicates once again that sample is of ultramafic type.

The Hasanoğlan lavas are characterized by SiO_2 (wt.%) contents between 42.90 and 49.40, while MgO (wt.%) and TiO_2 (wt.%) ranges within 2.35-9.34 and 2.38-3.56, respectively. The Ortaoba basalts, on the other hand, display relatively restricted major element contents except TiO_2, as indicated by 46.54-49.02 SiO_2 (wt.%), 6.38-8.65 MgO (wt.%) and 0.97-2.53 TiO_2 (wt.%) contents. The Kadirler lavas are characterized by highly variable contents similar to the İmrahor and Hasanoğlan basalts. They have SiO_2 (wt.%) contents ranging from 37.42 to 44.94 and MgO (wt.%) contents from 4.07 to 6.00. However, their TiO_2 (wt.%) values are restricted as reflected by contents ranging between 2.01 and 2.79. Relatively narrow range of TiO_2 contents displayed by the Hasanoğlan and Kadirler basalts may signify their generation from a single source, whereas widely changing TiO_2 values of Ortaoba presumably indicate presence of non-uniform origin for these extrusive rocks.

4.4. Classification of the Investigated Rocks

Most of the studied samples are characterized by low-grade hydrothermal alteration, thus the presence of selected element mobility is likely to occur on

the samples, particularly comprising the Large Ion Lithophile (LIL) elements (e.g. Pearce and Cann, 1973; Hart et al., 1974; Humphris and Thompson, 1978; Thompson, 1991; Staudigel et al., 1996). In addition, LOI values are highly variable (up to 13.7 wt.%), indicating some degree of alteration and the presence of secondary volatile and carbonate phases.

Most major elements (except Ti and P) together with LIL elements (except Th) represent highly inconsistent abundances, thus they are not reliable indicators to infer their petrogenesis. Therefore, the geochemical interpretation below is mainly based on the elements which are considered as relatively immobile under conditions of weathering and low-grade metamorphism (e.g. Pearce and Cann, 1973; Pearce, 1975; Floyd and Winchester, 1978; Ludden et al., 1982; Bienvenu et al., 1990; Staudigel et al., 1996; Kerrich et al., 1998).

In order to display the effect of low-grade metamorphism on the samples, Zr was used as stable fractionation index and plotted against various major oxides and trace elements (Figure 4.1). The elements which show mobility during low-grade alteration (e.g. K_2O, CaO, Rb, and Ba) are characterized by the wide range of scatter, whereas the elements considered as immobile under such conditions (e.g. TiO_2, P_2O_5, Ta and Nb) demonstrate rather consistent relationships.

When the samples are plotted on a rock classification diagram based on immobile elements (Winchester and Floyd, 1977), it is observed that they consist of three different groups as alkaline basalts, sub-alkaline basalts and the basalts transitional between alkaline and sub-alkaline types (Figure 4.2).

The basaltic lavas of Hasanoğlan and Kadirler are plotted in the alkaline field, whereas diabase dykes lie in the sub-alkaline field. However, it should be noticed that Ortaoba and İmrahor contain basic rocks of different characteristics such that three of the Ortaoba lavas are of sub-alkaline character, but the other two from the same locality exhibit alkaline character. When the İmrahor rocks are examined, it is seen that gabbro samples are clearly within the sub-alkaline field, while most of the basalts are plotted in the alkaline field. The two basalt samples and ultramafic sample, on the other hand, are represented by transitional features.

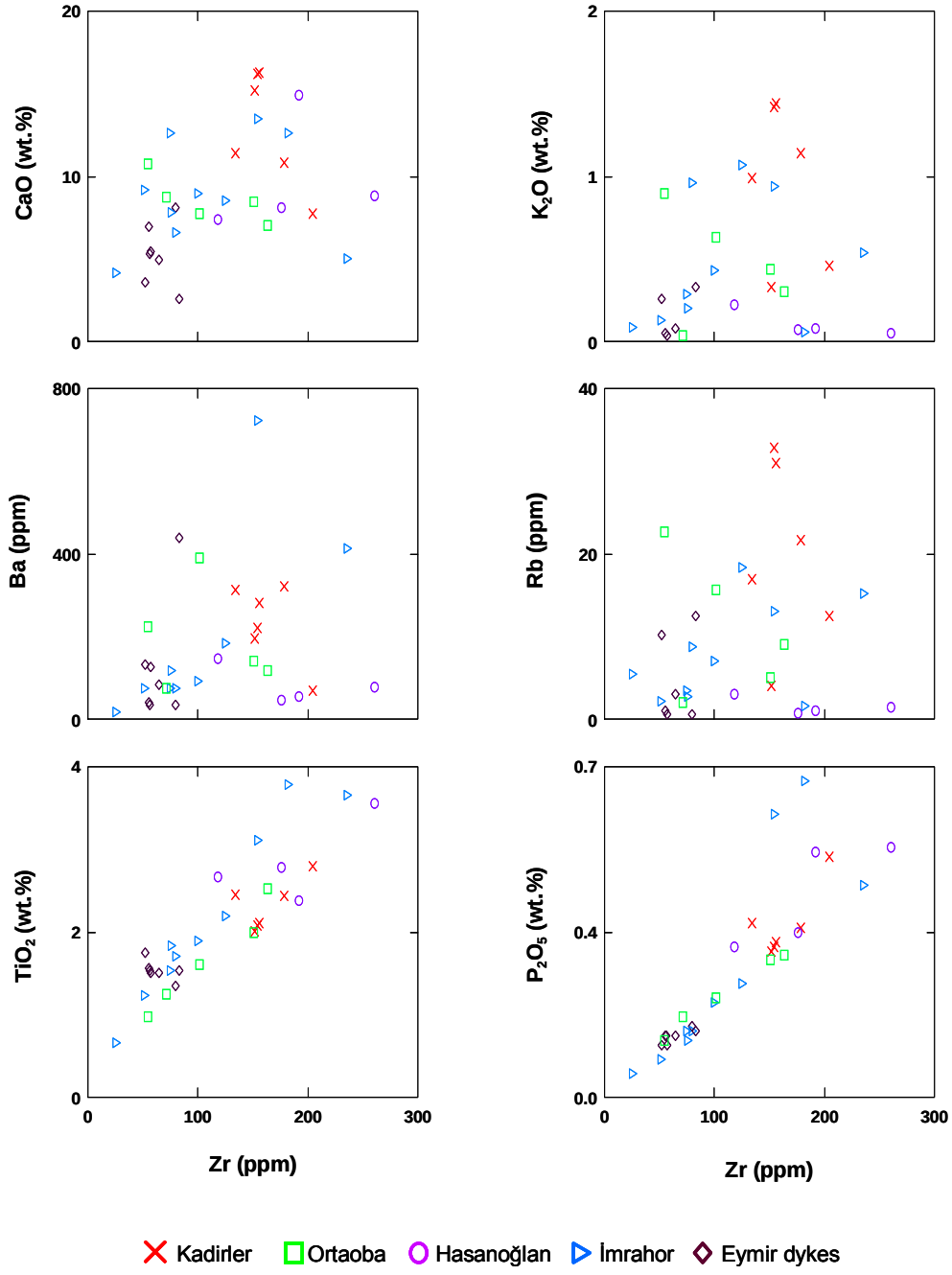

Figure 4.1. Behavior of mobile and relatively immobile elements in the presence of low-grade hydrothermal alteration.

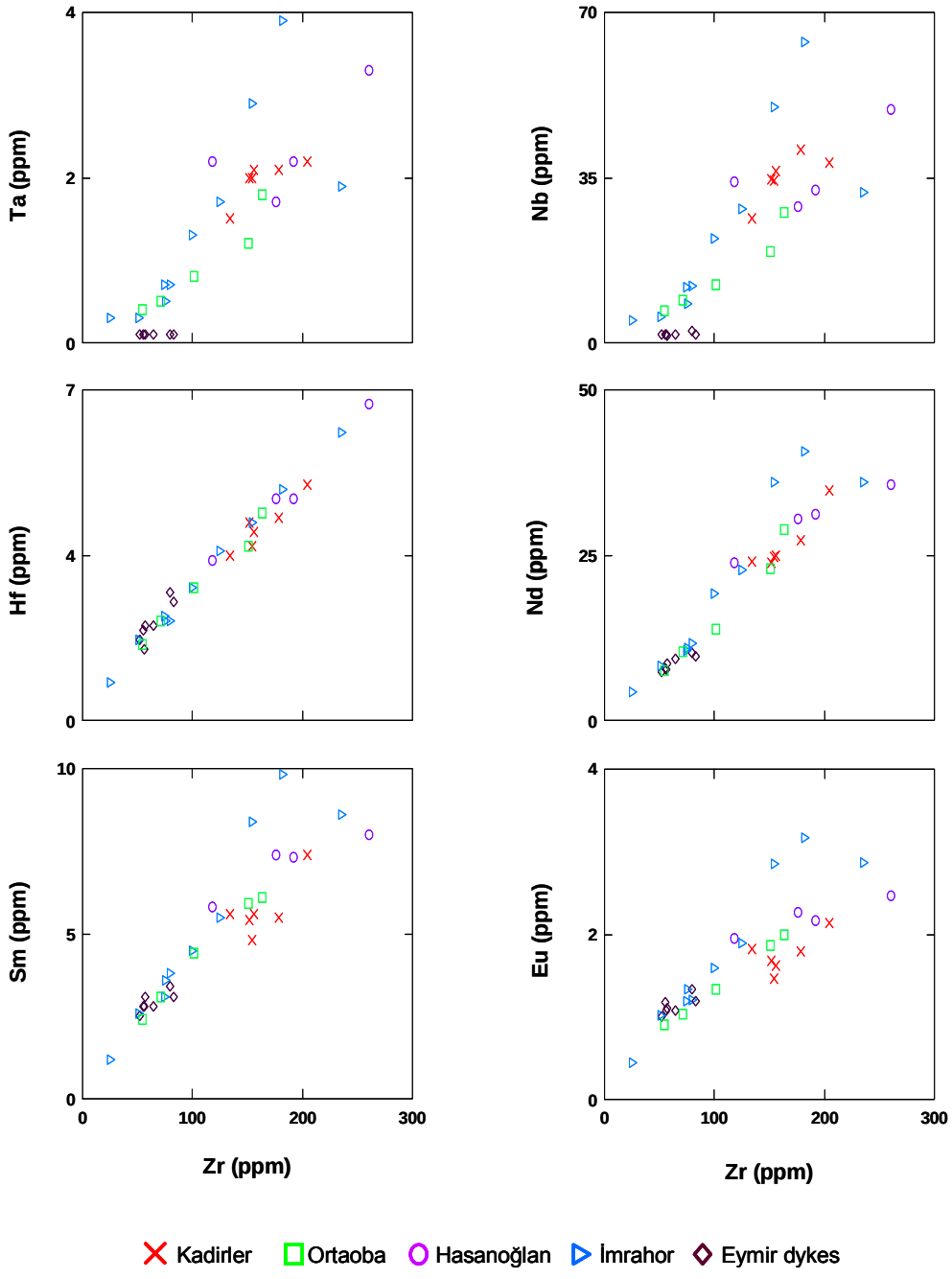

Figure 4.1 (continued).

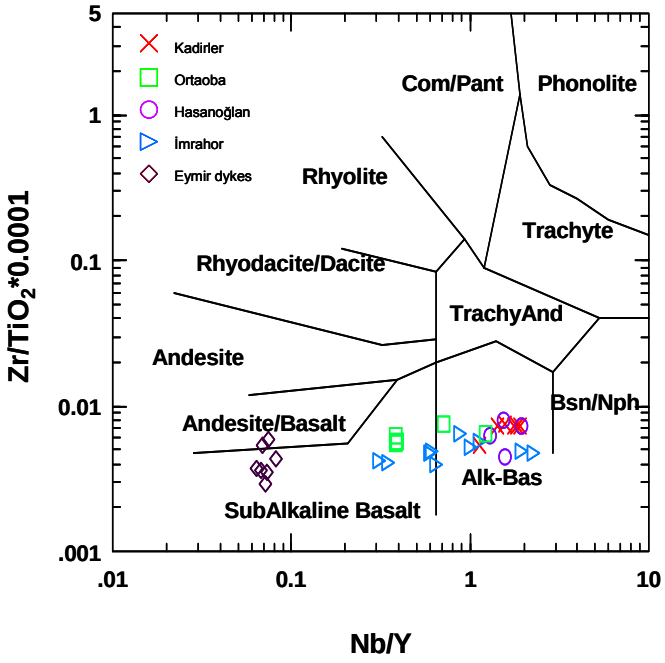

Figure 4.2. Classification of the samples on the diagram based on relatively immobile elements (after Winchester and Floyd, 1977).

4.5. Fractionation Trends of the Investigated Rocks

In most of the Harker diagrams including both major and trace elements, it is clearly observed that the diabase dyke samples exhibit different trends relative to the rest (Figure 4.3). It must be noted that the diabases have restricted SiO_2 and MgO contents, so their fractionation features will not be interpreted here.

The increasing Al_2O_3 contents with increasing SiO_2 may indicate the fractionation of ferro-magnesian minerals within the İmrahor and Kadirler volcanics. However, the Ortaoba and Hasanoğlan extrusive rocks do not present clear trends to interpret the fractionation. If MgO versus SiO_2 diagram is considered, the Kadirler lavas seem quite interesting, since they have increasing MgO contents with increasing SiO_2. This can be interpreted as the variable contents of SiO_2 due to secondary silicification and calcitization. The Hasanoğlan volcanics are again scattered, reflecting no identifiable trends. The Ortaoba lavas this time present consistent trends with gradually decreasing MgO against increasing SiO_2, indicating the importance of ferro-

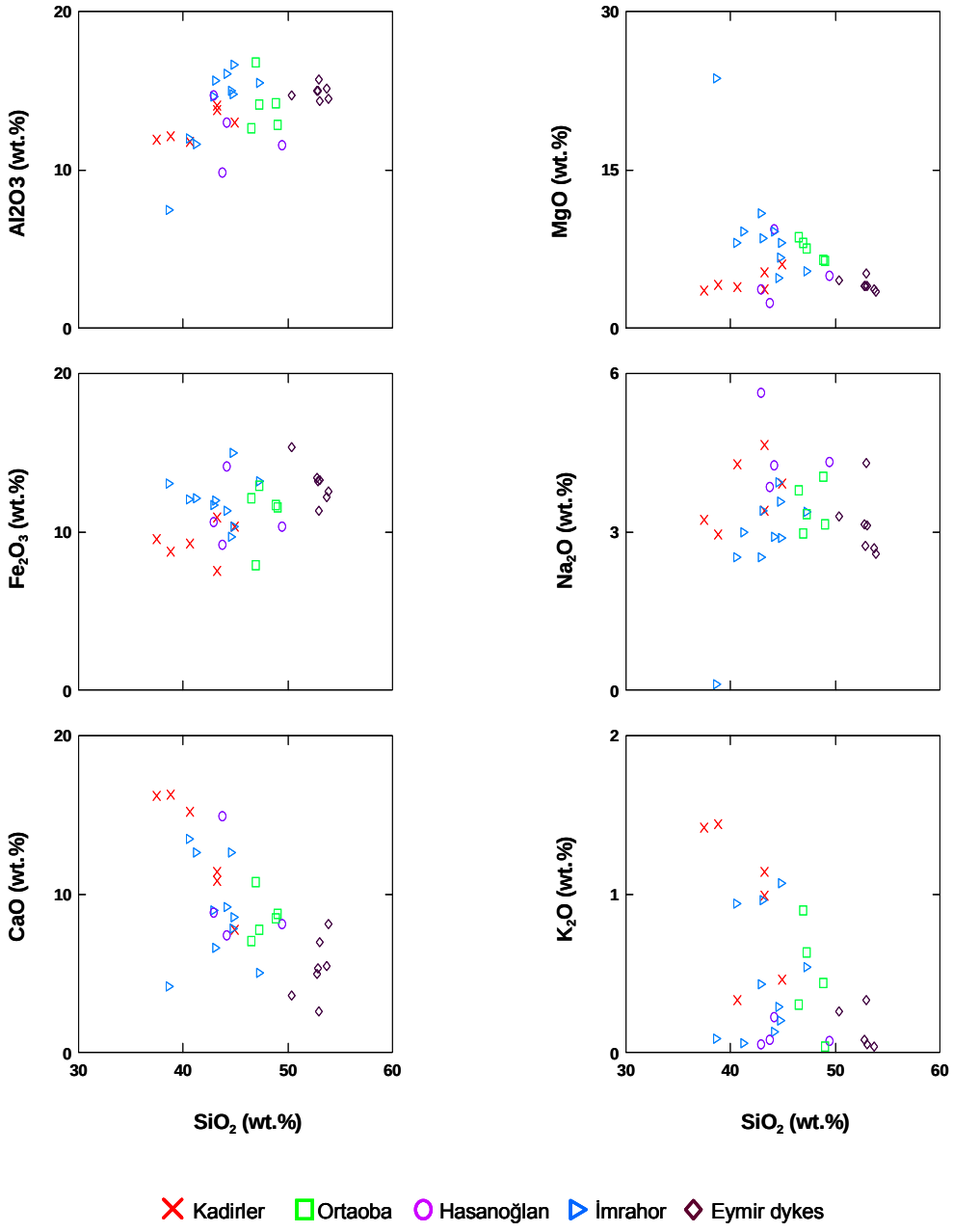

Figure 4.3. Major element Harker diagrams displaying fractionation trends of the studied basalts.

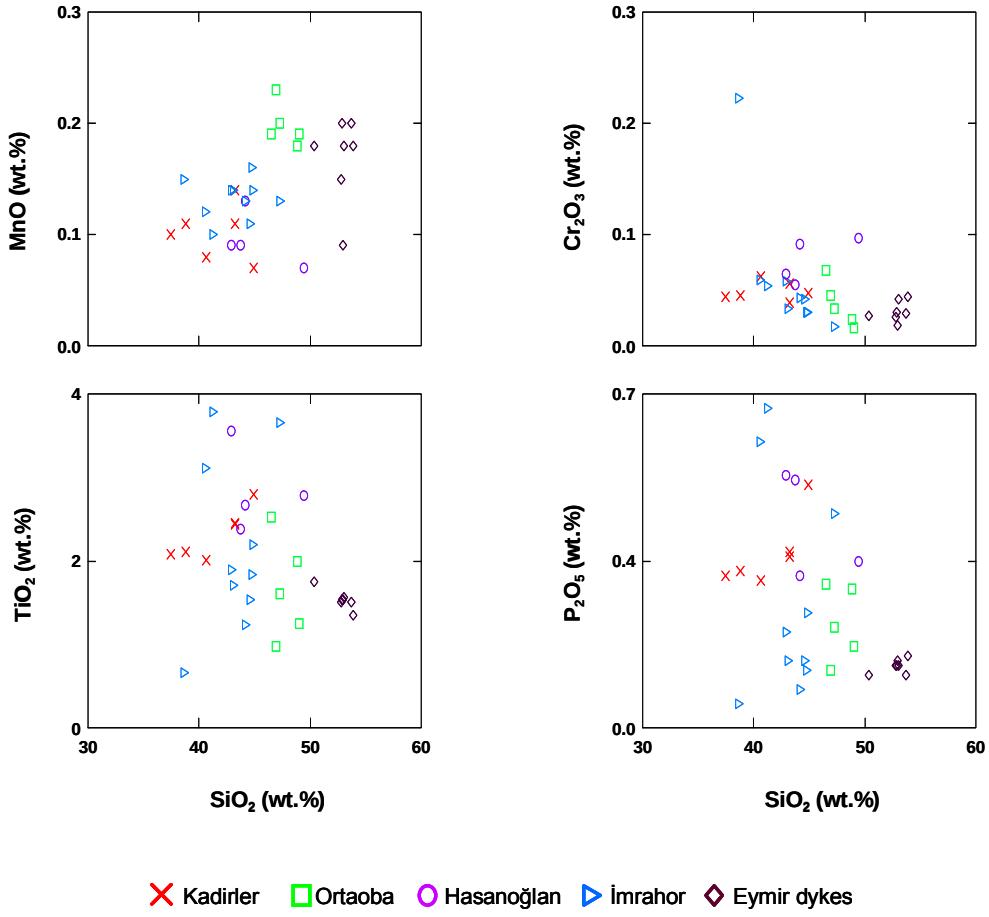

Figure 4.3 (continued).

magnesian mineral fractionation. Decreasing trends reflected by Fe_2O_3 contents also conformable to the fractionation of ferro-magnesian minerals. Since alkali contents are highly variable due to intense alteration, no lucid could be observed in terms of fractionation. TiO_2, P_2O_5 as well as MnO trends against SiO_2 also give no apparent idea. On the other hand, the decreasing contents of Cr_2O_3 observed in the İmrahor and Ortaoba indicate once more that the crystallization of ferro-magnesian minerals dominates the fractionation process.

The plots of trace elements against SiO_2 reveal similar results, supporting the predominant fractionation of ferro-magnesian mineral phases (Figure 4.4). Increasing Sc abundances with increasing apparently indicate this situation for

the Kadirler and İmrahor samples. It would not be appropriate to make any interpretation about the Hasanoğlan and Ortaoba samples because of the scattering in their trends. However, the substantial decrease in Ni contents suggests also the importance of crystallization of Fe-Mg minerals for the

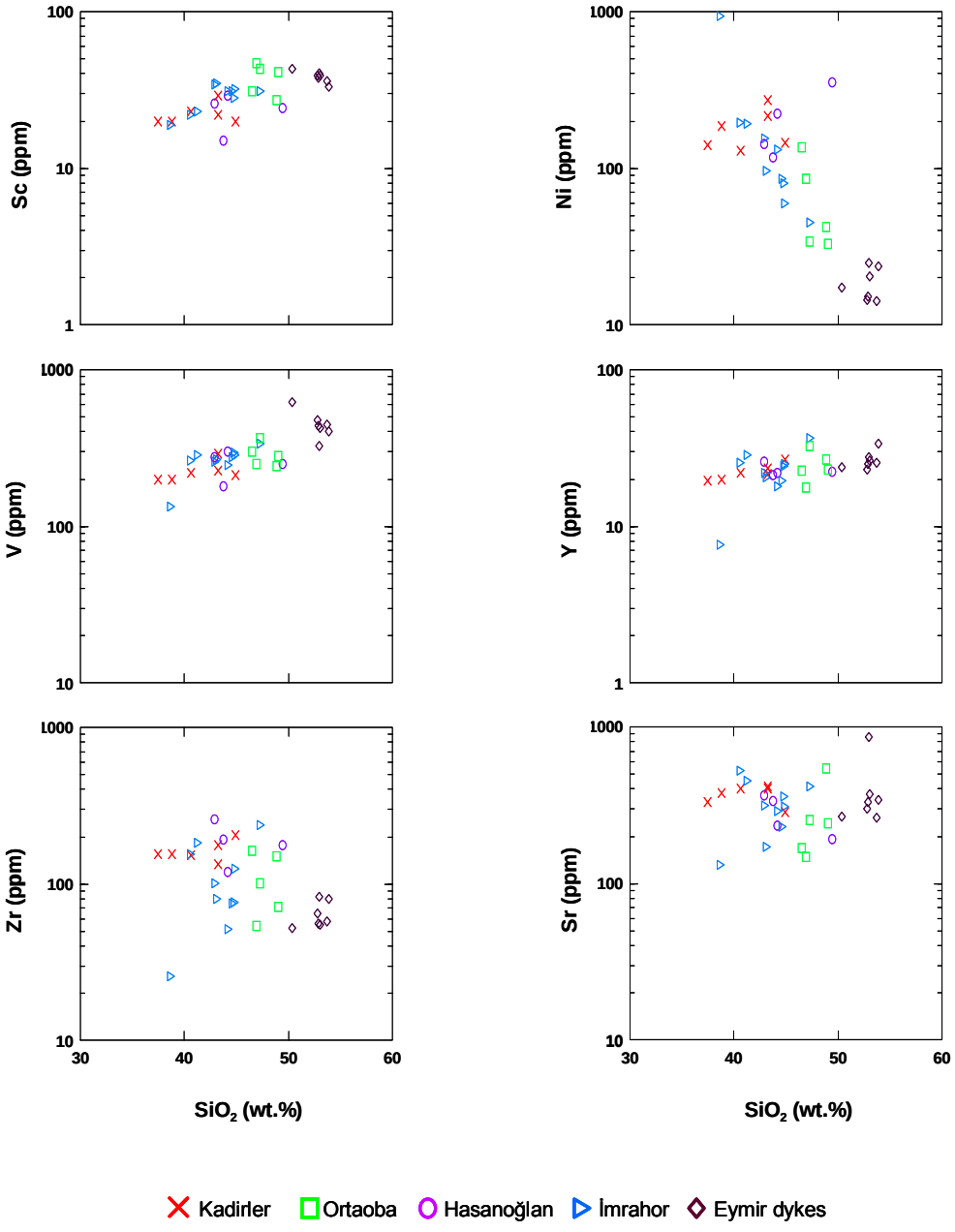

Figure 4.4. Trace element Harker diagrams displaying fractionation trends of the studied basalts.

Ortaoba basalts as well as the İmrahor basaltic rocks. This time, the Kadirler reflects scattered trends compared with the case in previous diagram. If the V and Y contents are taken into consideration, the Hasanoğlan lavas are also conformable to the fractionation trends observed in the other samples, thus it can be deduced that the Hasanoğlan extrusives are also under the influence of Fe-Mg fractionation.

As a result, the both major and trace element variations displayed by studied rocks indicate that fractional crystallization of ferro-magnesian phases may have played an important role in creating the observed trends during the magmatic evolution.

4.6. Source and Petrogenesis

Zr/Y ratio is not influenced by moderate degrees of fractional crystallization due to incompatibility of Zr and Y with the main fractionating phases in basaltic magmas, such as olivine, pyroxene and plagioclase (e.g. Abdel-Rahman, 2002, 2004). The Zr/Y ratios reflect a higher value if small degree of melting is considered, since the incompatibility of Zr is higher than that of Y in mantle phases (e.g. Pearce 1980; Nicholson and Latin, 1992). It is observed that the Zr/Y ratios decrease with decreasing Zr in the Hasanoğlan, Kadirler and İmrahor basalts, indicating their generation by variable degrees of melting (interpreted in Section 4.6).

When the samples are plotted on Zr/Y as Zr/Nb diagram, the alkaline samples appear to have been derived from a plume-related source (Figure 4.5). Although, the subalkaline and transitional samples from İmrahor and Ortaoba tend to exhibit transitional character, they may also be related with enriched mantle source. The diabase dykes are apparently plotted in a different field with relatively low Zr/Y but high Zr/Nb values, suggesting the contribution of a depleted mantle source during their generation (N-MORB, Zr/Y=2.64, Zr/Nb= 31.8; Sun and McDonough, 1989).

In order to clarify this situation, Y/Nb ratio can also be considered. The alkaline samples are characterized by lowest values of Y/Nb among the studied rocks

(Y/Nb=0.44-1.39), whereas the sub-alkaline and transitional samples have relatively higher values (Y/Nb=1.55-3.20). The diabases, on the other hand, show the highest values relative to the rest (Y/Nb=12.21-15.75). Thus, the relatively low values of Y/Nb for the samples except diabases may indicate their generation from enriched mantle sources, while very high values of Y/Nb displayed by diabases can be attributed to involvement of depleted mantle sources.

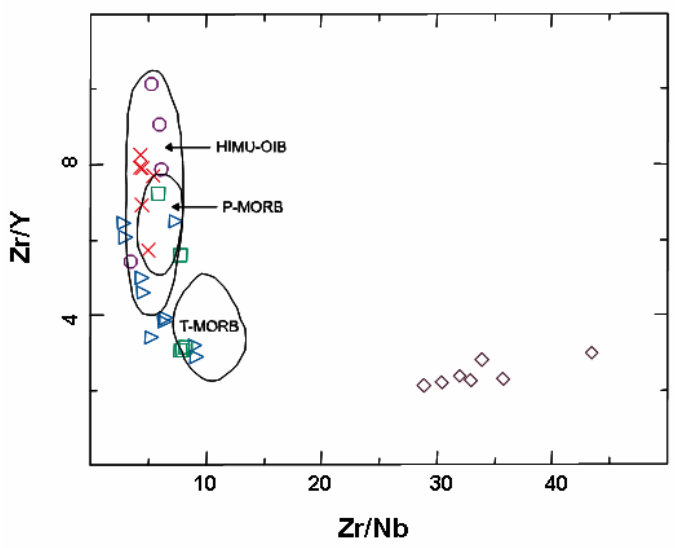

Figure 4.5. Zr/Y-Zr/Nb diagram constraining possible mantle sources for the basalts studied. (after Abdel-Rahman, 2002; T-MORB and P-MORB data from Menzies and Kyle, 1990; HIMU-OIB data from Weaver et al., 1987). For symbols see Figure 4.1.

All the basaltic samples except diabases have relatively high Nb/La and La/Yb ratios. The alkaline lavas have high ratios (Nb/La=1.12-1.78, La/Yb=8.06-22.52), while the subalkaline and transitional ones are dominated by rather small values (Nb/La=1.17-1.57, La/Yb=2.88-5.07). The diabases, on the other hand, display considerably low values (Nb/La=0.39-0.63, La/Yb=1.05-1.92) in comparison with the others. High ratios of Nb/La (>1) are the indication of asthenospheric mantle source (OIB-like), whereas lower ratios (<0.5) signify lithospheric mantle source (Bradshaw and Smith, 1994; Smith et al., 1999).

Thus, the all samples apart from diabases indicate an asthenospheric mantle source as reflected by the high ratios, while a lithospheric mantle source should have involved in the petrogenesis of the diabases.

Whether the garnet is a residual phase in the source or not can be revealed by REE abundances. The presence of residual garnet leads to depletion of HREE relative to LREE due to strong retention of the former in garnet (Wilson 1989; Spath et al., 1996), as also reflected by the high partition coefficients (e.g. Green et al., 1989; Jenner et al., 1994). The strong depletion of HREE with respect to LREE together with comparatively high $[La/Yb]_N$ ratios (9.8-27.5) indicates that garnet is a residual phase in the source of alkaline basalts (e.g. Frey et al., 1978). Furthermore, $[Tb/Yb]_N$ values of the Kadirler and alkaline Ortaoba basalts ($[Tb/Yb]_N$=1.75-2.38; 2.11-2.39, respectively) are consistent with those of alkaline basalts from Hawaii ($[Tb/Yb]_N$=1.89-2.45; Frey et al. 1991), which are also believed to derived from a garnet-bearing source. The Hasanoğlan and alkaline İmrahor basalts, however, display ratios ($[Tb/Yb]_N$=2.45-3.01; 2.13-3.72, respectively) that are not comparable with those of Hawaii basalts. The high Dy/Yb ratios of alkaline basalts (Dy/Yb=2.09-3.87) compared to that of chondrite (Dy/Yb= 1.49; Sun and McDonough, 1989) maintain previous results, suggesting that they have been derived from a garnet lherzolite source.

The subalkaline and transitional samples, exhibit less fractionated patterns and lower $[La/Yb]_N$ ratios (3.5-6.2) relative to the alkaline samples. At this point two possibilities exist for the source of the subalkaline and transitional basalts; a) a LREE-enriched garnet-bearing source, where garnet is consumed owing to large degrees of melting, b) a source characterized by relatively low LREE abundances with no garnet present. Therefore, second choice would be more appropriate, suggesting that a spinel lherzolite source could have been involved in their magma generation.

The transition from spinel to garnet lherzolite is assumed to occur at depths of at least 80 km in the presence of deep mantle plumes (e.g. McKenzie and O'Nions, 1991). When Yb, Sm and Ce concentrations of alkaline basalts are plotted on the curves which have been suggested by Ellam (1992) to estimate

melt segregation depths (Figure 4.6), they corresponds to depths of approximately 100 km, which is consistent with a garnet lherzolite source, supporting previous results.

As discussed in Abdel-Rahman (2002), there is an inverse relationship between degree of partial melting and highly/moderately incompatible element ratios (Pankhurst, 1977). The relatively linear trends displayed by the basaltic samples may be suggestive of the importance of partial melting as a prevailing petrogenetic process (Figure 4.7). However, it must be noticed that the diabases follows a different path compared to the rest.

As similar to the case mentioned above, an inverse link is observed between degree of partial melting and the ratio of an incompatible element to Al_2O_3 such that the ratio decrease with increasing degree of partial melting (Hoernle and Schmincke, 1993). The linear positive trends explain once more that the partial melting is a dominant process in magma generation of the studied basaltic rocks (Figure 4.8).

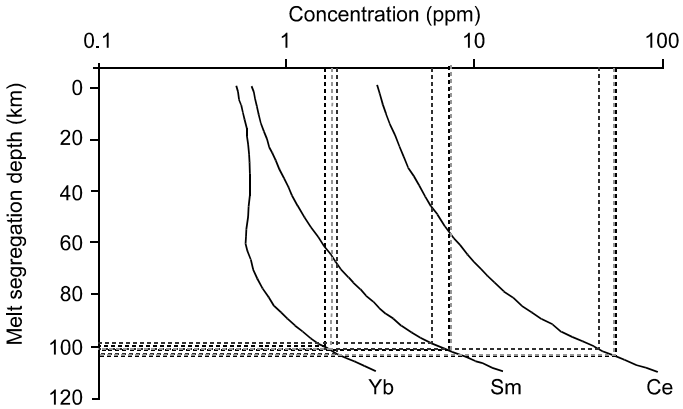

Figure 4.6. Estimation of segregation depths for alkaline samples (after Ellam, 1992).

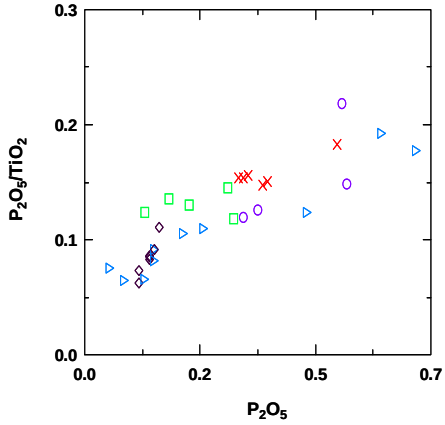

Figure 4.7. Plot of P_2O_5/TiO_2 vs. P_2O_5, indicating effect of partial melting on the investigated rocks. For symbols see Figure 4.1.

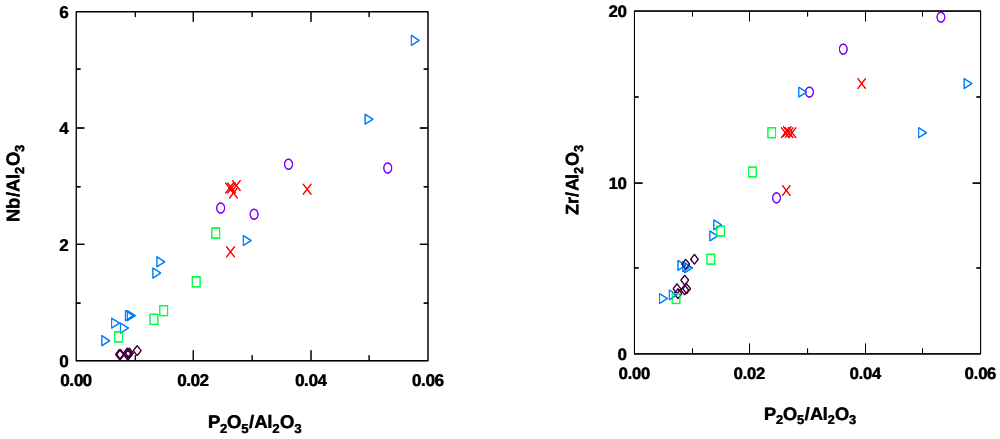

Figure 4.8. Ratio-ratio plots using Al_2O_3, which display the influence of partial melting on the studied samples. For symbols see Figure 4.1.

Another essential point is whether they have suffered crustal contamination or not. Since the investigated basalts are porphyritic, it must be considered that they may have been kept within crustal magma chambers, thus leading to interaction with continental crust by assimilation and fractional crystallization (AFC) processes (e.g. Moghazi, 2003). In order to unravel this situation, certain elemental ratios (such as La/Ta, La/Nb, Nb/Y and Th/Nb) should be considered. It is known that basaltic rocks influenced by crustal contamination are characterized by the ratios; La/Ta>22, La/Nb>1.5 (e.g. Hart et al., 1989). All the studied samples excluding the diabases exhibit low elemental ratios

La/Ta=9.18-15.40; La/Nb=0.56-0.90; Th/Nb=0.04-0.11), suggesting that the effect of crustal contamination is insignificant for those samples. The diabase dykes, unlike the others, show unusually high values (La/Ta=30.00-59.00; La/Nb=1.58-2.58; Th/Nb=0.26-0.56), which may be result of crustal contamination. Nevertheless, it must be emphasized that high La/Nb values are common features recognized in arc mafic rocks (e.g. Gill, 1981).

In the plot of Th/Yb vs. Nb/Yb as suggested by Pearce and Peate (1995; Figure 4.9), the samples apart from diabases are plotted in the MORB array, displaying negligible crustal effects. The diabase samples, however, fall in the oceanic arc field and overlap area between oceanic and continental arc field. Therefore, it may be suggested that high La/Ta, La/Nb, Th/Nb ratios, which is believed to be caused by crustal contamination, can also arise from the subduction enrichment of the mantle source. However, it is difficult at this time to say which process was effective or that the combination of two was involved during the evolution of diabase rocks.

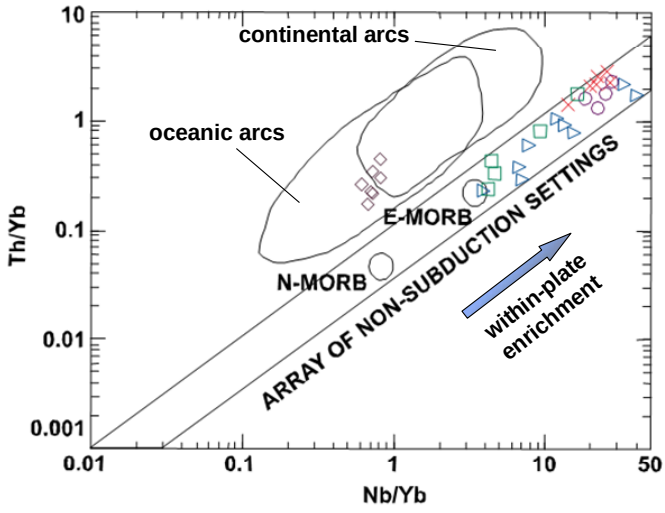

Figure 4.9. Th/Yb vs. Nb/Yb diagram displaying mantle enrichment for uncontaminated samples and effect of subduction enrichment on the diabases (after Pearce and Peate, 1995; N-MORB and E-MORB values from Sun and McDonough, 1989). For symbols see Figure 4.1.

The discrimination between crustal and mantle sources in the investigated rocks can be further constrained by Ce/U and Nb/U ratios (e.g. McDonough, 1990). In the diagram, all the rocks apart from diabases clearly plot inside the OIB field, whereas the diabases are outside the both MORB and OIB fields (Figure 4.10). In fact, their Nb/U values ($[Nb/U]_{ave}$=7.75) are similar to those of island-arc basalts (Nb/U~7; Sun, 1980). Therefore, the suggestion of enriched mantle sources for the samples except diabases is still valid. Furthermore, the diagram also implies that subduction enrichment might have been effective instead of crustal contamination for the diabases, since most of them fall in the places away from the average crust. However, this suggestion should be further supported by REE abundances which will be discussed in Section 4.7.

It should be noted that oceanic sediments may also result in contamination of magmas apart from AFC processes which is responsible for crustal contamination. It is suggested that pelagic sediments are characterized by highly enriched nature in terms of Th (e.g. Ben Othman et al., 1989). Unlike Th and Nb,

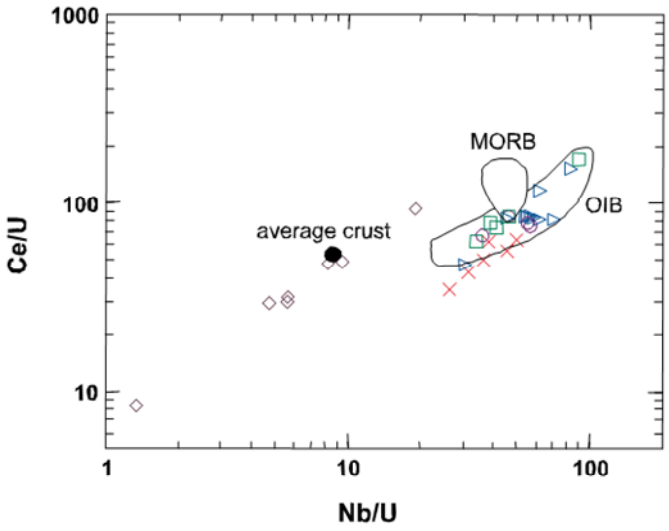

Figure 4.10. Ce/U vs. Nb/U diagram indicating possible source regions for the investigated rocks (after Moghazi, 2003; MORB data from Ito et al., 1987; OIB from Hofmann et al., 1986; Davies et al., 1989; average crust from Hofmann et al., 1986). For symbols see Figure 4.1.

which are assumed to be immobile in subduction fluids, U behave as a fluid-mobile element (e.g. Plank, 1996; Hoernle, 1998). Therefore, presence of U within continental materials added to the system can lead to high U abundances. However, the low concentrations of U in the diabases (U_{ave}=0.4 ppm) suggest that continental materials is not so effective during genesis of the diabases. This result is further confirmed by low Th/La values displayed by these rocks (Th/La=0.12-0.24), which are comparable to those observed in intra-oceanic arcs (Th/La=0.09, Mariana arc; McCullough and Gamble; 1991) unaffected by major crustal effects compared with continental margins (Th/La>45, Aeolian Arc; Ellam et al., 1988).

According to Condie (2003), the oceanic mantle can be regarded to include four end-member domains (for details see also Condie, 2005). These are deep depleted mantle (DEP), an enriched component (EN) including upper continental crust and continental lithosphere, a recycled component (REC) comprising EM1, EM2 and HIMU, and finally a shallow depleted mantle (DM). If Zr/Nb and Nb/Th ratios are compared, the diabases are clearly separated from the group, plotted in arc- related basalts (ARC) field (Figure 4.11a). The rest of samples, however, display affinity to OIB-type basalts, indicating their derivation from recycled component. Zr/Y and Nb/Y ratios also confirm the involvement of a recycled component for the alkaline samples, but the subalkaline and transitional ones are apparently differentiated in this case (Figure 4.11b). It is interesting, however, that the diabase samples appear within N-MORB field, reflecting a shallow-depleted mantle source. Thus, both arc-related and MORB component could be possible for magma generation of the diabase samples.

The type of source for OIB-like samples is another subject to emphasize. According to Hart (1988), asthenospheric sources of OIB can be seperated into four reservoirs based on Sr, Nd and Pb isotopes: HIMU (high $^{238}U/^{204}Pb$ mantle end-member), which is characterized by the lowest $^{87}Sr/^{86}Sr$ among OIBs (Hofmann, 1997), is considered to be generated from subducted oceanic crust. However, EMI (enriched mantle 1) and EMII (enriched mantle 2) reflect the addition of subducted sediments (pelagic for EMI and terrigenous for EMII), and the last type is represented by depleted MORB mantle (DMM).

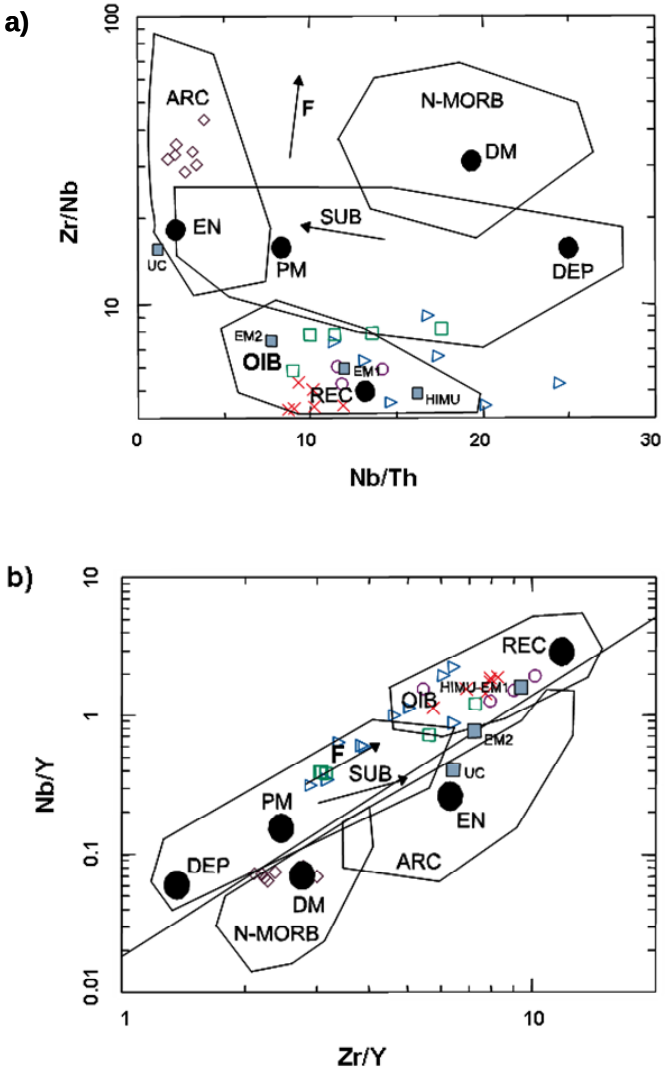

Figure 4.11. Diagrams illustrating probable mantle sources from which the studied samples derived (after Condie, 2005; fields are based on Weaver, 1991; Condie, 2003). For symbols see Figure 4.1.

These reservoirs can also be differentiated using elemental ratios (for details see Weaver, 1991). In this respect, La/Nb, Zr/Nb and Th/Nb values were discussed to reveal the source characteristics of OIB-type basalts in the study areas.

La/Nb ratios of the Kadirler (La/Nb=0.56-0.81), Hasanoğlan (La/Nb=0.66-0.90) and İmrahor basalts (La/Nb=0.56-0.80) suggest that they are more akin to HIMU-OIB (La/Nb=0.66-0.77; Weaver, 1991), whereas the Ortaoba basalts

(La/Nb= 0.82-0.88) seem to have relatively higher values, which are comparable with EMI-OIB (La/Nb=0.64-1.19; Weaver, 1991).

Zr/Nb values are consistent with the previous results such that the Zr/Nb ratios displayed by Kadirler, Hasanoğlan and İmrahor basalts (4.3-5.4; 3.5-6.1; 2.9-7.4) are in the range of those of HIMU-OIB (Zr/Nb=3.2-5.0; Weaver, 1991), while the Ortaoba basalts in the range of EMI-OIB.

Although Th/Nb values also suggest that the Kadirler, Hasanoğlan and İmrahor basalts (Th/Nb=0.08-0.12; 0.06-0.09; 0.04-0.09, respectively) are of HIMU-OIB type (Th/Nb=0.078-0.101; Weaver, 1991), the values shown by the Ortaoba basalts (Th/Nb= 0.09-0.11) are similar to those from HIMU-OIB rather than EMI-OIB (Th/Nb=0.105-0.122; Weaver, 1991).

Therefore, on the basis of La/Nb, Zr/Nb and Th/Nb ratios, it may be suggested, the OIB-like basalts from Kadirler, Hasanoğlan and İmrahor might have been derived from a HIMU-type source, whereas the Ortaoba basalts should be related to an EMI-type source.

4.7. Tectonic Discrimination of the Studied Samples

Considering that each tectonic environment is characterized by distinctive geochemical signature (e.g. Wood et al., 1979; Meschede, 1986), the investigated basic rocks were plotted on a series of tectonic discrimination diagrams to classify them with respect to their immobile trace element contents.

In the Ti versus V discrimination diagram (Shervais, 1982), the basic rock samples are widely scattered in the ocean-floor basalts (OFB) field. The Hasanoğlan and Kadirler lavas are confined in the within-plate basalts (WPB) field defined by Ti/V ratios from 50 to 100 (Figure 4.12). This result is consistent with their alkaline characters mentioned in Section 4.4, since alkaline lavas are mostly generated at the intra-plate tectonic settings (e.g. Fitton and Upton, 1987; Wilson 1989).

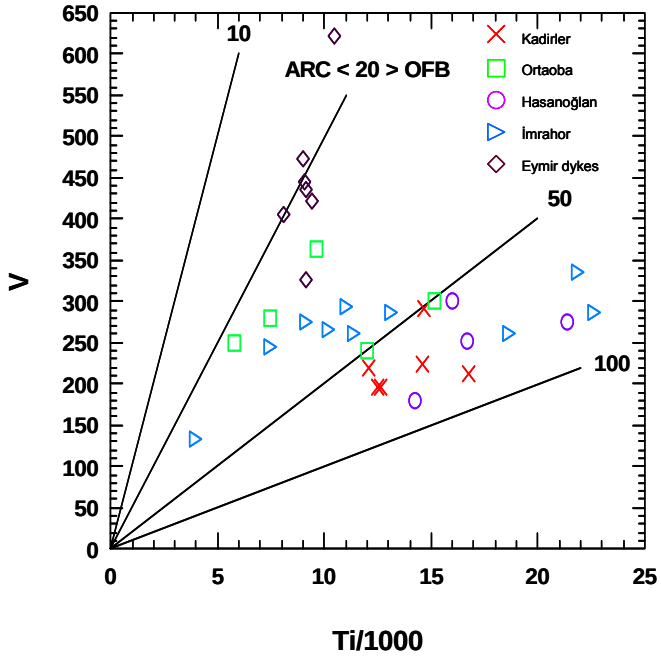

Figure 4.12. Tectonomagmatic discrimination plots for the studied samples (after Shervais, 1982).

The samples from İmrahor and Ortaoba comprise different types, appearing in the mid-oceanic ridge basalts (MORB) - back-arc basin basalts (BABB) field, WPB field and transitional zone between the two as indicated by Ti/V ratios between 20 and 100. The two samples from Ortaoba are plotted just on the boundary separating MORB-BABB from WPB, thus it is hard to infer anything about their tectonic environment. However, their alkaline nature together with their appearance on the transitional zone in this diagram may show contribution of a plume-related or enriched mantle source in their generation.

The İmrahor basaltic rocks, on the contrary to the Ortaoba lavas, are plotted in the WPB field in addition to the MORB-BABB fields. The alkaline basalts appear in the WPB field and sub-alkaline gabbro samples are plotted in the MORB-BABB field as can be expected; however, the other alkaline samples are confined in the area characterizing MORB and BABB.

The diabase dykes are mostly assembled close to the ARC-OFB boundary; however the samples are precisely separated from the other dolerites, plotting

in ARC and MORB-BABB fields respectively. Note that the ultramafic sample is away from the rest of İmrahor samples and plot in the MORB-BABB field.

In the Zr/Y versus Zr tectonic discrimination diagram as defined by Pearce and Norry (1979), a similar scene could be observed such that the Hasanoğlan and Kadirler basalts indicate a within-plate environment (Figure 4.13). The diabase dykes from İmrahor are plotted in the overlap area between island-arc basalts (IAB) and MORB. The Ortaoba and İmrahor lavas are expectedly scattered over the diagram.

The alkaline lavas from Ortaoba are included in the WPB field, hence supporting the “non-depleted source” idea obtained from the previous diagram. The sub-alkaline lavas of Ortaoba; on the other hand, could not be clearly interpreted as one of them is involved in the IAB field and the other two lie on the boundary that separate the IAB and MORB fields.

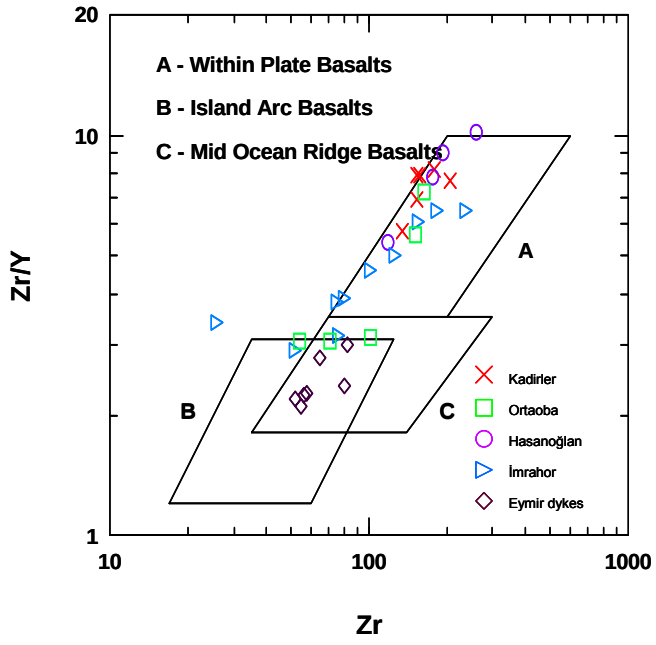

Figure 4.13. Tectonomagmatic discrimination plots for the studied samples (after Pearce and Norry, 1979).

The entire alkaline lavas of İmrahor are plotted in the WPB field at this time. It should be noticed that two samples, which are unexpectedly plotted in the MORB-BABB field in the previous diagram, clearly reflect WPB character in this case. The transitional lavas, however, are plotted in the WPB field, bringing to mind the idea of plume-contribution related to their tectonic origin. The sub-alkaline gabbros from İmrahor are plotted in MORB and IAB fields, respectively but very close to the boundaries, and the ultramafic sample is again separated from the rest, plotting in an indefinable place.

If the Zr-Nb-Y discrimination diagram (Meshede, 1986) is considered, it is seen that the rock samples are certainly assembled in the three fields as WPB, E-MORB and N-MORB-VAB (Figure 4.14). The Hasanoğlan and Kadirler lavas are plotted in the WPB field, conforming to the previous diagrams. The İmrahor dyke samples are entirely confined in the field that characterizes N-MORB and VAB. This is also an agreeable result; however it is still not clear whether they are VAB, MORB or BABB.

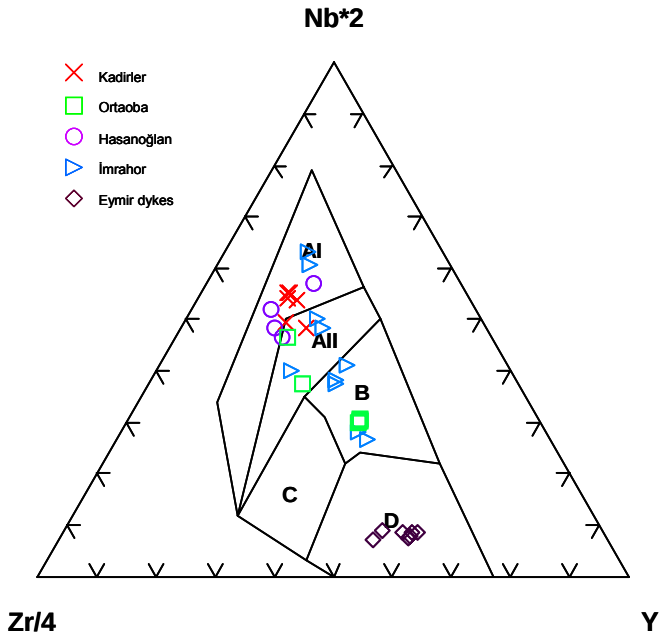

Figure 4.14. Tectonomagmatic discrimination plots for the studied samples (after Meshede, 1986. Fields: AI and AII: WPB; B: P-MORB; C: WPT and VAB; D: N-MORB and VAB).

The same two from Ortaoba are once more separated from the group, plotting in the WPB field, on the other hand, the rest of the group appear in the E-MORB field. This scene when compared with the other diagrams indicates that the two alkaline samples are probably related to an intra-plate tectonic setting, while the sub-alkaline ones reflect a mid-oceanic ridge, however more data is required to prove that they are of plume-related MORB.

The alkaline İmrahor basalts are in agreement with the former results, plotting in the WPB field. The sub-alkaline gabbros, transitional basalts and ultramafic sample as expected are restricted in the different field, E-MORB. At this point, it can be deduced that the alkaline İmrahor lavas are probably of within-plate origin, whereas the sub-alkaline and transitional ones presumably reflect a mid-oceanic ridge, nevertheless it is not apparent whether they are of N-MORB or E-MORB.

In the Ti-Zr-Y discrimination diagram (Pearce and Cann, 1973), no problem arises from the lavas of Hasanoğlan and Kadirler since they are plotted in the WPB field as usual and the Ortaoba lavas also display appropriate distribution, confining within the two fields (Figure 4.15). The alkaline Ortaoba samples are plotted in the WPB field, whereas the remaining sub-alkaline ones are restricted in the field that corresponds to MORB, IAT and CAB. All the İmrahor samples other than diabase dykes (except one sample) are interestingly gathered in the WPB field this time. Only one sample is located at the junction of the three fields. Most of the İmrahor dykes this time are restricted in only one field, IAT. Two samples are plotted in the MORB-IAT-CAB field and one sample is at the boundary.

When the Hf-Th-Ta tectonic discrimination diagram (Wood et al., 1979) is taken into consideration, similar results come out relative to the previous diagrams (Figure 4.16). The entire Hasanoğlan and Kadirler basalts appear in the alkaline within-plate basalt field. Four samples from Ortaoba are plotted in the E-MORB, whereas one sample is confined in the alkaline WPB field just next to the boundary. This result is quite normal since alkaline samples are plotted in the WPB field in the previous diagrams. Furthermore, the three sub-alkaline samples and here they are seen as E-MORB; like in the Nb-Zr-Y

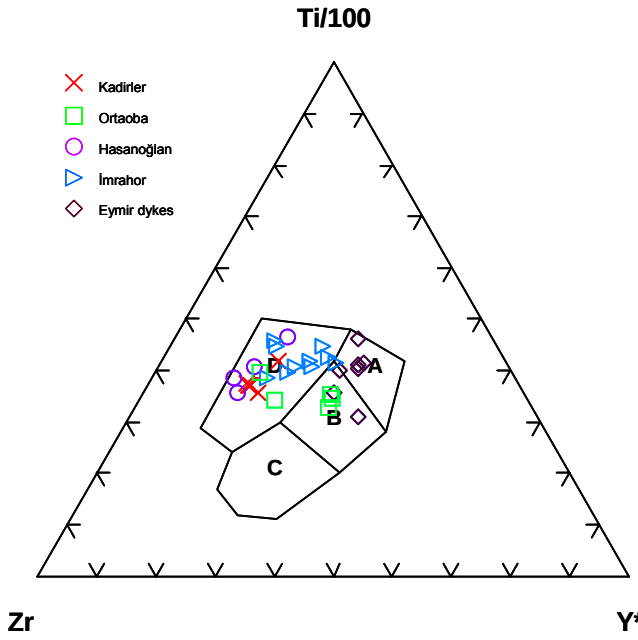

Figure 4.15. Tectonomagmatic discrimination plots for the studied samples (after Pearce and Cann, 1973. Fields: A: IAT; B: MORB and IAT; C: CAB; D: WPB).

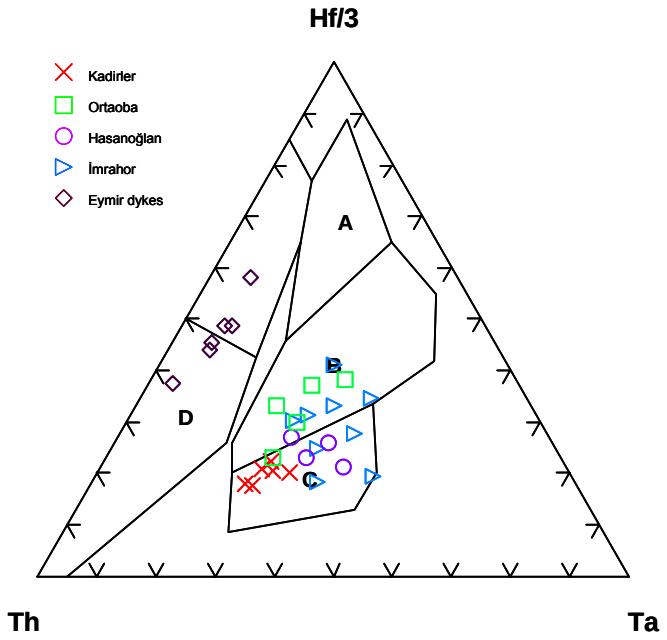

Figure 4.16. Tectonomagmatic discrimination plots for the studied samples (after Wood et al., 1979. Fields: A: N-MORB, B: P-MORB; C: WPB; D: Destructive plate margin basalts).

diagram of Meshede (1986). The İmrahor dykes seems very harmonious; all of them are plotted in the destructive plate margin basalts field. When compared with the previous results, this time, the whole dyke samples fall inside a single field and it may be suggested that they are probably related to an arc-related origin.

The basic rocks of İmrahor once more signify the presence of various tectonic settings such that they are plotted in both the alkaline WPB and E-MORB fields. The most of the alkaline samples that are of within-plate character in the former diagrams appear consistently in the alkaline WPB and sub-alkaline gabbro and ultramafic samples are plotted in the E-MORB field, supporting the previous results. However, one of the alkaline basalt samples is plotted in the E-MORB. Transitional lavas, on the other hand, look also consistent as reflected by their appearance in the E-MORB. At this time, it can be suggested that the sub-alkali Ortaoba and İmrahor samples together with transitional İmrahor basalts are probably of E-MORB type as also supported by the tectonomagmatic discrimination diagram of Meshede (1986).

Tectonic settings of the studied rocks based on the interpretations of the tectonodiscrimination diagrams are summarized in Table 4.1.

4.8. Inter-Element Relationships and Multi-element Variations

The Kadirler and Hasanoğlan basalts have Zr/Nb ratios (3.5-6.1) similar to oceanic-island basalts (Zr/Nb=5.83; Sun and McDonough 1989), while the Ortaoba extrusive rocks are more variable Zr/Nb ratios ranging between 5.9 and 8.2. The sub-alkali Ortaoba lavas (Zr/Nb=7.9-8.2) are more akin to E-type MORB (Zr/Nb=8.8; Sun and McDonough 1989). The alkaline ones, on the other hand, have ratios (Zr/Nb=5.9-7.8) more comparable to OIB. The İmrahor samples span a large range with ratios between 3.1 and 9.2, among which the sub-alkali and transitional samples (Zr/Nb=6.4-9.2) are similar to E-MORB, whereas the alkali basalts (Zr/Nb=3.1-7.4) are more akin to OIB. The İmrahor dykes, in contrast to the rest of samples, reflects highly depleted Nb contents as indicated by Zr/Nb ratios of 28.9- 43.4.

Table 4.1. Summary of geochemical features of studied samples based on discrimination diagrams.

Location	Lithology	Character	Tectonic setting
Hasanoğlan	Basalt	Alkaline	WPB
Kadirler	Basalt	Alkaline	WPB
Ortaoba	Basalt	Alkaline and Sub-alkaline	WPB and P-MORB
İmrahor	Basalt	Alkaline and Transitional	WPB and P-MORB
	Gabbro	Sub-alkaline	WPB and P-MORB
	Ultramafic	Transitional	WPB and P-MORB
Eymir Complex	Diabase	Sub-alkaline	IAB, N-MORB

Multi-element variation diagrams (or spider-diagrams) when compared with REE patterns are powerful tools to identify possible tectonic suits of the investigated rocks. In this part, in order to make the identification simpler, the patterns produced by basic rocks from each locality were given separately and the different patterns derived from the same locality were also indicated in different colors and symbols. It should also be noted that the order of trace elements in multi-element variation diagrams were selected based on Pearce (1983). The normalization values are according to Pearce (1983) for multi-element variation diagrams and Sun and McDonough (1989) for REE variation diagrams.

In the multi-element variation diagram, the Hasanoğlan lavas are characterized by enrichment relative to MORB in the whole spectrum of trace elements (except K and Rb), displaying a humped pattern (Figure 4.17). These features may indicate a within-plate tectonic setting for the generation of Hasanoğlan basalts (e.g. Sun and McDonough, 1989; Chaffey et al. 1989). On the other hand, the marked depletion displayed by K and Rb is most probably due to the low-grade hydrothermal alteration leading to mobility of these elements. When REE is considered, the Hasanoğlan lavas exhibit highly fractionated patterns

with varying degrees of LREE enrichment relative to HREE ($[La/Yb]_N$=18.1-27.3), indicating OIB-type characteristics (Figure 4.18).

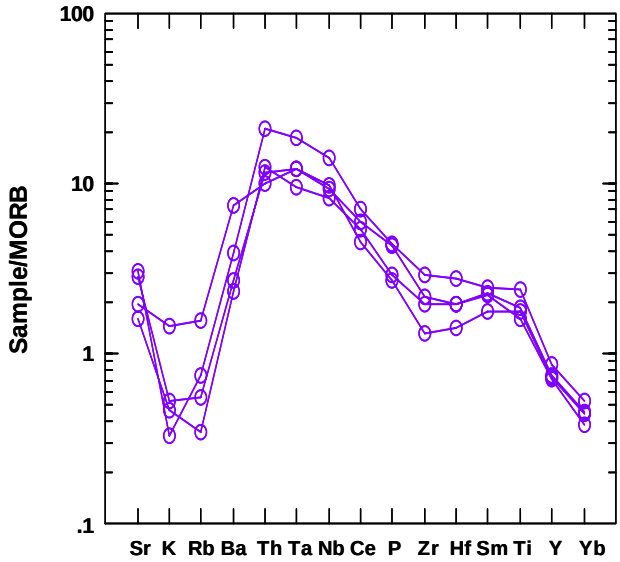

Figure 4.17. MORB-normalized trace element patterns for the Hasanoğlan extrusives (normalization values from Pearce, 1983).

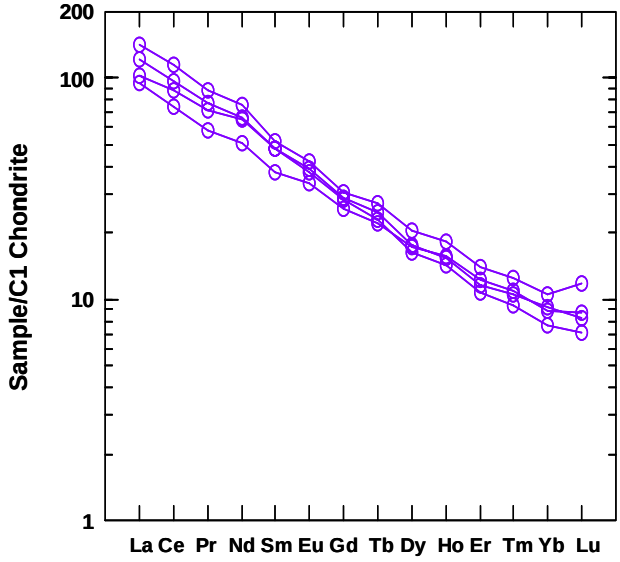

Figure 4.18. C1 Chondrite-normalized REE patterns for the Hasanoğlan extrusives (normalization values from Sun and McDonough, 1989).

The İmrahor basalts are characterized by highly variable nature in the multi-element variation diagram, which is presumably indicative for the presence more than one source (Figure 4.19). Indeed, if enrichment levels are taken into account, it is revealed that the İmrahor basalts contain two different types of lavas. One type displays variable enrichment relative to MORB, indicating an intra-plate character for these basaltic rocks (e.g. Sun and McDonough, 1989; Dupuy et al., 1989). Note that the effect of intense alteration on the sample A-22 which shows marked depletion in K content but extreme enrichment in Ba relative to the other samples. The other type is characterized by relative depletion compared to the first one; however, these samples also represent enrichment relative to N-MORB. Both groups have similar REE characteristics so that they are characterized by varying degrees of enrichment in LREE relative to HREE (Figure 4.20). Nevertheless, it can be noticed that the first group have more-enriched nature ($[La/Yb]_N$=11.7-27.5) especially in LREE, suggesting that they are of OIB-type ($[La/Yb]_N$=20.9; Sun and Donough, 1989), whereas the second group ($[La/Yb]_N$=3.5-6.2) reflects characteristics of E-type MORB ($[La/Yb]_N$=3.2; Sun and McDonough, 1989).

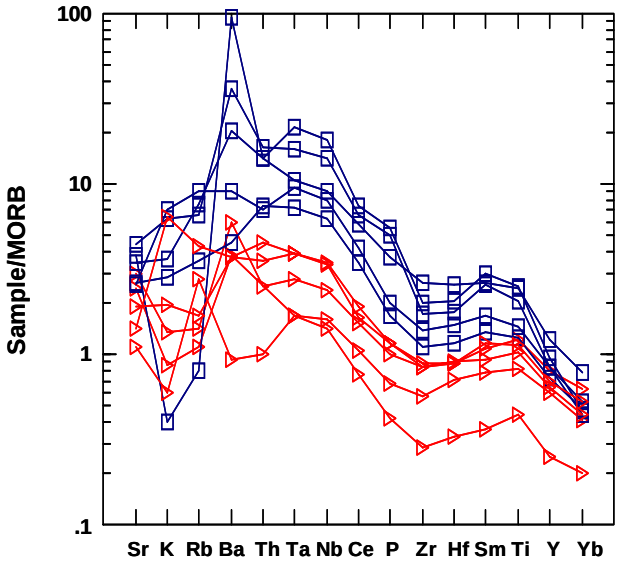

Figure 4.19. MORB-normalized trace element patterns for the basic igneous rocks of İmrahor (normalization values from Pearce, 1983).

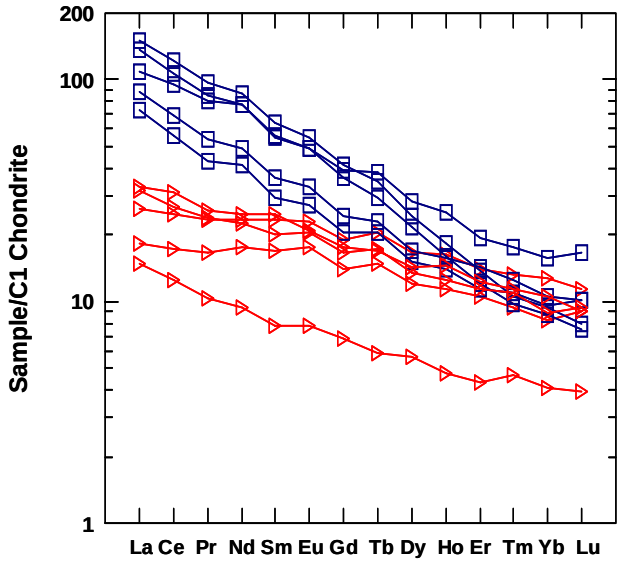

Figure 4.20. C1 Chondrite-normalized REE patterns for the basic igneous rocks of İmrahor (Normalization values from Sun and McDonough, 1989).

The diabase dykes of Eymir Complex display different trace element patterns compared to those of the other samples as indicated by significant depletion in Nb abundances, suggesting a subduction-related event for their origin (Figure 4.21). The considerable Nb depletion (Zr/Nb=28.9-43.4) together with the relatively flat patterns (Figure 4.22) reflected by REE elements ($[La/Yb]_N$=1.9-2.2) may indicate that they should have been generated above a supra-subduction zone.

The selective enrichment of the LIL elements relative to the HFS elements, especially indicated by Th enrichment followed by negative Nb anomaly is generally assumed to be diagnostic features of volcanic arc basic rocks (e.g. Pearce, 1982; Gamble et al., 1993; Thirlwall et al., 1994) and this Nb anomaly is commonly considered to be derived from subduction component (e.g. Green 1995). However, if their transitional character between MORB and IAB, as reflected by numerous diagrams, is taken into account, it can be suggested that they may have been generated above a back-arc basin (e.g. Kay et al., 1986; Stern et al., 1990). It is documented that back-arc basins are characterized by a wide range of geochemical compositions as indicated by

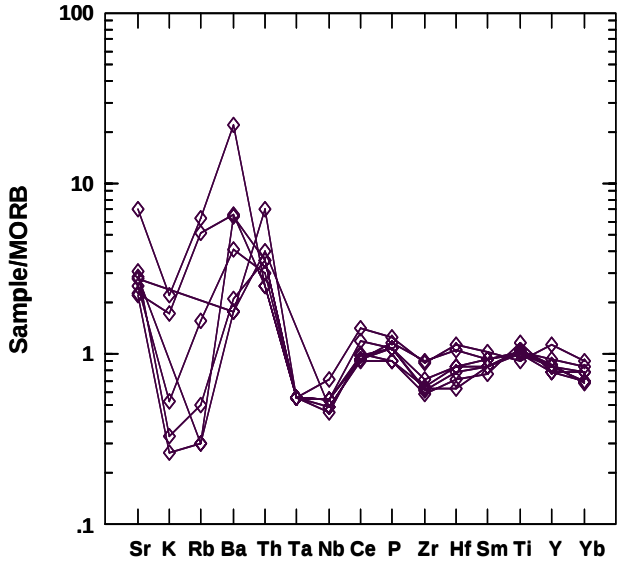

Figure 4.21. MORB-normalized trace element patterns for the diabase dykes of Eymir Complex from İmrahor area (normalization values from Pearce, 1983).

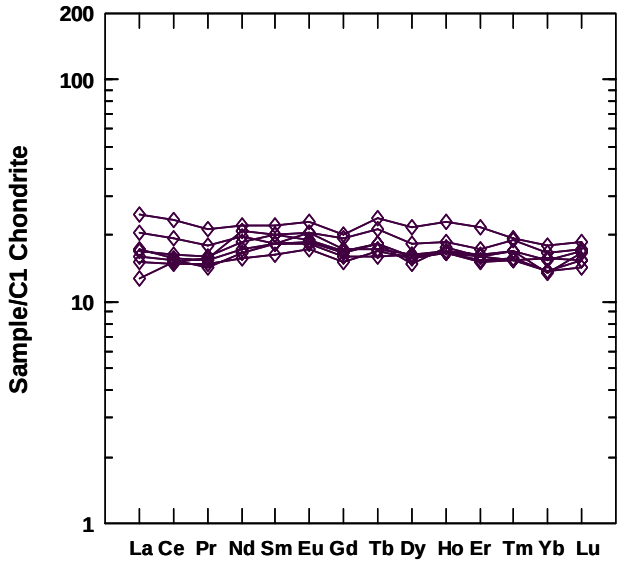

Figure 4.22. C1 Chondrite-normalized REE patterns for the diabase dykes of Eymir Complex from İmrahor area (normalization values from Sun and McDonough, 1989).

basalts with distinctive subduction signatures which may be sometimes impossible differentiate from arc basalts to basalts with little or no evidence of subduction, based on the distance from the trench area (e.g. Hochstaedter et al., 1990; Ewart et al. 1998; Gribble et al. 1998). Flat rare-earth patterns are also reported in some back-arc basin basalts (e.g. Leat et al., 2000; Corcoran and Dostal, 2001; Fretzdorff et al. 2002).

Thus, on the basis of these features pointed out above, geochemical characteristics of the diabase dykes are comparable to those of back-arc basins rather than island-arcs. Furthermore, it must be emphasized that the flat patterns of the REE may indicate the absence of a residual garnet from the source, thus corresponding to melting depths shallower than those dominated by garnet lherzolite (e.g. Arndt et al., 1993).

The Ortaoba volcanics are represented by enriched patterns relative to N-MORB as observed in the previous examples. Similar to the İmrahor samples, these lavas also consist of two different groups as revealed by their multi-element patterns (Figure 4.23). The first group is characterized by relative enrichment compared to the other, thus they are more akin to OIB (e.g. Thirlwall 1997; Norman and Garcia, 1999). Furthermore, if REE abundances are considered (Figure 4.24), the first group reflects more fractionated nature with $[La/Yb]_N$ ratios changing between 9.8 and 16.2, whereas, the second group have $[La/Yb]_N$ ratios of 4.2-4.6, suggesting their E-MORB character.

The Kadirler lavas are characterized by humped multi-element patterns, indicating their generation in a within-plate tectonic setting (Figure 4.25; Sun and McDonough, 1989; Chaffey et al. 1989). On the other hand, relatively low Zr/Nb ratios (4.3-5.4) together with the typical fractionated REE pattern ($[La/Yb]_N$=9.8-22.7) suggest that they are comparable to OIB (Figure 4.26).

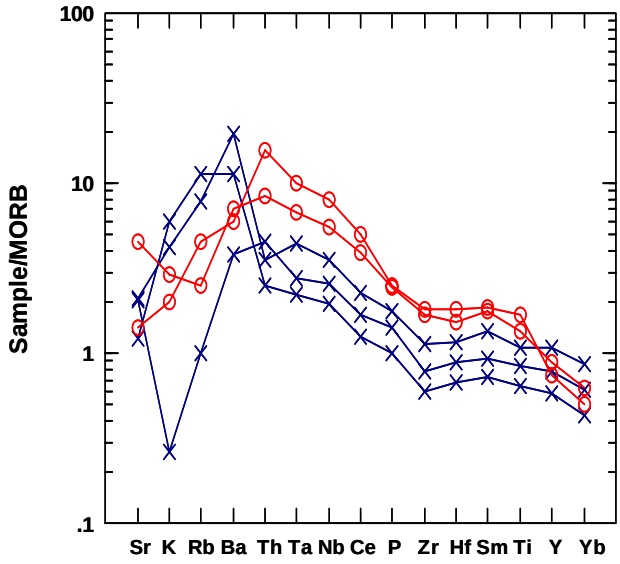

Figure 4.23. MORB-normalized trace element patterns for the Ortaoba lavas (normalization values from Pearce, 1983).

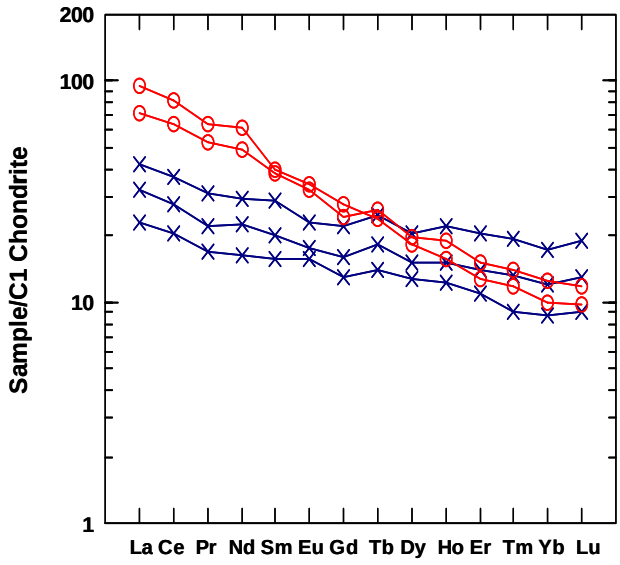

Figure 4.24. C1 Chondrite-normalized REE patterns for the Ortaoba lavas (Normalization values from Sun and McDonough, 1989).

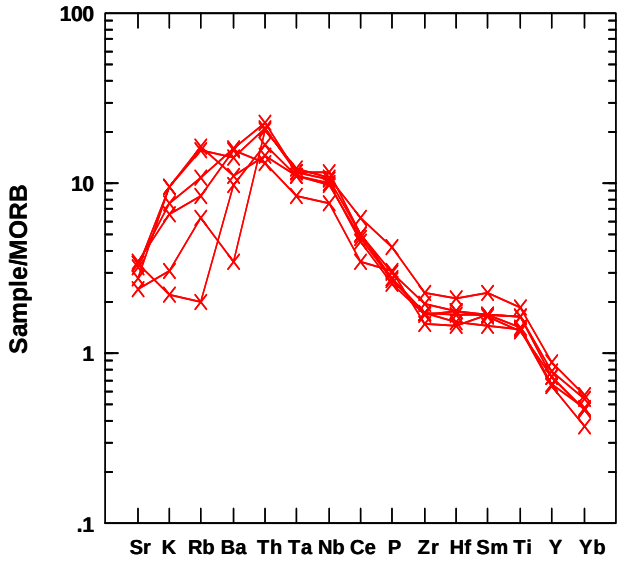

Figure 4.25. MORB-normalized trace element patterns for the Kadirler lavas (normalization values from Pearce, 1983).

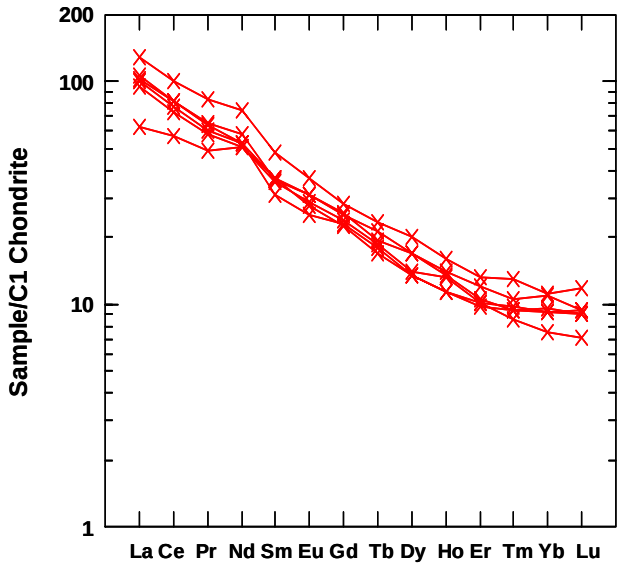

Figure 4.26. C1 Chondrite-normalized REE patterns for the Kadirler lavas (normalization values from Sun and McDonough, 1989).

4.9. Discussion on the Geochemical Characteristics of the Studied Rocks within the Karakaya Complex

Large variations in terms of major element compositions displayed by the İmrahor and Ortaoba basic rocks indicate a non-uniform origin of these samples. Especially considering the TiO_2 contents the difference is obvious: the İmrahor samples have TiO_2 (wt.%) contents ranging between 0.66 and 3.78% and the Ortaoba lavas between 0.97 and 2.53%. The alkaline İmrahor and Ortaoba basalts are characterized by the contents from 1.90 to 3.78%, which are conformable to OIB (>2% TiO_2; e.g. Harris, 1983). In the tectonomagmatic discrimination diagrams, these basalts are plotted in the within-plate field, suggesting that they may be OIB-like. Furthermore, the humped trace element patterns (Zr/Yb=3.1-7.8) together with fractionated REE patterns ($[La/Yb]_N$=9.8-27.5) clearly show their oceanic island origin. On the other hand, the sub-alkaline samples from both localities reveal that they are similar to P-MORB (TiO_2 (wt.%)=1.46-1.59%; Schilling et al., 1983) with TiO_2 in the interval of 0.97-1.84% rather than N-MORB (TiO_2 (wt.%)=1.15-1.31%; Schilling et al. 1983). Their sub-alkaline to transitional character as well as their appearance in the MORB and P-MORB fields in the discrimination diagrams indicate their generation in a spreading center. However, the trace element and REE patterns unravel that they are not related to N-MORB. The enrichment relative to N-MORB observed in the spider diagrams together with LREE enrichment patterns certainly suggests the contribution of a non-depleted source in their generation. The inter-element ratios (Zr/Yb=6.4-9.2 and $[La/Yb]_N$=3.5-6.2) also support their P-type MORB origins.

The diabase dykes, however, are very different compared to the rest of İmrahor samples, since they bear no enriched source signature. The TiO_2 (wt.%) contents changing in a narrow interval (1.35-1.75%) indicate a uniform origin for these basalts. Although these contents are similar to those observed in P-type MORB, they are plotted in the fields that characterize both MORB and IAB in the tectonic discrimination diagrams. It should be also noted that in the Hf-Th-Ta diagram (Wood et al., 1979), they are entirely within the range of destructive plate margin basalts. The multi-element variation patterns reveal their generation above a supra-subduction zone as indicated by the considerable depletion in Nb contents. This is also evidenced by their Zr/Nb

ratios changing between 28.9 and 43.4. However, at this point the question is whether they have been formed in above an island-arc (IAB-type), continental-arc (CAB-type) or back-arc basin (BABB-type).

Island arc volcanic rocks display noticeably dissimilar geochemical characteristics compared with MORB and OIB, possessing high abundances of LREE and LIL elements relative to HFS elements (e.g. Saunders et al., 1980; Gamble et al., 1993; Thirlwall et al., 1994; Pearce and Peate, 1995), which is thought to be result from refertilization of the mantle wedge by slab-derived fluids (e.g. Gill 1981, Arculus and Powell, 1986; Pearce and Parkinson; 1993; Arculus, 1994) and it is widely accepted that high LIL/HFSE ratios are indication of subduction-related events (e.g. Arculus and Powell, 1986; Hawkesworth et al., 1993; Brenan et al. 1994). This feature is very apparent on the multi-element plot as reflected by nearly flat pattern after variable enrichment of LIL elements. If REE patterns are examined, their relatively flat patterns also support the subduction-related origin for these samples. Nevertheless, their transitional features as reflected by both MORB- and IAB-like characteristics may display that they were formed in supra-subduction zone extensional regimes (back-arc basin) (e.g. Stern et al., 1990; Ewart et al., 1994; Pearce et al., 1995; Petford and Atherton, 1995). The TiO_2 (wt.%) contents (1.35-1.75%) are also more appropriate to BABB (TiO_2=0.7-2%; Hawkins, 1976; Hawkins and Melchior, 1985; Eissen et al., 1991; Pearce et al., 1995) instead of IAB (generally <TiO_2=1; Woodhead et al., 1998).

Another confirmation regarding back-arc origin of the diabase dykes comes from the La/Yb vs. Nb/La diagram (Figure 4.27). It is observed that the diabase samples entirely fall inside the BABB field and well-separated from the fields of MORB and arc basalts, suggesting their generation in a back-arc basin setting.

Such arc-related enriched basalts are typical features of modern back-arc basin basalts built on thin continental crust (e.g. Petford and Atherton, 1995). In addition, in mature oceanic arcs, high- to medium-K calc-alkaline magmas infrequently display strongly enriched levels in HFSE (e.g. Pearce, 1983; Pearce and Peate, 1995). Thus, an intra-oceanic back-arc basin may be more

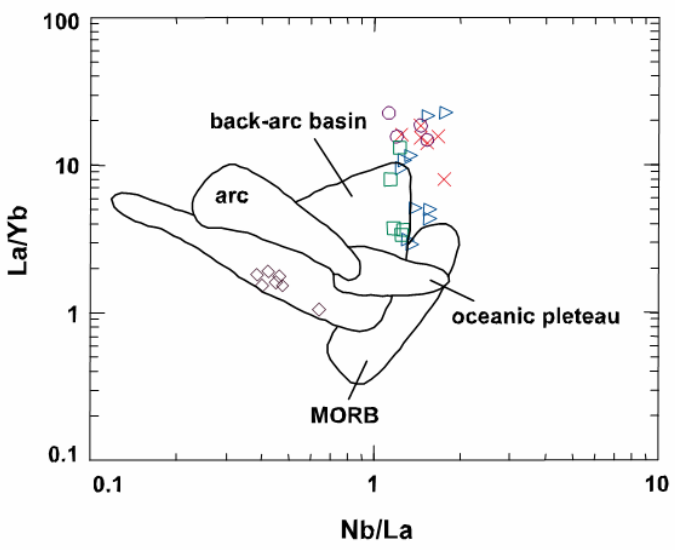

Figure 4.27. Plot of La/Yb vs. Nb/La for discrimination of investigated rocks (after Ichiyama and Ishiwatari, 2004). Fields from; arc (Hochstaedter et al., 1996); back-arc basin (Allan and Gorton, 1992); MORB (Sun et al., 1979); oceanic plateau (Floyd, 1989; Tejada et al., 2002). For symbols see Figure 4.1.

appropriate for tectonic setting of the diabase dykes (e.g. Gribble et al. 1998) instead of an intra-continental back-arc setting (e.g. Saleh and Boyle 2001).

The Kadirler and Hasanoğlan lavas in contrast to the İmrahor and Ortaoba are dominated by single tectonic setting, which can be noticed at the first sight by their restricted TiO_2 contents with 2.38-3.56% for the Hasanoğlan and 2.01-2.79% for the Kadirler. Such TiO_2 contents are more akin to OIB as the beginning. The supporting results also come from the discrimination diagrams and multi-element variations, indicating that they are alkaline within-plate basalts. In addition, their REE patterns with varying degrees of enrichment of LREE relative to HREE ($[La/Yb]_N$=9.8-27.3) are also conformable to their OIB-character.

CHAPTER 5

DISCUSSION

In the extent of this study, several tectono-stratigraphic units including the pre-Permian Eymir Metamorphic Complex, Middle Triassic (Anisian) Bahçecik Formation, Triassic Olukman Formation, Middle-Upper Triassic (Ladinian?-Carnian) Ortaoba Unit, and Middle Triassic (Anisian) pillow basalt-limestone association within the Karakaya Complex from the Central and Northwestern Turkey were studied in terms of geological relations, petrography, petrology and tectonic setting.

In this chapter, the data obtained will be discussed within the framework of Karakaya Complex dilemma starting with the field data.

In the Imrahor area, the Eymir Metamorphic Complex is represented by a low-grade dynamothermally metamorphosed volcano-sedimentary assemblage as documented in the previous works (e.g. Akyürek et al. 1984; Koçyiğit 1987). The contact relationships and age of this metamorphic unit, however, is controversial. While Koçyiğit (1987) regarded the unit as a tectonic entity with a thrust contact to the surrounding units, Akyürek et al. (1984) interpreted the contact of this unit with the clastic rocks of the Karakaya Complex as depositional. In the study area, the Eymir Metamorphic Complex tectonically underlies the Olukman Formation (generalized field relationships of the units in the İmrahor area are illustrated in Figure 5.1). Petrographical observations also support this result, as indicated by obvious difference in terms of type of metamorphism between the two units. The presence of Na-amphibole-bearing HP/LT metavolcanics in the metamorphic complex in contrast to incipiently metamorphosed and weakly foliated metaclastic/metavolcanic rocks of the Bahçecik Formation clearly suggests that they should be tectonically related and a transitional contact as suggested by Akyürek et al. (1984) is not possible. The age of complex is ascribed to Lower Triassic based on the fossil

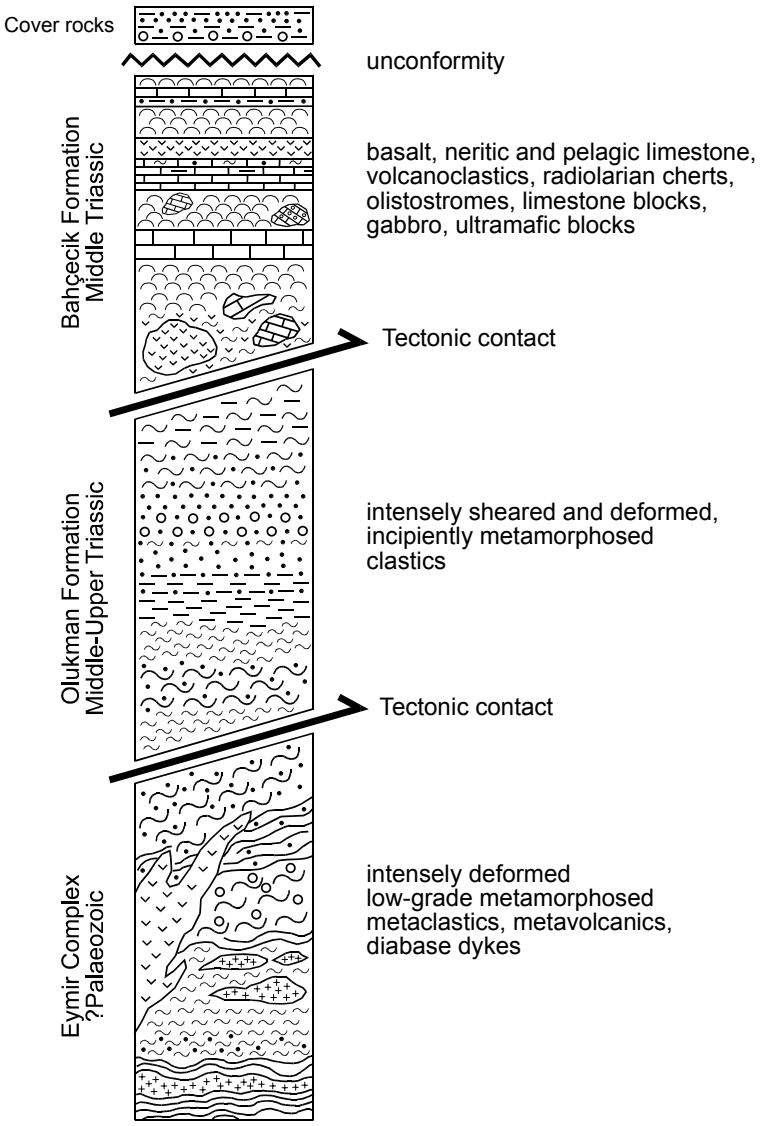

Figure 5.1. Generalized field relationships of the studied units in the İmrahor area (not to scale).

fauna within the transitional zone (Akyürek et al., 1979a,b, 1980, 1981, 1984). Since such a transitional zone is not confirmed in this study, it can be suggested that the Lower Triassic age should probably corresponds the lower parts of the Olukman Formation. However, it is important to note that both the Bahçecik and Olukman formations include clasts of metamorphic rocks, akin to those of the metamorphic complex, which would suggest that Eymir was already formed and even metamorphosed and yielded clasts for the Karakaya

units. Therefore, a pre-Karakaya age suggested by various authors (e.g. Koçyiğit et al., 1991) is still valid for the age of Eymir unit.

The contact between the Bahçecik Formation and the Olukman Formation, in the study area, is also represented by a thrust fault. This is clearly recognized in the field (Figures 2.13, 2.14) such that a zone consisting of highly sheared and deformed rocks including gabbro, ultramafics, basalts and greywackes. Along the thrust, the Bahçecik Formation is thrust onto the clastics of the Olukman Formation. This result is again contrasting with that of Akyürek et al. (1984), who suggested that the two formations are intercalated with each other. The fossil assemblages found in the shallow-water limestones of the unit alternated with basalts indicate a Middle Anisian (Middle Triassic) age (determined by Prof. Dr. Demir Altıner). This age data is also conformable with Anisian age suggested by Özgül (1993; with fossil determinations of Prof. Dr. Demir Altıner). The same unit is assigned to Middle-Upper Triassic by Akyürek et al. (1984). In this study, no age data was acquired from the Olukman Formation.

In brief, the geological observations within the framework of this study confirms the tectonic melange character of the complex, including most probably a pre-Karakaya subduction/accretion complex with HP/LT metamorphism (Eymir Metamorphic Complex), a volcano-sedimentary complex with mass-flow deposits, turbidites and olistolites formed in close vicinity of an oceanic seamount (Bahçecik Formation and Kadirler rocks), another volcano-sedimentary unit with MOR-type rocks (Ortaoba Unit) and a sedimentary melange with clastic rocks of continental crust origin as well as limestone blocks derived from a platform margin (Olukman Formation). Their tectonic juxtaposition should be post Late-Triassic but pre-Early Jurassic as previously suggested by various authors (e.g. Okay 2000).

The petrographical examination reveals that these main tectono-stratigraphic units in the study area are represented by variably metamorphosed rock types, including metabasalts, metaclastics, slates, phyllites and schists.

All the basalts studied are characterized by hydrothermal alteration as reflected by a variety of colors in hand specimen; dark green, dark blue and

red, though some appear in nearly blackish tones. Furthermore, most of them exhibit spherical degassing structures mostly filled by secondary minerals. The Ortaoba basalts are distinctive with their greenish colors and absence of vesicles or amygdales. On the other hand, the Kadirler and Hasanoğlan basalts comprise lots of amygdales (e.g. Figure 3.36). Most of the Kadirler lavas are blackish colored, while the Hasanoğlan basalts generally display blackish and reddish tones of colors. The basalts from İmrahor are more akin to those of Kadirler and Hasanoğlan, since they generally show amygdaloidal texture with blackish and reddish tones of color.

Under microscope, the presence of low-grade metamorphism is confirmed in all of the basalts such that the primary mineral phases are intensely overprinted by secondary ones (petrographical features of geochemically analyzed samples are summarized in Table 5.1). All the basalts are holocrystalline and porphyritic and pre-dominant primary mineral phases are clino-pyroxene and plagioclase. Olivine appears as another primary mineral but less common than the former two. The alkaline Ortaoba and Ti-augite bearing basalts from İmrahor are especially distinguished by their large crystal sizes of both phenocrysts and microcrysts in groundmass. Interestingly, olivine could not be determined among the mineral assemblage of the Ortaoba basalts. The existence of Ti-augite in some of the Ortaoba and İmrahor extrusives is also another unique feature of these basalts that the rest do not display. However, the Ti-augite bearing basalts from Ortaoba and İmrahor are actually different. Ti-augite is apparently the most abundant primary mineral in the İmrahor basalts, whereas the Ortaoba lavas are rather dominated by plagioclase. Olivine, in all cases, appears as psedomorphs, totally replaced by serpentine minerals. Kaersutite is another distinguishing characteristic of Ti-augite bearing basalts of İmrahor (Figure 3.2). It should be noted that Ti-augite bearing basalts of Ortaoba do not include kaersutite. The Ti-augite bearing Ortaoba basalts are characterized by a secondary mineral assemblage of actinolite, epidote group, chlorite, and absence of prehnite/pumpellyite. On the other hand, in the Kadirler, Hasanoğlan and most of the İmrahor basalts actinolite is absent. Therefore, the Ortaoba lavas indicate higher metamorphic temperatures when compared with the rest.

Table 5.1. Summary of petrographical features of the geochemically analyzed rocks.

Location	Rock type	Texture	Mineralogy		Distinctive features
			Primary	Secondary	
İmrahor	basalt (Ti-augite-bearing)	aphanitic, partly amygdaloidal, holocrystalline, porphyritic, seriate, sub-ophitic	cpx + plag + oli ± kae ± bm	chl + serp + pist + zoi/clizoi ± preh + ser + cc	presence of Ti-aug and kae, relatively large crystals
	gabbro	phaneritic, holocrystalline, porphyritic, sub-ophitic	cpx + plag + oli	serp + chl + act + preh + ser	well-developed sub-ophitic texture
	ultramafic	phaneritic, holocrystalline, equigranular, mesh-texture,	oli + cpx + kae + bm	serp + act	high oli content, well-developed mesh-texture
Hasanoğlan	basalt	aphanitic, amygdaloidal, holocrystalline, porphyritic, seriate, glomeroporphyritic, sub-ophitic	cpx + plag + oli	chl + pist + zoi/clizoi + serp + cc + qz	Highly amygdaloidal
Ortaoba	basalt	aphanitic, holocrystalline, porphyritic, seriate, sub-ophitic	cpx + plag	act + chl + pist + zoi/clizoi + cc + qz	absence of vesicles
Kadirler	basalt	aphanitic, holocrystalline, porphyritic, seriate, glomeroporphyritic, sub-ophitic	oli + cpx + plag	chl + pist + serp + cc + qz + ser	highly amygdaloidal, intense calcitization
Eymir Complex	diabase	micro-phaneritic, holocrystalline, equigranular	hb + plag + qz	chl + act + pist + zoi/clizoi + Na-amph + preh + ser ± cc	presence of hb

Thin section examination reveals that the clastic rocks are represented by both incipiently-metamorphosed ones and metaclastics. They are generally grayish, brownish colored, less commonly greenish and governed by same types of clastics. Although this leads to confusion in differentiating the two in hand specimen, under microscope there is a clear difference in terms of degree of metamorphism. The clasts in metamorphic ones are highly elongated in especially finer-grained clastics. Furthermore, the presence of considerable pyroxene fragments (e.g. Figure 3.23) is also a distinctive feature for the metaclastics.

As indicated by geological and petrographical features, the units studied are of very different characteristics. Note that all the units in the study areas, except for the Olukman Formation, are characterized by the presence of basic igneous rocks. In this respect, the geochemical characteristics of the basic rocks were examined to decipher their tectonic origin.

It is important to mention that hydrothermal alteration is of considerable degree, as reflected by high LOI values and unusual major element contents. Therefore, the geochemical nature of the samples was interpreted in terms of relatively immobile elements during low-grade metamorphism.

In the rock classification diagram (Winchester and Floyd, 1977), the samples are grouped into three that is, the alkaline basalts, sub-alkaline basalts and transitional basalts (Figure 4.2). While the Hasanoğlan and Kadirler extrusives are of alkaline character, the Ortaoba and İmrahor includes all three groups mentioned above. If the tectonic discrimination diagrams are considered (Figures 4.12 to 4.16) together, it is observed that the Hasanoğlan and Kadirler basalts represent WPB. Amongst the Ortaoba and İmrahor samples, the alkaline rocks are characterized by WPB, whereas subalkaline ones apart from diabase rocks are similar to both WPB and P-MORB (or E-MORB). Diabases from Eymir, on the other, are very different compared to the rest, indicating IAB and N-MORB. Such a scene suggests at this point that diabases should have been derived from different tectonic setting and sources relative to the others. Multi-element and REE patterns also support this hypothesis. They are variably enriched in LIL elements, but associated with depletion (note the

distinctive negative Nb anomaly in Figure 4.21) as indicated by flat-lying patterns with near-MORB abundances. Thus, they should have been generated above a supra-subduction zone. The multi-element and REE variations (Figures 4.19, 4.20, 4.23, 4.24) also make clear the question that the Ortaoba and İmrahor samples are really composed of basic rocks of different types, namely OIB- and P-MORB type? The alkaline Hasanoğlan, Kadirler, and İmrahor samples display variable enrichment in most of the elements as reflected by humped patterns which is characteristics of WPB and their enrichment levels indicate that they are more akin to OIB-type. The sub-alkaline types, in contrast to the former, are more depleted, but they are also characterized by an enriched nature. Thus, these samples are affinity to P-MORB, rather than OIB. REE abundances also confirm this result, since the OIB-type samples have higher LREE compared to the P-MORB-type equivalents, followed by a considerable depletion in HREE, thus indicating more fractioned patterns.

In the alkaline OIB-type samples, as mentioned above, there is a substantial depletion in HREE relative to LREE, indicating the presence of garnet as a residual phase in the mantle source. Thus, these basalts should have been derived from a garnet lherzolite source. The P-MORB-type samples do not show such a considerable decrease (Figures 4.20 and 4.24). On the other hand, their relatively low LREE abundances compared with those of alkaline basalts eliminate the possibility that their generation in response to large degrees of melting from a garnet lherzolite source. Therefore, the possibility of a spinel lherzolite source devoid of garnet phase is more likely for the P-MORB-type basic rocks. Unlike the OIB- and P-MORB-type samples, the diabase dykes must reflect involvement of different type of sources during their generation owing to a subduction-related origin. Indeed, low HFSE abundances (near N-MORB) clearly indicate that a depleted mantle source have been involved during their genesis. The relatively low Zr/Y, Nb/La but high Zr/Nb ratios also support this result, suggesting a lithospheric mantle source. The opposite character of OIB-and P-MORB-type samples indicates an astenospheric mantle source, confirming the previous results.

The effect of crustal contamination is another issue to explain for the basic rocks studied. The relatively low ratios in terms of certain elements (La/Ta, La/Nb, Nb/Y and Th/Nb) suggest that crustal effects are of no significance for all the rocks excluding the diabases. The multi-element patterns of OIB- and P-MORB type are also conformable with this suggestion. The ratios mentioned above, however, seem misleading for the diabase rocks, since multi-element abundances exhibit no signature of crustal contamination. This problem actually lies in their back-arc origins, opened on an oceanic lithosphere. This is displayed by their both MORB and IAB character such that LIL and HFS element abundances are apparently lower relative to continental-arc basalts. Thus, low abundances of both LILE and HFSE in the diabase rocks result in high ratios which are not actually caused by crustal contamination.

Similar to the basic rock samples examined in this study, the basic volcanics in the previous geochemical studies are also hydrothermally altered to a certain degree. They comprise three groups when plotted on the rock classification; namely alkaline, sub-alkaline and transitional basalts, resembling the samples in this study (Figure 5.2).

When tectonomagmatic discrimination diagrams are considered (Figure 5.3 to 5.6), it is seen that the basaltic samples in the previous studies are clearly dominated by various types of tectonic settings, including N-MORB, IAT and WPB, which confirms again our results. On the other hand, this study includes P-MORB-type rocks which are not present in the previous studies excluding Floyd (1993).

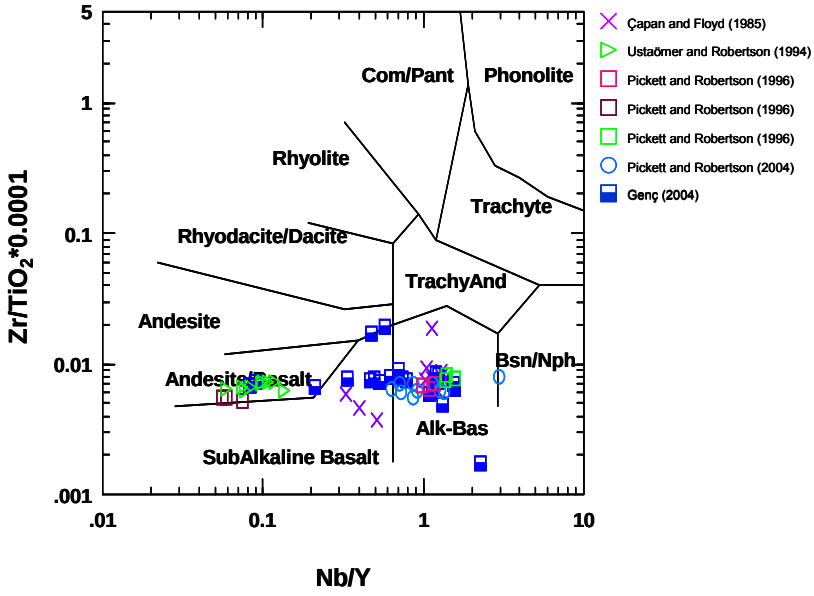

Figure 5.2. The classification of samples from the previous studies on the diagram based on relatively immobile elements (after Winchester and Floyd, 1977; for samples of Pickett and Robertson (1996), brown square: Ortaoba Unit, red square: Nilüfer Unit, green square: Çal Unit).

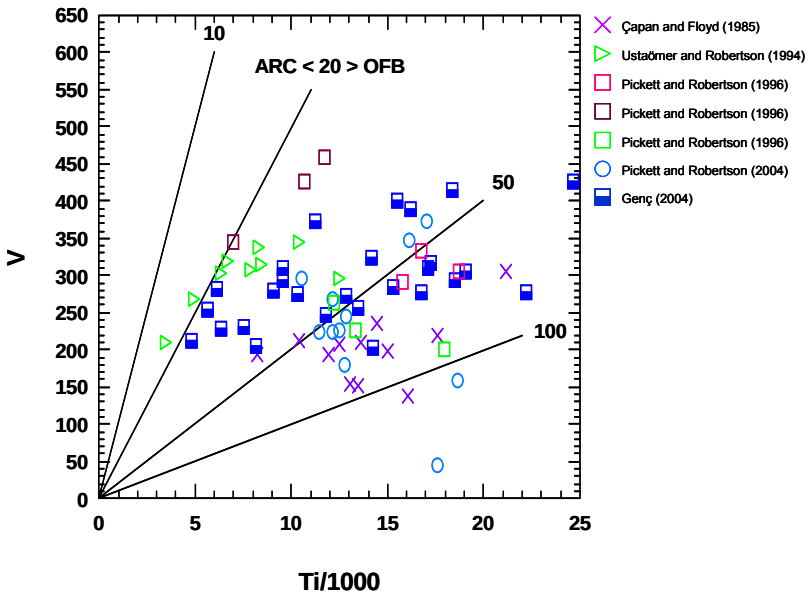

Figure 5.3. Tectonomagmatic discrimination plots for samples from the previous studies (after Shervais, 1982).

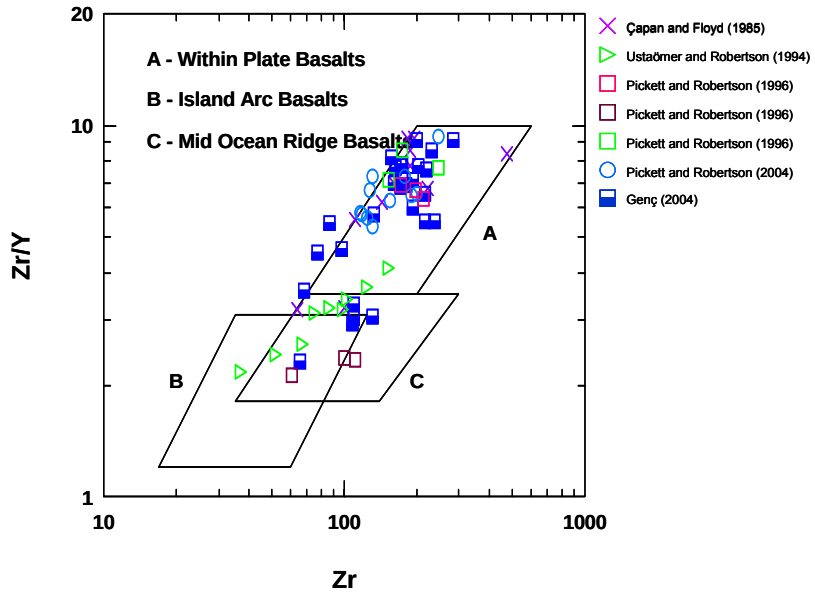

Figure 5.4. Tectonomagmatic discrimination plots for samples from the previous studies (after Pearce and Norry, 1979).

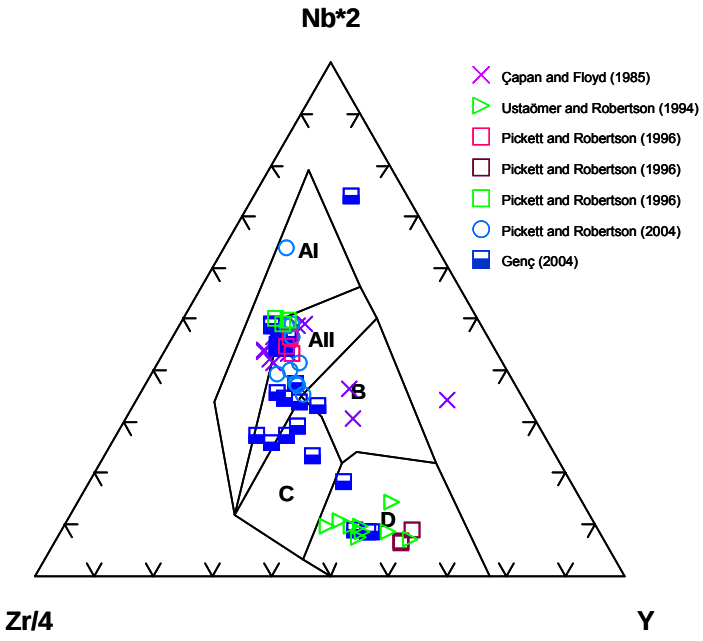

Figure 5.5. Tectonomagmatic discrimination plots for samples from the previous studies (after Meshede, 1986. Fields: AI and AII: WPB; B: P-MORB; C: WPT and VAB; D: N-MORB and VAB).

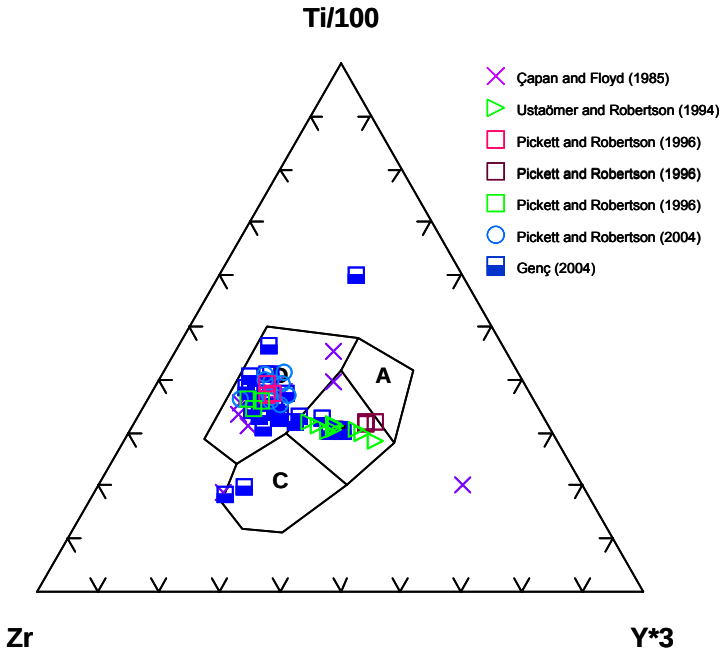

Figure 5.6. Tectonomagmatic discrimination plots for samples from the previous studies (after Pearce and Cann, 1973. Fields: A: IAT; B: MORB and IAT; C: CAB; D: WPB).

Multi-element and REE patterns indicate that the Ankara Group (Çapan and Floyd, 1985), the Nilüfer Unit (Pickett and Robertson, 1996, 2004; Yalınız and Göncüoğlu, 2002; Genç 2004) and the Çal Unit (Pickett and Robertson, 1996) are represented by OIB-type within-plate extrusives, whereas the Küre Unit (Ustaömer and Robertson, 1994) is characterized by back-arc basin lavas (Figure 5.7). It should be noted that the "Nilüfer" samples of Genç (2004) comprise also basalts which are akin to MORB-type with relatively low enrichment levels. However, all the samples were regarded as within-plate basalts in the study of Genç (2004).

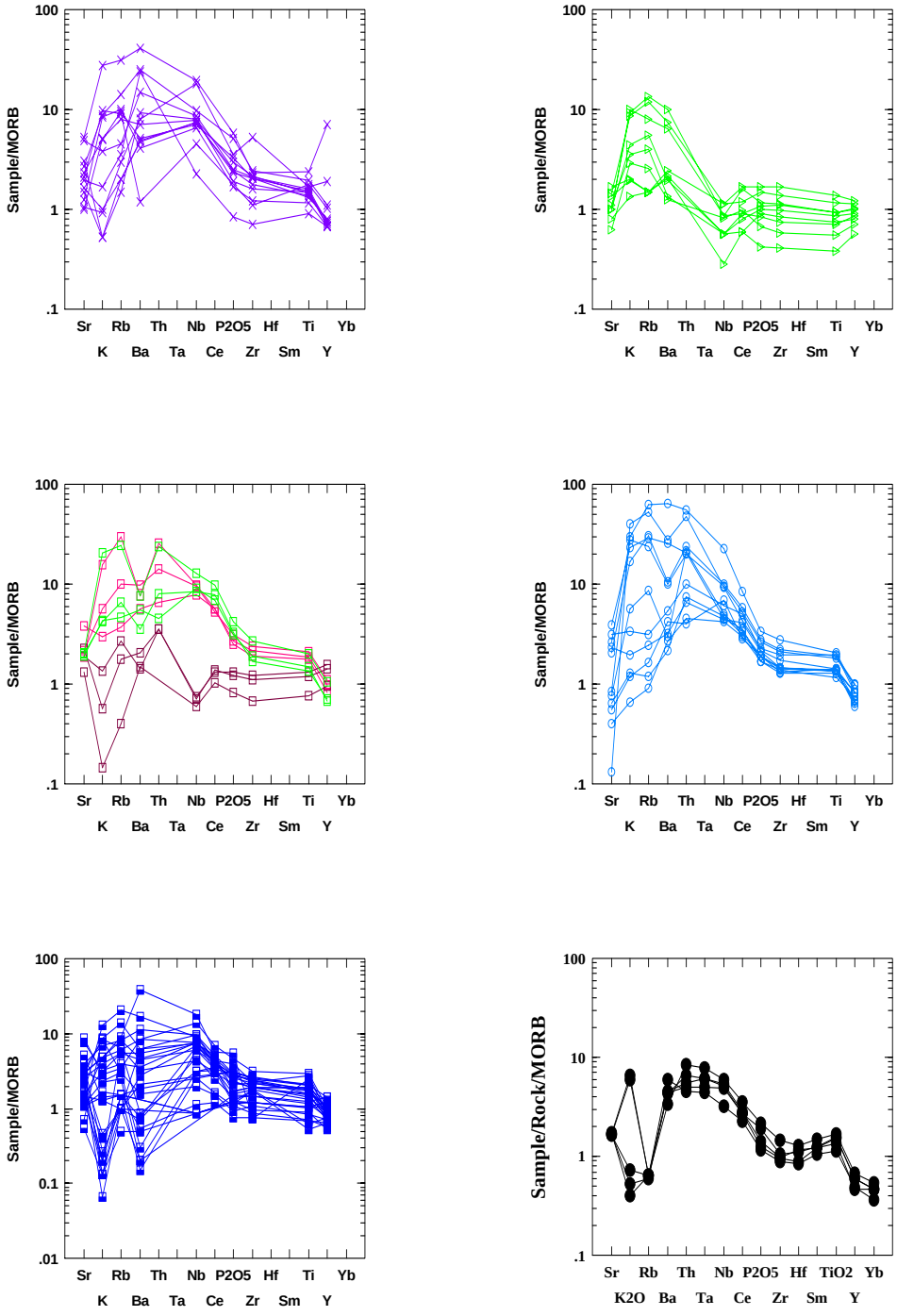

Figure 5.7. MORB-normalized trace element patterns for samples from the previous studies (normalization values from Pearce, 1983; for symbols see Figure 5.2. Samples for the last diagram (indicated by black dots) from Yalınız and Göncüoğlu, 2002).

In this study, the alkaline İmrahor and Hasanoğlan samples from the Bahçecik Formation are represented by OIB-type basalts, whereas the sub-alkaline and transitional İmrahor samples are characterized by P-MORB features. As mentioned above, the Triassic Ankara Group samples of Çapan and Floyd (1985) are of OIB character and Floyd (1993) also documented the presence of basalts with OIB and P-MORB features in the Ankara Group. Therefore, the existence of OIB- and P-MORB type basic rocks within the Karakaya Group in Ankara region is confirmed by this study. On the other hand, the geochemical nature of diabase dykes within the Eymir Complex has been unraveled for the first time in this study and it was suggested that they are arc-related rocks generated above a supra-subduction zone. In this respect, they are analogous to the Küre extrusives as deduced from Figure 4.21. This study indicates that the Ortaoba Unit is dominated by P-MORB type rocks whereas only two samples comprises alkaline OIB-type basalts similar to the Nilüfer Unit (Figure 4.23). However, the Ortaoba basalts were interpreted as N-MORB by Pickett and Robertson (1996). Thus, the presence of basalts with P-MORB characteristics within the Ortaoba Unit has been first documented by this study. The Kadirler basalts were also identified in terms of geochemical aspects for the first time, and described as OIB-type basalts.

In the light of the data acquired from field and geochemical data, the tectonic evolution of the studied units can be summarized as follows:

The Olukman Formation represents a sedimentary melange which was developed in a tectonically active environment as indicated by its clastic nature composed of turbiditic deposits with varying sizes and thickness. Thus, these rapid changes in lithology within the Olukman Formation indicate a tectonically unstable environment during its deposition. The olistostromal parts including neritic limestone clasts which are cemented by a clastic material may signify that limestone clasts should probably have been incorporated into clastics by gravity sliding along a slope. Furthermore, the presence of a small lense of pillow basalts from the Bahçecik Formation within the Olukman Formation also support this idea such that the lava flows accumulating along the margin of slope together with syn-depositional limestones have been transported with mass flows and incorporated into the clastic rocks of the Olukman. The highly

deformed and sheared nature of the unit should be related with a later tectonic event.

The Bahçecik Formation, on the other hand, comprise significant amounts of basic igneous rocks, thus the geochemical implications are of considerable importance for the unit to clarify its tectonic evolution. As mentioned in the previous parts, the Bahçecik Formation consists of basalt flows alternating with both neritic and pelagic limestones. The association of OIB-type basalts with neritic limestones and P-MORB-type basalts with both types of limestones demonstrates that the type of magmatism should have changed in the course of time with the variations in the formation depth. However, the alternation of shallow-water limestones only with OIB-type lavas may suggest a seamount origin for the Bahçecik Formation. In this respect, the neritic limestones should have been deposited along a shallow platform related to an oceanic island with an alkaline volcanic activity characterized by OIB-type basaltic flows taking place in the same time. The basalts with P-MORB signatures, on the other hand, indicate that the volcanism was also effective in the deeper parts of the oceanic environment as reflected by their alternation with pelagic limestones and radiolarian cherts.

The presence of P-MORB magmatism is more favorable with an extension within an oceanic crust, as no indication of a continental crust contamination is observed. In this model, OIB-type magmas, which are derived from an asthenospheric garnet lherzolite source, are plume-related. Thus, at the first stages, the oceanic lithosphere starts to extend in response to the uprising of the asthenospheric mantle and the first products of magmatism will be of OIB-type generating oceanic seamounts. Since, the water depth is relatively shallow at the margins of the volcanic island in this stage; the neritic limestones should have been deposited in alternation with lava-flows. The sedimentary infill along the slopes of the volcanic edifice of the seamount will mainly including volcanic detritus and blocks derived from the platform margins. The mass-flow-type volcanoclastic rocks of the Bahçecik Formation as well as the similar deposits in Ortaoba (Pickett and Robertson, 2004) very probably represent these slope deposits.

The alternation of P-MORB volcanic rocks with pelagic limestones indicates deposition in a deeper environment. Moreover, these are formed later than the seamount-type rocks. This would suggest that the enriched MOR-type volcanic rocks are somehow related to the plume activity that produced the OIB-type rocks mentioned above. If this is the case, the ongoing extension within the oceanic plate above the plume may have resulted in formation of a MOR, with chemical characteristics of plume-related MOR volcanics. The existence of gabbro and ultramafics with P-MORB character also confirm this model, probably indicating the lower parts of newly-developed oceanic crust. Therefore, the Bahçecik Formation reflects an immature (or aborted) oceanic crust formation as indicated by the absence of true MORB (N-MORB). By this the juxtaposition of the OIB and P-MORB-type volcanic rocks should have been realized during the formation of the Karakaya melange. It should be pointed out, that this tectonic interpretation is highly speculative, as the geochemical data yet is limited.

The Eymir Complex on the other hand is characterized by a metamorphic complex with HP/LT minerals (Figure 3.26) indicating a subduction/accretion history. The turbiditic clastics, which are the dominant rock assemblage in the complex, should have been transported into their depositional area by mass flows. The basaltic rocks associated with the clastics reflect syn-depositional volcanism. However, when the subduction occurred, all the rock units were intensely sheared and deformed as they were accreted and incorporated into the accretionary prism. The presence of cross-cutting diabase dykes indicates the magmatic activity after the subduction event. As shown by their geochemical signatures (back-arc basin), the Eymir Complex was formed in a supra-subduction setting. The model proposed in this study is that, these dykes have intruded into the subduction/accretion complex probably in a back-arc basin setting.

The Ortaoba Unit is represented by a deep-marine depositional setting as indicated by absence of carbonates within the unit. The unit most probably reflects a slope, because the associated volcano-clastics are of P-MORB features. Such a geochemical indication also suggests the influence of a plume-related source during the generation of basaltic lava flows the Ortaoba

volcanics are considered as the counterparts of the P-MORB-type volcanic rocks of the Bahçecik Formation. The Ladian (?)-Carnian age of the Ortaoba unit is indicative for its formation in a plume-related MOR-type setting towards Late Triassic time.

To summarize the discussion, the problem of the “Karakaya Complex” which corresponds to a melange of greywacke, conglomerate, siltstone intercalated with spilitic basalt, radiolarite and mudstone with exotic limestone blocks, is still remained unsolved regarding its geodynamic setting. The models including an Early Triassic intra-continental rift basin (Yılmaz, 1981; Şengör and Yılmaz 1981; Koçyiğit 1987; Altıner and Koçyiğit 1993; Genç and Yılmaz 1995; Göncüoğlu et al., 2000) as well as a the subduction-accretion prism introduced by Tekeli (1981) and followed by others (e.g. Pickett and Robertson, 1996; Okay, 2000) can not be fully confirmed by the geochemical data obtained in this study.

This study suggest that the Karakaya Complex is characterized by rocks of various tectonic settings (seamount, plume-related MOR and back-arc basin) which have been later assembled and incorporated in a prism, forming a tectonic melange. Therefore, it would be incorrect to ascribe the Karakaya Unit to a single tectonic environment. Our model, here, actually partly confirms the two types of hypothesis mentioned in the previous paragraph. A rift model could be accepted, but excluding intra-continental type, since this study indicates the rift basin has been opened above an oceanic lithosphere. Therefore, in the model suggested by this study, a rift basin or marginal basin opened on a continental lithosphere is not confirmed. On the other hand, a subduction/accretion model is partly supported by the subduction-related diabase dykes, however no other sign of subduction have been reflected by the studied rocks. This study confirms the model proposed by Pickett and Robertson (1996, 2004) that the Nilüfer Unit is represented by seamounts dominated by OIB-type magmatism. A large oceanic plateau or igneous province suggested for the Nilüfer Unit by Okay (2000) and Genç (2004) have not been confirmed, as already suggested by Yalınız and Göncüoglu (2002).

CHAPTER 6

CONCLUSIONS

1. The rock-units in the studied areas are composed of a number of tectono-stratigraphic units (the Olukman Formation, the Bahçecik Formation, the Ortaoba Unit, the Nilüfer Unit and the informal pillow basalt-limestone association) which represent the Karakaya Complex and a pre-Karakaya basement unit (the Eymir Complex).

2. Detailed geochemical work on 32 samples from the igneous rocks in these units revealed the following:

a- the basic igneous rocks of the Bahçecik Formation display affinity to OIB and P-MORB, whereas The Ortaoba lavas are of P-MORB character. The Nilüfer-type basalts from the Ortaoba and Kadirler areas are characterized by OIB features.

b- the diabase dykes cross-cutting the Eymir Complex represent a back-arc basin setting above supra-subduction zone.

3. All the basaltic samples apart from the diabase dykes indicate asthenospheric mantle sources, whereas the latter signify involvement of depleted mantle sources.

4. The OIB-type basalts are associated with neritic limestones, and yielded early Middle Triassic (Middle Anisian) ages while P-MORB-type basalts are accompanied by dominantly by pelagic limestones with late Middle-early Upper Triassic fossils.

5. It is suggested that the volcanism in the Karakaya Complex is characterized by rocks of various tectonic settings (seamount, plume-related MOR and back-

arc basin) which have been later assembled and incorporated in a prism, forming a tectonic melange.

6. The state-of-art information obtained by this study and the re-evaluation of preliminary geochemical data shows that none of the previously suggested tectonic models fulfill the petrogenetic requirements and the solution of the Karakaya Problem is only possible by multidisciplinary work including detailed petrological study of the igneous events and their ages.

REFERENCES

Abdel-Rahman, A. M., 2002. Mesozoic volcanism in the Middle East: geochemical, isotopic and petrogenetic evolution of extension-related alkali basalts from central Lebanon. Geological Magazine, 139, 621-640.

Abdel-Rahman, A. M., and Nassar, P.E., 2004. Cenozoic volcanism in the Middle East: petrogenesis of alkali basalts from northern Lebanon. Geological Magazine, 141, 545-563.

Akyürek, B., 1981. İç Anadolu'nun jeolojisi sempozyumu. Ankara melanjının kuzey bölümünün temel jeoloji özellikleri, TJK yayını, 41-52, Ankara.

Akyürek, B., and Soysal, Y., 1983. Biga Yarımadası Güneyinin (Savaştepe-Kırkağaç-Bergama-Ayvalık) temel jeoloji özellikleri. Maden Tetkik ve Arama Enstitüsü Dergisi, 95/96, 1-13.

Akyürek, B., Bilginer, E., Dağer, Z., and Sunu, O., 1979a. Hacılar (K. Çubuk-Ankara) bölgesinde Alt Triyas'ın varlığı. Türkiye Jeoloji Kurumu Bülteni, 22/2, 169-174.

Akyürek, B., Bilginer, E., Çatal, E., Dağer, Z., Soysal, Y., and Sunu, O., 1979b. Eldivan-Şabanözü (Çankırı) dolayında ofiyolit yerleşimine ilişkin bulgular. JMO yayınları, S.9, Ankara.

Akyürek, B., Bilginer, E., Çatal, E., Dağer, Z., Soysal, Y., and Sunu, O., 1980. Eldivan-Şabanözü (Çankırı), Hasayaz-Çandır (Kalecik-Ankara) dolayının jeolojisi. Maden Tetkik ve Arama Enstitüsü, Rapor No : 6741 (unpublished).

Akyürek, B., Duru, M., Sütçü, Y.F., Papak, İ. Şaroğlu, F., Pehlivan, N., Gönenç, O., Granit, S., and Yaşar, T., 1996. Ankara ilinin çevre jeolojisi ve doğal kaynaklar projesi (1994 yılı Jeoloji grubu çalışmaları). Maden Tetkik ve Arama Enstitüsü, Rapor No: 9961 (unpublished).

Akyürek, B., Bilginer, E., Akbaş, B., Hepşen, N., Pehlivan, Ş., Sunu, O., Soysal, Y., Dağer, Z., Çatal, E., Sözeri, B., Yıldırım, H., and Hakyemez, Y., 1982. Ankara-Elmadağ-Kalecik dolayının jeolojisi. Maden Tetkik ve Arama Enstitüsü, Rapor No : 7298 (unpublished).

Akyürek, B., Bilginer, E., Akbaş, B., Hepşen, N., Pehlivan, Ş., Sunu, O., Soysal, Y., Dağer, Z., Çatal, E., Sözeri, B., Yıldırım, H., and Hakyemez, Y., 1984. Ankara-Elmadağ-Kalecik dolayının temel jeolojik özellikleri. Jeoloji Mühendisliği, 20, 31-46.

Akyüz, H.S. and Okay, A.I., 1996. A section across a Tethyan suture in northwestern Turkey. International Geology Review, 38, 405-418.

Akyüz, H.S., and Okay, A.I., 1998. Manyas güneyinin (Balıkesir) jeolojisi ve mavişistlerin tektonik konumu. Maden Tetkik ve Arama Enstitüsü Dergisi, 120, 1-13.

Al-Saleh, A.M., and Boyle, A.P., 2001. Neoproterozoic ensialic back-arc spreading in the eastern Arabian Shield: geochemical evidence from Halaban Ophiolite. Journal of African Earth Sciences, 33, 1-15.

Allan, J.F., and Gorton, M.P., 1992. Geochemistry of igneous rocks from Legs 127 and 128, Sea of Japan. Proceedings of the Ocean Drilling Program, Scientific Results, 128, 905-929.

Altıner, D., and Koçyiğit, A., 1993. Third remark on the geology of the Karakaya basin. An Anisian megablock in northern central Anatolia: micropaleontologic, stratigraphic and tectonic implications for the rifting stage of Karakaya basin, Turkey. Revue de Paleobiologie, 12, 1-17.

Altınlı, E., 1975. Geology of the Central Sakarya. Proceedings of the 50th Anniversary of the Turkish Republic Earth Science Congress. Mineral Research and Exploration Institute of Turkey (MTA) Publications, 159-191 (in Turkish with English abstract).

Arculus, R.J., 1994. Aspects of magma genesis in arcs. Lithos, 33, 189-208.

Arculus, R.J., and Powell, J.R., 1986. Source component mixing in the regions of arc magma generation. Journal of Geophysical Research, 91, 5913-5926.

Arndt, N.T., Czamanske, G.K., Wooden, J.L., and Fedorenko, V.A., 1993. Mantle and crustal contributions to continental flood volcanism. Tectonophysics, 223, 39–52.

Bailey, E.B., and McCallien, W.J., 1953. Serpentinite lavas, the Ankara melange and the Anatolian thrust. Transactions of the Royal Society of. Edinburgh, 62, 403-442.

Batman, B., 1977. Haymana kuzeyinin jeolojik evrimi ve yöredeki melanjın incelenmesi: Doçentlik Tezi, 172 pp, Yerbilimleri Enst. Beytepe, Ankara.

Batman, B., 1978. Haymana kuzeyinin jeolojik evrimi ve yöredeki melanjın incelenmesi I: Stratigrafi birimleri. Yerbilimleri, 4, 95-124.

Ben Othman, D., White, W.M., and Patchett, J., 1989. The geochemistry of marine sediments, island arc magma genesis, and crust-mantle recycling. Earth and Planetary Science Letters, 94, 1-21.

Bienvenu, P., Bougeault, H., Joron, J.-L., Treuil, M., and Dmitriev, L., 1990. MORB alteration: rare-earth elementrnon-rare-earth hygromagmatophile element fractionation. Chemical Geology, 82, 1-14.

Bingöl, E., 1975. Batı Anadolu'nun jeotektonik evrimi. Maden Tetkik ve Arama Enstitüsü Dergisi, 86, 14-34.

Bingöl, E., Akyürek, B., and Korkmazer, B., 1973. Biga yarımadasının jeolojisi ve Karakaya Formasyonunun bazı özellikleri. Proceedings of the 50th Anniversary of the Turkish Republic Earth Science Congress. Mineral Research and Exploration Institute of Turkey (MTA) Publications, 70-77 (in Turkish).

Blanc, P., 1965. Serie stratigraphique de Çal Köy (Anatolie Occidentale, Turquie): presence de spilites dans le Permien. Soc. Geol. Fr. C.R., 3, 100-102.

Blanc, P., 1969. Etude petrographique de la granidiorite de Yenice, Peninsula de Çanakkale. Ph. D. Thesis. University of Paris, France.

Bozkurt, E., 1990. Karakaya Napı içinde yeni bir Karbonifer ve Permiyen bulgusu. Maden Tetkik ve Arama Dergisi, 110, 181-188.

Bradshaw, T.K., and Smith, E.I., 1994. Polygenetic Quaternary volcanism at Crater Flat, Nevada. Journal of Volcanology and Geothermal Research 63, 165-182.

Brenan, J.M., Shaw, H.F., Phinney, D.L., and Ryerson, F.J., 1994. Rutile-aqueous fluid partitioning of Nb, Ta, Hf, Zr, U and Th: implications for high field strength element depletions in island arc basalts. Earth and Planetary Science Letters, 128, 327-339.

Brinkmann, R., 1971. Jungpalaozoikum und alteres Mesozoikum in NW-Anatolien. Maden Tetkik ve Arama Dergisi, 76, 56-67.

Chaffey, D. J., Cliff, R.A., and Wilson, B.M., 1989. Characterization of the St. Helena magma source. In: Saunders, A.D., and Norry, M.J. (eds.), Magmatism in the Ocean Basins. Geological Society, London, Special Publications, 42, 257-276.

Condie, K.C., 2003. Incompatible element ratios in oceanic basalts and komatiites: tracking deep mantle sources and continental growth rates with time. Geochemistry Geophysics Geosystems, 4, 252-268.

Condie, K.C., 2005. High field strength element ratios in Archean basalts: a window to evolving mantle sources of mantle plumes? Lithos, 79, 491-504.

Corcoran, P.L., and Dostal, J., 2001. Development of an ancient back-arc basin overlying continental crust; the Archean Peltier Formation, Northwest Territories, Canada. Journal of Geology, 109, 329-348.

Çalgın, R., Pehlivanoğlu, H., Ercan, T., and Şengün, M., 1973. Ankara civarı jeolojisi, Maden Tetkik ve Arama Enstitüsü, Rapor No: 6487 (unpublished).

Çapan, U.Z., and Floyd, P.A., 1985. Geochemical and petrographic features of metabasalts within units of Ankara melange, Turkey. Ofioliti, 10, 3-18.

Çapkınoğlu, Ş., and Bektaş, O., 1998. Karakaya Kompleksi'ne ait Karasenir Formasyonu (Amasya) içindeki kireçtaşı olistolitlerinden Erken Devoniyen konodontları. Maden Tetkik ve Arama Dergisi, 120, 159-170.

Davies, G.R., Norry, M.J., Geralch, D.C. and Cliff, R.A., 1989. A combined chemical and Pb–Sr–Nd isotope study of the Azores and Cape Verde hotspots: the geodynamic implications. In: Saunders, A.D., and Norry, M.J., (eds.), Magmatism in the Ocean Basins. Geological Society, London, Special Publications, 42, 231-256.

Doğan, M., 1990. Pontid kuşağı Paleotetis ofiyolitlerinin jeokimyasal verilerle petrolojik, magmatik ve tektonik modellenmesi. Doktora Tezi, İstanbul Üniversitesi, 200 pp, İstanbul.

Dupuy, C., Barsczus, H.G., Dostal, J., Vidal, Ph., and Liotard, J.-M., 1989. Subducted and recycled lithosphere as the mantle source of ocean island basalts from southern Polynesia, central Pacific. Chemical Geology, 77, 1-18.

Eissen, J.P., Lefevre, C., Maillet, P., Morvan, G., and Nohara, M., 1991. Petrology and geochemistry of the central north Fiji basin spreading center (southwest Pacific) between 16 degrees and 22 degrees. Marine Geology, 98, 201-239.

Ellam, R.M., 1992. Lithospheric thickness as a control on basalt geochemistry. Geology, 20, 153-156.

Ellam, R.M., Menzies, M.A., Hawkesworth, C.J., Leeman, W.P., Rosi, M., and Serri, G., 1988. The transition from calc-alkaline to potassic orogenic magmatism in the Aeolian Islands, Southern Italy. Bulletin of Volcanology, 50, 386-398.

Ercan, T., Ergül, E., Akçaören, F., Çetin, A., Granit, S., and Asutay, J., 1990. Balıkesir-Bandırma arasının jeolojisi, Tersiyer volkanizmasının petrolojisi ve bölgesel yayılımı. Maden Tetkik ve Arama Enstitüsü Dergisi, 110, 113-130.

Erk, A.S., 1977. Ankara civarında Genç Paleozoyiğin Kulm fliş formasyonu. Maden Tetkik ve Arama Dergisi, 88, 73-94.

Erol, O., 1956. Ankara güneydoğusundaki Elma Dağı ve çevresinin jeolojisi ve jeomorfolojisi üzerinde bir araştırma. MTA yayınları, Seri. D, 9, Ankara.

Ewart, A., Bryan, W.B., Chappell, B.W., and Rudnick, R.L., 1994. Regional geochemistry of the Lau-Tonga arc and backarc systems. Proceedings of the Ocean Drilling Program, Scientific Results, 135, 385-425.

Ewart, A., Niu, Y., Collerson, K. D., Regelous, M., and Wendt, J. I., 1998. Geochemical evolution within the Tonga-Kermadec-Lau arc-back-arc systems: the role of varying mantle wedge composition in space and time. Journal of Petrology, 39, 331-368.

Fitton, J.G. and Upton, B.G.J., 1987. Alkaline Igneous Rocks. Geological Society, London, Special Publications, 30, 568 pp.

Floyd, P.A., 1989. Geochemical features of intraplate oceanic plateau basalts. In: Saunders, A.D., and Norry, M.J., (eds.), Magmatism in the Ocean Basins. Geological Society, London, Special Publications, 42, 215-230.

Floyd, P.A., 1993. Geochemical discrimination and petrogenesis of alkalic basalt sequences in part of the Ankara melange, central Turkey. Journal of the Geological Society, London, 150, 541-550.

Floyd, P.A., and Winchester, J.A., 1978. Identification and discrimination of altered and metamorphosed volcanic rocks using immobile elements. Chemical Geology, 21, 291-306.

Fretzdorff, S., Livermore, R.A., Devey, C.W., Leat, P.T., and Stoffers, P., 2002. Petrogenesis of the backarc East Scotia Ridge, south Atlantic ocean. Journal of Petrology, 43, 1435-1467.

Frey, F.A., Green, D.H., and Roy, S.D., 1978. Integrated models of basalt petrogenesis: a study of quartz tholeiites to olivine melilitites from south-eastern Australia utilizing geochemical and experimental petrological data. Journal of Petrology, 19, 463-513.

Gamble, J.A., Smith, I.E.M., McCulloch, M.T., Graham, I.J., and Kokelaar, B.P., 1993. The geochemistry and petrogenesis of basalts from the Taupo volcanic zone and Kermadec island, S.W. Pacific. Journal of Volcanology and Geothermal Research, 54, 265-290.

Genç, S.C., and Yılmaz, Y., 1995. Evolution of the Triassic continental margin, northwest Anatolia. Tectonophysics, 243, 193-207.

Genç, Ş., Selçuk, H., Cevher, F., Gözler,Z., Karaman, T., Bilgi, C., and Akçören, F. 1986. İnegöl (Bursa) – Pazaryeri (Bilecik) arasının jeolojisi. Maden Tetkik ve Arama Enstitüsü Dergisi, 95/96, 1-13, Rapor No: 7912, 68 pp (unpublished).

Genç, Ş.C., 2004. A Triassic large igneous province in the Pontides, northern Turkey: geochemical data for its tectonic setting. Journal of Asian Earth Sciences, 22, 503-516.

Gill, J.B., 1981. Orogenic Andesites and Plate Tectonics. New York, Springer-Verlag, 390 pp.

Göncüoğlu, M.C., Dirik, K., and Kozlu, H., 1997. Pre-Alpine and Alpine Terranes in Turkey: explanatory notes to the terrane map of Turkey. Annales Geologique de Pays Hellenique, 37, 515-536.

Göncüoğlu, M.C., Erendil, M., Tekeli, O., Aksay, A., Kuşçu, İ., and Ürgün, B., 1987. Geology of the Armutlu Peninsula. IGCP Project 5, Guide Book. Field Excursion along W-Anatolia, 12-18.

Göncüoğlu, M.C., Kuwahara, K., Tekin, K.U., and Turhan, N., 2004. Upper Permian (Changxingian) radiolarian cherts within the clastic successions of the “Karakaya Complex” in NW Anatolia. Turkish Journal of Earth Sciences, 13, 201-213.

Göncüoğlu, M.C., Turhan, N., Şentürk, K., Özcan, A., and Uysal, Ş., 2000. A geotraverse across NW Turkey: tectonic units of the Central Sakarya region and their tectonic evolution. In: Bozkurt, E., Winchester, J., and Piper, J.A., (eds.), Tectonics and magmatism in Turkey and the Surrounding Area. Geological Society, London, Special Publications, 173, 139-161.

Gözler, M.Z., Ergül, E., Akçaören, F., Genç, S.C., Akat, Ü., and Acar, Ş., 1984. Çanakkale Boğazı doğusu-Marmara Denizi güneyi-Bandırma-Balıkesir-Edremit ve Ege Denizi arasındaki alanın jeolojisi ve kompilasyonu. Maden Tetkik ve Arama Enstitüsü Raporu [in Turkish with English abstract].

Green, T.H., 1995. Significance of Nb/Ta as an indicator of geochemical processes in the crust-mantle system. Chemical Geology, 120, 347-359.

Green, T.H., Sie, S.H., Ryan, C.G., and Cousens, D.R., 1989. Proton microprobe-determined partitioning of Nb, Ta, Zr, Sr and Y between garnet, clinopyroxene and basaltic magma at high pressure and temperature. Chemical Geology, 74, 201-216.

Gribble, R.F., Stern, R.J., Newman, S., Bloomer, S.H. and O'Hearn, T., 1998. Chemical and isotopic composition of lavas from the northern Mariana Trough; implications for magma genesis in back-arc basins. Journal of Petrology, 39, 125-154.

Harris, C., 1983. The petrology of lavas and associated plutonic inclusions of Ascension Island. Journal of Petrology, 24, 424-470.

Hart, S.R., 1988. Heterogeneous mantle domains signatures, genesis and mixing chronologies. Earth and Planetary Science Letters, 90, 273-296.

Hart, S.R., Erlank, A.J., and Kable, E.J.D., 1974. Sea Floor Basalt Alteration: Some Chemical and Sr Isotopic effects. Contributions to Mineralogy and Petrology, 44, 219-230.

Hart, W.K., Wolde, G.C., Walter, R.C., and Mertzman, S.A., 1989. Basaltic volcanism in Ethiopia: constraints on continental rifting and mantle interactions. Journal of Geophysical Research, 94, 7731-7748.

Hawkesworth, K., Gallagher, K., Hergt, J.M., and McDermott, F., 1993. Mantle and slab contributions in arc magmas. Annual Review of Earth and Planetary Science, 21, 175-204.

Hawkins, J.W., 1976 Petrology and geochemistry of basaltic rocks of the Lau Basin. Earth and Planetary Science Letters, 28, 283-297.

Hawkins, J.W., and Melchior J.T., 1985. Petrology of Mariana trough and Lau basin basalts. Journal of Geophysical Research, 90, 11431-11468.

Hochstaedter, A.G., Gill, J.B., and Morris, J.D., 1990. Volcanism in the Sumisu Rift, II. Subduction and nonsubduction related components. Earth and Planetary Science Letters, 100, 195-209.

Hochstaedter, A.G., Kepezhinskas, P., Defant, M., Drummond, M., and Koloskov, A., 1996. Insights into the volcanic arc mantle wedge from magnesian lavas from the Kamchatka arc. Journal of Geophysical Research, 101, 697-712.

Hoernle, K., 1998. Geochemistry of Jurassic oceanic crust beneath Gran Canaria (Canary Islands): Implications for crustal recycling and assimilation. Journal of Petrology, 39, 859-880.

Hoernle, K., and Schmincke, H. U., 1993. The role of partial melting in the 15 Ma geochemical erosion of Gran Canaria: a blob model for the Canary hotspot. Journal of Petrology, 34, 599-626.

Hofmann, A.W., 1997. Mantle geochemistry: the message from oceanic volcanism. Nature, 385, 219-229.

Hofmann, A.W., Jochum, K.P., Seufert, M., and White, W.M., 1986. Nb and Pb in oceanic basalts: new constraints on mantle evolution. Earth and Planetary Science Letters, 79, 33-45.

Humpris, S.J., and Thompson, G., 1978. Hydrothermal alteration of oceanic basalts by seawater. Geochimica et Cosmochimica Acta, 42, 107-125.

Ito, E., White, W.M., and Gobel, C., 1987. The O, Sr, Nd and Pb isotope geochemistry of MORB. Chemical Geology, 62, 157-176.

Jenner, G.A., Foley, S.F., Jackson, S.E., Green, T.H., Fryer, B.J., and Longerich, H.P., 1994. Determination of partition coefficients for trace elements in high pressure–temperature experimental run products by laser ablation microprobe-inductively coupled plasmamass spectrometry (LAM-ICP-MS). Geochimica et Cosmochimica Acta, 58, 5099-5130.

Kay, R.W., Rubbenstone, J.L., and Kay, S.M., 1986. Aleutian terrains from Nd isotopes. Nature, 322, 605-609.

Kaya, O., 1991. Stratigraphy of the Pre-Jurassic sedimentary rocks of the western parts of Turkey; type area study and tectonic considerations. type area study and tectonic considerations. Newsletter for Stratigraphy, 23, 123-140.

Kaya, O., and Mostler, H., 1992. A Middle Triassic age for low-grade greenschist facies metamorphic sequence in Bergama (İzmir), western Turkey: the first paleontological age assignment and structural-stratigraphic implications. Newsletter for Stratigraphy, 26, 1-17.

Kaya, O., Wiedmann, J., and Kozur, H., 1986. Preliminary report on the stratigraphy, age and structure of the so-called Late Paleozoic and/or Triassic “mélange or “suture zone complex” of northwestern and western Turkey. Yerbilimleri, 13, 1-16.

Kaya O., Özkoçak, O., and Lisenbee, A., 1989. Stratigraphy of the pre-Jurassic blocky sedimentary rocks to the south of Bursa, NW Turkey. Mineral Research and Exploration of Turkey (MTA) Bulletin, 109, 15-24.

Kerrich, R.W., Wyman, D., Fan, J., and Bleeker, W., 1998. Boninite series: low-Ti tholeiite associations from the 2.7 Ga Abitibi greenstone belt. Earth and Planetary Science Letters, 164, 303-316.

Koçyiğit, A., 1987. Tectono-stratigraphy of the Hasanoglan (Ankara) region: evolution of the Karakaya orogen. Yerbilimleri, 14, 269-293

Koçyiğit, A., 1991. An example of an accretionary forearc basin from northern Central Anatolia and its implications for the history of subduction of Neo-Tethys in Turkey. Geol .Soc.Am. Bull., 103, 22-36.

Koçyiğit, A., 1992. Southward-vergent imbricate thrust zonein Yuvaköy: A record of the latest compressional event related to the collisional tectonic regime in Ankara-Erzincan Suture zone, TAPG Bulletin, 4/I, 111-118.

Koçyiğit, A., and Lünel, A.T., 1987. Geology and tectonic setting of Alcı region, Ankara. METU Journal of Pure and Applied Sciences, 20, 35-57.

Koçyiğit, A., Kaymakçı, N., Rojay, B., Özcan, E., Dirik, K., and Özçelik, Y., 1991. İnegöl-Bilecik-Bozüyük arasında kalan alanın jeolojik etüdü. Orta Doğu Teknik Üniversitesi-Türkiye Petrolleri Anonim Ortaklığı projesi raporu, n° 90-03-09-01-05, 1395.

Kozur, H., 1997. Pelagic Permian and Triassic of the western Tethys and its paleogeographic and stratigraphic significance. Abstracts, XLVIII. Berg- und Hüttenmannischer Tag, Technische Universitat Bergakademie Freiberg, 21-25.

Kozur, H., and Kaya, O., 1994. First evidence of pelagic Late Permian conodonts from NW Turkey. Neues Jahrbuch für Geologie und Paleontologie Monatshefte, 6, 339-347.

Kozur, H., Aydın, M., Demir, O., Yakar, H., Göncüoğlu, M.C., and Kuru, F., 2000. New stratigraphic and palaeogeographic results from the Palaeozoic and early Mesozoic of the Middle Pontides (northern Turkey) in the Azdavay, Devrekani, Küre and Inebolu areas: Implications for the Carboniferous-Early Cretaceous geodynamic evolution and some related remarks to the Karakaya oceanic rift basin. Geologica Croatica, 53, 209-268.

Leat, P.T., Livermore, R.A., Millar, I.L., and Pearce, J.A., 2000. Magma Supply in Back-arc Spreading Centre Segment E2, East Scotia Ridge. Journal of Petrology, 41, 845-866.

Leven, E.Ja., and Okay, A.I., 1996. Foraminifera from the exotic Permo-Carboniferous limestone blocks in the Karakaya Complex, northwest Turkey. Rivista Italiana Paleontologia e Stratigrafia, 102, 139-174.

Ludden, J., Gelinas, L., and Trudel, P., 1982. Archaean metavolcanics from the Rouyn-Noranda district, Abitibi greenstone belt, Quebec, Part 2. Mobility of trace elements and petrogenetic constraints. Canadian Journal of Earth Sciences, 19, 2276-2287.

McCulloch, M.T., and Gamble, J.A., 1991. Geochemical and geodynamical constraints on subduction zone magmatism. Earth and Planetary Science Letters, 102, 358-374.

McDonough, W. F., 1990. Constraints on the composition of the continental lithospheric mantle. Earth and Planetary Science Letters, 101, 1-18.

McKenzie, D., and O'Nions, R. K., 1991. Partial melt distributions from inversion of rare earth element concentrations. Journal of Petrology, 32, 1021-1091.

Menzies, M.A., and Kyle, R., 1990. Continental volcanism: a crust-mantle probe. In: Menzies, M.A., (ed.), Continental Mantle, Oxford: Oxford Science Publishers, 157-177.

Meschede, M., 1986. A method of discriminating between different types of mid-ocean ridge basalts and continental tholeiites with the Nb-Zr-Y diagram. Chemical Geology, 56, 207-218.

Moghazi, A.M., 2003. Geochemistry of a Tertiary continental basalt suite, Red Sea coastal plain, Egypt: petrogenesis and characteristics of the mantle source region. Geological Magazine, 140, 11-24.

Nicholson, H., and Latin, D., 1992. Olivine tholeiites from Krafla, Iceland: evidence for variation in melt fraction within a plume. Journal of Petrology, 33, 1105-1124.

Norman, T., 1973. Ankara melanjının yapısı hakkında. Cumhuriyetin 50. Yılı Kongresi Bildiriler Kitabı, 77-94.

Norman, M.D., and Garcia, M.O., 1999. Primitive magmas and source characteristics of the Hawaiian plume: petrology and geochemistry of shield picrites. Earth and Planetary Science Letters, 168, 27- 44.

Okan, Y., 1982. Elmadağ formasyonunun (Ankara) yaşı ve alt bölümleri. Türkiye Jeoloji Kurumu Bülteni, 25, 95-104.

Okay, A.I., 1984a. Distribution and characteristics of the northwest Turkish blueschists. In: Dixon, J.E., and Robertson, A.H.F., (eds.), The geological evolution of the Eastern Mediteranean. Geological Society, London Special Publications, 17, 455-466.

Okay, A.I., 1984b. Kuzeybatı Anadolu'da yer alan metamorfik kuşaklar, in Proceedings Ketin Symposium, Ankara, February 1984, 83-92.

Okay, A.I., 1989. Tectonic units and sutures in the Pontides, northern Turkey. In: Şengör, A.M.C., (ed.), Tectonic Evolution of the Tetyhan Region. Kluwer, 109-115.

Okay, A.I., 2000. Was the Late Triassic orogeny in Turkey caused by the collision of an oceanic plateau ? In: Bozkurt, E., Winchester, J., and Piper, J.A., (eds.), Tectonics and magmatism in Turkey and the Surrounding Area. Geological Society London Special Publication, 173, 139-161.

Okay, A.I., and Mostler, H., 1994. Carboniferous and Permian radiolarite blocks in the Karakaya Complex in northwest Turkey. Turkish Journal of Earth Sciences, 3, 23-28.

Okay A.I., and Tüysüz, O., 1999. Tethyan sutures of northern Turkey. In: Durand, B., Jolivet, L., Horvath, F., and Seranne, M., (eds.), The Mediterranean Basins: Tertiary Extension within the Alpine Orogen. Geological Society, London, Special Publications, 156, 475-515.

Okay, A.I., and Altıner, D., 2004. Uppermost Triassic limestone in the Karakaya Complex – stratigraphic and tectonic significance. Turkish Journal of Earth Sciences, 13, 187-199.

Okay, A.I., and Göncüoğlu, M.C., 2004. The Karakaya Complex: A review of Data and Concepts. Turkish Journal of Earth Sciences, 13, 77-95.

Okay, A.I., Siyako, M., and Bürkan, B.A., 1991. Geology and tectonic evolution of the Biga Peninsula, northwest Turkey. Bulletin of the Technical University of Istanbul, 44, 191-256.

Okay, A.I., Satır, M., Maluski, H., Siyako, M., Monie, P., Metzger, R., and Akyüz, S., 1996. Paleo- and Neo-Tethyan events in northwest Turkey: geological and geochronological constraints. In: Yin, A., and Harrison, M., (eds.), Tectonics of Asia, Cambridge University Press, 420-441.

Özgül, L., 1993. Tectono-stratigraphy of the İmrahor (Ankara) region. B. Sc. Research Project, Middle East Technical University, 47 pp, Ankara.

Özkoçak, O., 1969. Etude geologique du Massif Ultrabasique d'Orhaneli et da sa proche bordure (Bursa, Turquie). Thesis, Univ. De Paris; 191 pp, Paris (unpublished).

Pankhurst, R.J., 1977. Open system fractionation and incompatible element variations in basalts. Nature, 268, 36-38.

Pearce, J.A., 1975. Basalt geochemistry used to investigate past tectonic environments on Cyprus. Tectonophysics, 25, 41-67.

Pearce, J.A., 1980. REE values for various OIB etc. From lead isotope study of young volcanic rocks mid-oceanic ridges, oceanic islands and island arcs. Philosophical Transactions of the Royal Society of London, Series A 297, 409-445.

Pearce, J.A., 1982. Trace element characteristics of lavas from destructive plate boundaries. In: Thorpe, R.S., (ed.), Andesites, 525-548. New York: John Wiley and Sons.

Pearce, J.A., 1983. The role of sub-continental lithosphere in magma genesis at destructive plate margins. In: Hawkesworth, C.J., and Norry, M.J., (eds.), Continental basalts and mantle xenoliths, 230-249. Nantwich: Shiva.

Pearce, J.A., and Cann, J.R., 1973. Tectonic setting of basic volcanic rocks determined using trace element analysis. Earth and Planetary Science Letters, 19, 290-300.

Pearce, J.A., and Norry, M., 1979. Petrogenetic implications of Ti, Zr, Y and Nb variations in volcanic rocks. Contributions to Mineralogy and Petrology, 69, 33-47.

Pearce, J.A., and Parkinson, I.J., 1993. Trace element models for mantle melting: application to volcanic arc petrogenesis. In: Prichard H.M., Alabaster T., Harris N.B.W., and Neary C. R., (eds.), Magmatic Processes and Plate Tectonics. Geological Society, London, Special Publications, 76, 373-403.

Pearce J.W., and Peate D.W., 1995. Tectonic implications of the composition of volcanic arc magmas. Annual Review of Earth and Planetary Science, 23, 251-285.

Pearce, J.A., Ernewein, M., Bloomer, S.H., Parson, L.M., Murton, B.J., and Johnson, L.E., 1995. Geochemistry of Lau Basin volcanic rocks: influence of ridge segmentation and arc proximity. In: Smellie J.L., (ed.), Volcanism Associated with Extension at Consuming Plate Margins. Geological Society, London, Special Publications, 81, 53-75.

Petford, N., and Atherton, M.P., 1995. Cretaceous–Tertiary volcanism and syn-subduction crustal extension in northern central Peru. In: Smellie, J.L., (ed.), Volcanism Associated with Extension at Consuming Plate Margins. Geological Society, London, Special Publications, 81, 233-248.

Pickett, E.A., and Robertson, A.H.F., 1996. Formation of the Late Paleozoic-Early Mesozoic Karakaya complex and related ophiolites in northwestern Turkey by Palaeotethyan subduction-accretion. Journal of Geological Society, London, 153, 995-1009.

Pickett, E., and Robertson, A.H.F., 2004. Significance of the volcanogenic Nilufer unit and related components of the Triassic Karakaya Complex for Tethyan Subduction/Accretion Processes in NW Turkey. Turkish Journal of Earth Sciences, 13, 97-143.

Plank, T., 1996. The brine of the Earth. Nature, 380, 202-203.

Rojay, B., and Göncüoğlu, M. C., 1997. Tectonic setting of some pre-Liassic low grade metamorphics in northern Anatolia. Yerbilimleri, 19, 109-118.

Saunders, A.D., Tarney, J., Marsh, N.G., and Wood, D.A., 1980. Ophiolites as ocean crust or marginal basin crust: a geochemical approach. In: Panayiotou, A., (ed.), Ophiolites. Proceedings of the International Ophiolite Symposium, Cyprus, 1979, 193-204.

Schilling, J.G., Zajac, M., Evans, R., Johnston, T., White W., Devine, J.D., and Kingsley, R., 1983. Petrologic and geochemical variations along the Mid-Atlantic Ridge from 27ºN to 73ºN. American Journal of Science, 283, 510-586.

Shervais, M., 1982. Ti-V plots and the petrogenesis of modern and ophiolitic lavas. Earth and Planetary Science Letters, 59, 101-118.

Smith, E.I., Sanchez, A., Walker, J. D., and Wang, K., 1999. Geochemistry of mafic magmas in the Hurricane Volcanic Field, Utah: implications for small- and largescale chemical variability of the lithospheric mantle. Journal of Geology, 107, 433-448.

Spath, A., Le Roex, A.P., and Duncan, R.A., 1996. The geochemistry of lavas from the Comores Archipelago, Western Indian Ocean: petrogenesis and mantle source region characteristics. Journal of Petrology, 37, 961-991.

Stampfli, G. M., 2000. Tethyan Oceans. In: Bozkurt, E., Winchester, J., and Piper, J.A., (eds.), Tectonics and Magmatism in Turkey and the Surrounding Area. Geological Society, London, Special Publications, 173, 1-24.

Staudigel, H., Plank, T., White, B., and Schmincke, H.U., 1996. Geochemical fluxes during seafloor alteration of the basaltic upper oceanic crust: DSPS sites 417 and 418. Geophysical Monograph, 96, 19-38.

Stern, R.J., Lin, P.-N., Morris, J.D., Jackson, M.C., Fryer, P., Bloomer, S.H., and Ito, E., 1990. Enriched back-arc basin basalts from the northern Mariana Trough: implications for the magmatic evolution of back-arc basins. Earth and Planetary Science Letters, 100, 210-225.

Sun, S.-s., 1980. Lead isotope study of young volcanic rocks from mid-ocean ridges, ocean islands and island arcs. Philosophical Transactions of the Royal Society of London, Series A 297, 409-445.

Sun, S.-s., and McDonough, W.F., 1989. Chemical and isotopic systematics of oceanic basalts: implications for mantle composition and processes. In: Saunders, A.D., and Norry, M.J., (eds.), Magmatism in the Ocean Basins. Geological Society, London, Special Publications, 42, 313-345.

Sun, S.-s., Nesbitt, R.W., and Sharaskin, A.Y., 1979. Geochemical characteristics of mid-ocean ridge basalts. Earth and Planetary Science Letters, 44, 119-138.

Şengör, A.M.C., 1979. Mid-Mesozoic closure of Permo-Triassic Tethys and its implications. Nature 279, 590-593.

Şengör, A.M.C., and Yılmaz, Y., 1981. Tethyan Evolution of Turkey: a plate tectonics approach. Tectonophysics, 75, 181-241.

Şengör, A.M.C., Yılmaz, Y. and Ketin, I., 1980. Remnants of a pre-Late Jurassic ocean in northern Turkey: Fragments of Permian-Triassic Paleo-Tethys. Geological Society of America Bulletin, 91, 599-609.

Şengör, A.M.C., Yılmaz, Y., and Sungurlu, O., 1984. Tectonics of the Mediterranean Cimmerides: nature and evolution of the western termination of Paleo-Tethys. In: Dixon, J.E., and Robertson, A.H.F., (eds.), The Geological Evolution of the Eastern Mediteranean. Geological Society, London, Special Publications, 17, 77-112.

Tankut, A., 1984. Basic and ultrabasic rocks from the Ankara Melange, Turkey. In: Dixon, J.E., and Robertson, A.H.F., (eds.), The geological evolution of the Eastern Mediteranean. Geological Society, London Special Publications, 17, 449-454.

Tejada, M.L.G., Mahoney, J.J., Neal, C.R., Duncan R.A., and Petterson, M.G., 2002. Basement geochemistry and geochronology of central Malaita, Solomon Island, with implications for the origin and evolution of the Ontong Java Plateau. Journal of Petrology, 43, 449-484.

Tekeli, O., 1981. Subduction complex of pre-Jurassic age, northern Anatolia, Turkey. Geology, 9, 68-72.

Thirlwall, M.F., 1997. Pb isotopic and elemental evidence for OIB derivation from young HIMU mantle. Chemical Geology, 139, 51-74.

Thirlwall, M.F., Smith, T.E., Graham, A.M., Theodoru, N., Hollings, P., Davidson, J.P., and Arculus, R.J., 1994. High field strength element anomalies in arc lavas: source or process? Journal of Petrology, 35, 819-838.

Thompson, G., 1991. Metamorphic and hydrothermal processes: basalt-seawater interactions. In: Floyd, P.A., (ed.), Oceanic Basalts. Blackie, Glasgow and London, 148-173.

Turhan, N., Okuyucu, C., and Göncüoğlu, M.C., 2004. Autochthonous Upper Permian (Midian) Carbonates in the Western Sakarya Composite Terrane, Geyve Area, Turkey: Preliminary Data. Turkish Journal of Earth Sciences, 13, 215-229.

Tüysüz, O., and Yiğitbaş, E., 1994. The Karakaya basin: a Palaeo-Tethyan marginal basin and its age of opening. Acta Geologica Hungarica, 37, 327-250.

Ustaömer, T., and Robertson, A.H.F., 1994. Late Paleozoic marginal basin and subduction-accretion: the Paleotethyan Küre Complex, Central Pontides, northern Turkey. Journal of the Geological Society, London, 151, 291-305.

Ustaömer, T., and Robertson, A.H.F., 1999. Geochemical evidence used to test alternative plate tectonic models for the pre-Upper Jurassic (Palaeotethyan) units in the Central Pontides, N Turkey. Geological Journal, 34, 25-53.

Ünalan, G., Yüksel, V., Tekeli, T., Gönenç, O., Seyirt, Z., and Hüseyin, S., 1976. Haymana-Polatlı yöresinin (GB Ankara) Üst Kretase-Alt Tersiyer stratigrafisi ve paleocoğrafik evrimi. TJK Bülteni, 19/2, 159-176.

Weaver, B.L., 1991. The origin of ocean island basalt end-member compositions: trace element and isotopic constraints. Earth and Planetary Science Letters, 104, 381-397.

Weaver, B.L., Wood, D.A., Tarney, J., and Joron, J.L., 1987. Geochemistry of ocean island basalts from the South Atlantic: Ascension, Bouvet, St. Helena, Gough and Tristan da Cunha. In: Fitton, J.G., and Upton, B.G.J., (eds.), Alkaline Igneous Rocks. Geological Society, London, Special Publications, 30, 253-267.

Wiedmann, J., Kozur, H., and Kaya, O., 1992. Faunas and age significance of the pre-Jurassic turbidite-olistostrome unit in the western parts of Turkey. Newsletter for Stratigraphy, 26, 133-144.

Wilson, M., 1989. Igneous Petrogenesis. London: Unwin Hyman, 466 pp.

Winchester, J.A., and Floyd, P.A., 1977. Geochemical discrimination of different products using immobile elements. Chemical Geology, 20, 325-343.

Wood, D.A., Joron, J.L., and Treuil, M., 1979. A reappraisal of the use of trace elements to classify and discriminate between magma series erupted in different settings. Earth and Planetary Science Letters, 45, 326-336.

Woodhead, J.D., Eggins, S.M., and Johnson, R.W., 1998. Magma genesis in the New Britain island arc: further insights into melting and mass transfer processes. Journal of Petrology, 39, 1641-1668.

Yalınız, M.K., and Göncüoglu, M.C., 2002. Geochemistry and petrology of “Nilüfer-type” metabasic rocks of eastern Kozak Massif, NW Turkey. 1.International Symposium Faculty of Mines (ITU) on Earth Sciences and Engineering 16-18 May, 2002, Istanbul, Abstracts, 158.

Yılmaz, A., and Yılmaz, H., 2004. Geology and structural evolution of the Tokat Massif (Eastern Pontides, Turkey). Turkish Journal of Earth Sciences, 13, 231-246.

Yılmaz, Y., 1981. Sakarya kıtası güney kenarının tektonik evrimi. İstanbul Yerbilimleri, 1, 33-52.

Yılmaz, Y., 1990. Allochtonous terranes of Tethyan Middle East: Anatolia and the surrounding regions. Philosophical Transactions of Royal Society, London A 331, 611-624.

APPENDIX A

PLATE

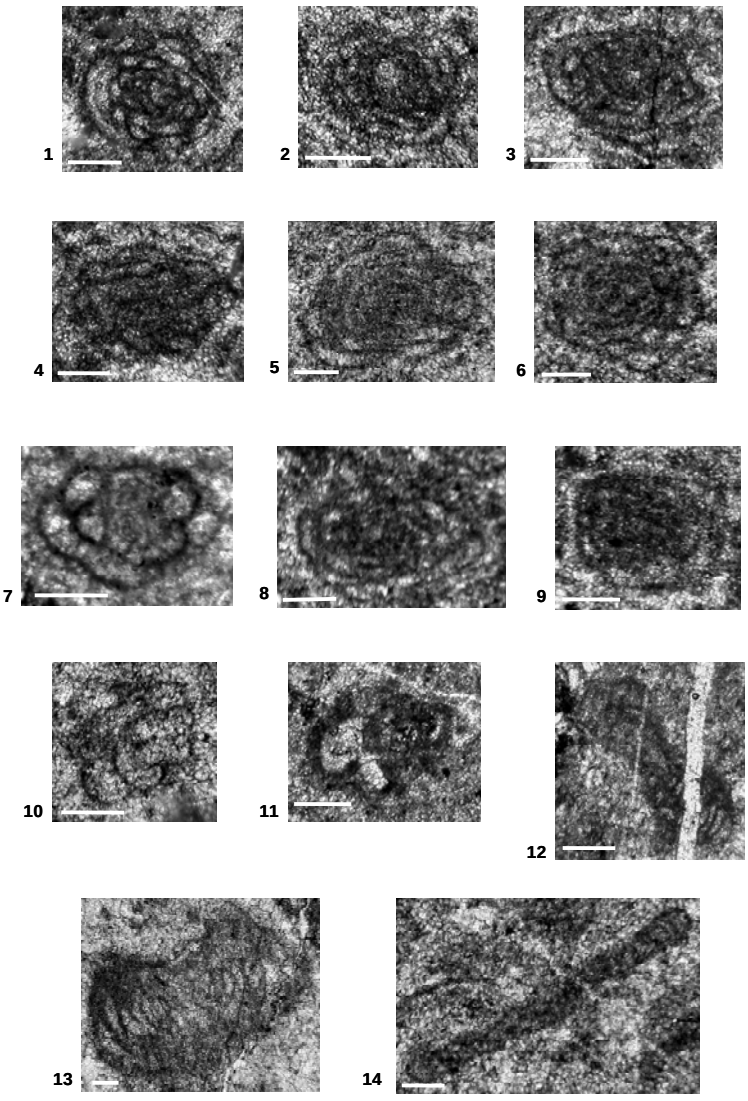

Figure 1-6, 8-9: *Pliammina densa* (PANTIC, 1965). 1: Sample M13; 2-6, 8-9: Sample M2.

Figure 7: *Meandrospira dinarica* (KOCHANSKY-DEVIDE and PANTIC, 1965). Sample M6.

Figure 10: *Meandrospira deformata* (SALAJ, 1967). Sample M13.

Figure 11: *Endoteba* sp. Sample M13.

Figure 12: *Aulotortus?* sp. Sample M7.

Figure 13: *Aulotortus? Eotriasicus* (ZANINETTI, RETTORI and MARTINI, 1994). Sample M9.

Figure 14: *Paulbronnimannella whittakeri* RETTORI. Sample M2.

Scale bar indicates 300µ in 1-5, 8,9,11,12; 200µ in 6,7,10,13,14.

APPENDIX B

GEOCHEMICAL DATA ACQUIRED FROM THE STUDY AREAS

	Hasanoğlan basalt				Ortaoba basalt		
ELEMENT	**A-1**	**A-2**	**A-3**	**A-4**	**A-5**	**A-6**	**A-7**
SiO_2	44.19	49.40	43.71	42.90	46.94	47.22	49.02
Al_2O_3	12.98	11.52	9.80	14.66	16.74	14.09	12.80
Fe_2O_3	14.11	10.32	9.16	10.64	7.92	12.93	11.53
MgO	9.34	5.01	2.35	3.66	8.13	7.55	6.38
CaO	7.36	8.13	14.94	8.83	10.77	7.76	8.73
Na_2O	4.26	4.32	3.84	5.63	2.96	3.34	3.15
K_2O	.22	.07	.08	.05	.90	.63	.04
TiO_2	2.67	2.78	2.38	3.56	.97	1.61	1.25
P_2O_5	.32	.35	.52	.53	.12	.21	.17
MnO	.13	.07	.09	.09	.23	.20	.19
Cr_2O_3	.092	.097	.055	.065	.045	.033	.016
Ni	235	360	116	135	97	43	27
Sc	29	24	15	26	47	43	41
LOI	4.0	7.7	13.1	9.1	4.3	4.2	6.6
SUM	99.70	99.81	100.04	99.74	100.04	99.79	99.89
Ba	147.0	47.0	53.8	78.0	224.1	389.5	76.3
Be	1	<1	1	<1	1	<1	<1
Co	61.4	62.1	28.7	45.4	47.7	47.1	41.9
Cs	1.3	<.1	.3	<.1	3.9	1.9	3.4
Ga	20.0	17.4	11.5	21.4	17.0	17.4	16.0
Hf	3.4	4.7	4.7	6.7	1.6	2.8	2.1
Nb	34.2	28.9	32.5	49.5	6.8	12.3	9.0
Rb	3.1	.7	1.1	1.5	22.6	15.7	2.0
Sn	1	2	2	2	<1	1	<1
Sr	234.6	190.7	336.7	365.2	148.3	254.0	243.5
Ta	2.2	1.7	2.2	3.3	.4	.8	.5
Th	2.0	2.5	2.3	4.2	.5	.7	.9
U	.6	.8	.7	.9	.2	.3	.1
V	301	251	180	276	249	363	280
W	.2	.2	.4	.9	.9	.5	.8
Zr	118.5	175.8	192.2	260.4	54.1	101.2	70.8
Y	21.9	22.3	21.2	25.7	17.6	32.3	23.2
La	22.5	24.2	29.1	33.9	5.4	9.9	7.7
Ce	45.8	54.4	58.9	70.8	12.5	22.4	17.0
Pr	5.51	6.80	7.34	8.31	1.61	2.95	2.12
Nd	23.9	30.4	31.2	35.6	7.6	13.8	10.5
Sm	5.8	7.4	7.3	8.0	2.4	4.4	3.1
Eu	1.95	2.26	2.17	2.46	.91	1.34	1.03
Gd	5.24	5.92	5.76	6.22	2.65	4.51	3.30
Tb	.82	.93	.86	1.01	.52	.93	.68
Dy	4.36	4.48	4.18	5.19	3.22	5.18	3.81
Ho	.89	.87	.81	1.04	.69	1.25	.86
Er	2.05	1.93	1.77	2.34	1.80	3.37	2.32
Tm	.28	.27	.24	.32	.23	.49	.34
Yb	1.52	1.56	1.30	1.81	1.48	2.91	2.06
Lu	.22	.21	.18	.30	.23	.48	.33

	Ortaoba basalt		İmrahor diabase				
ELEMENT	**A-8**	**A-9**	**A-10**	**A-11**	**A-12**	**A-13**	**A-14**
SiO_2	46.54	48.88	53.91	52.83	53.73	50.35	52.92
Al_2O_3	12.64	14.19	14.45	14.95	15.13	14.68	14.95
Fe_2O_3	12.09	11.70	12.53	13.40	12.21	15.34	13.22
MgO	8.65	6.43	3.46	4.01	3.68	4.49	3.99
CaO	7.03	8.49	8.08	4.92	5.47	3.58	5.33
Na_2O	3.79	4.05	2.59	3.15	2.69	3.29	2.73
K_2O	.30	.44	.04	.08	.04	.26	.04
TiO_2	2.53	2.00	1.35	1.50	1.51	1.75	1.53
P_2O_5	.30	.29	.15	.13	.11	.11	.13
MnO	.19	.18	.18	.15	.20	.18	.20
Cr_2O_3	.068	.024	.044	.026	.029	.027	.030
Ni	158	51	20	20	20	20	26
Sc	31	27	33	39	36	43	38
LOI	5.6	3.1	3.1	4.6	5.0	5.6	4.6
SUM	99.75	99.78	99.88	99.75	99.81	99.66	99.65
Ba	118.4	140.4	35.8	82.6	127.7	132.2	35.0
Be	<1	1	1	1	1	1	1
Co	46.3	39.9	31.5	32.9	29.4	38.6	30.6
Cs	1.8	.7	.1	.3	.2	.4	<.1
Ga	19.9	18.9	20.1	19.2	20.4	20.8	19.4
Hf	4.4	3.7	2.7	2.0	2.0	1.7	1.5
Nb	27.7	19.3	2.5	1.9	1.6	1.7	1.7
Rb	9.0	5.0	.6	3.1	.6	10.2	<.5
Sn	2	2	1	1	<1	<1	<1
Sr	169.3	546.7	340.0	298.9	263.9	269.0	328.5
Ta	1.8	1.2	.1	.1	.1	.1	<.1
Th	3.1	1.7	1.4	.6	.7	.5	.8
U	.6	.5	.3	.4	1.2	.3	.3
V	300	241	406	473	446	623	435
W	.8	.4	.4	.1	.4	.2	1.3
Zr	163.0	151.0	79.9	64.5	57.2	51.8	56.0
Y	22.5	26.9	33.8	23.2	25.2	23.6	25.0
La	22.7	17.0	5.9	4.9	4.0	3.6	3.8
Ce	50.4	39.0	14.3	11.8	10.0	9.0	9.4
Pr	6.10	5.00	2.04	1.70	1.53	1.40	1.37
Nd	28.9	23.0	10.3	9.3	8.7	7.3	7.7
Sm	6.1	5.9	3.4	2.8	3.1	2.5	2.8
Eu	1.99	1.87	1.34	1.07	1.10	1.01	1.08
Gd	5.67	5.04	4.17	3.26	3.48	3.08	3.40
Tb	.90	.98	.89	.60	.68	.63	.69
Dy	4.65	5.03	5.49	4.12	3.77	4.01	4.09
Ho	.89	1.08	1.30	.95	1.00	.95	.95
Er	2.11	2.50	3.58	2.63	2.66	2.55	2.50
Tm	.30	.36	.49	.39	.43	.40	.39
Yb	1.71	2.11	3.07	2.67	2.63	2.33	2.35
Lu	.25	.30	.47	.39	.43	.36	.39

	Diabase	İmrahor gabbro		İmrahor basalt		
ELEMENT	**A-15**	**A-16**	**A-17**	**A-18**	**A-19**	**A-20**
SiO_2	53.05	44.82	44.24	44.93	42.95	40.64
Al_2O_3	14.32	14.80	16.04	16.65	14.61	12.00
Fe_2O_3	13.28	14.96	11.34	10.35	11.69	12.01
MgO	4.02	6.69	9.17	8.03	10.84	8.11
CaO	6.96	7.82	9.18	8.55	8.98	13.50
Na_2O	3.11	3.57	2.91	2.89	2.51	2.51
K_2O	.05	.20	.13	1.07	.43	.94
TiO_2	1.57	1.84	1.24	2.19	1.90	3.11
P_2O_5	.13	.12	.08	.24	.20	.60
MnO	.18	.16	.13	.14	.14	.12
Cr_2O_3	.042	.030	.043	.030	.058	.059
Ni	20	77	128	62	156	194
Sc	39	28	31	32	34	22
LOI	3.1	4.7	5.4	4.8	5.6	6.3
SUM	99.81	99.72	99.92	99.89	99.93	99.93
Ba	41.7	119.3	76.0	182.9	91.5	722.0
Be	1	1	1	1	1	1
Co	31.8	54.5	51.7	37.6	47.2	50.7
Cs	.1	.4	1.1	.4	.4	.7
Ga	19.2	20.0	17.6	22.5	18.8	20.4
Hf	1.9	2.1	1.7	3.6	2.8	4.2
Nb	1.9	8.4	5.6	28.3	22.0	49.8
Rb	1.0	2.8	2.2	18.3	7.0	13.0
Sn	1	<1	<1	1	1	1
Sr	369.7	360.2	292.0	308.2	313.4	526.0
Ta	.1	.5	.3	1.7	1.3	2.9
Th	.7	.5	<.1	1.4	1.5	3.3
U	.2	.1	<.1	.5	.4	.8
V	421	293	245	287	260	261
W	.6	.3	.1	.1	.1	.4
Zr	54.9	76.4	51.6	125.3	100.7	155.1
Y	26.2	24.1	17.9	25.0	21.8	25.5
La	4.1	6.2	4.3	21.0	17.3	32.1
Ce	9.7	15.3	10.5	42.1	34.2	65.0
Pr	1.47	2.23	1.59	5.11	4.05	8.11
Nd	8.0	11.0	8.2	22.8	19.2	36.1
Sm	2.8	3.6	2.6	5.5	4.5	8.4
Eu	1.18	1.33	1.02	1.90	1.59	2.86
Gd	3.53	3.93	2.87	4.97	4.20	7.44
Tb	.65	.76	.56	.86	.76	1.09
Dy	4.18	4.25	3.05	4.34	3.84	5.48
Ho	.96	.93	.64	.89	.79	.91
Er	2.70	2.31	1.75	2.37	1.90	1.99
Tm	.43	.34	.24	.32	.28	.25
Yb	2.31	2.15	1.39	1.80	1.62	1.49
Lu	.42	.29	.23	.26	.26	.19

	İmrahor basalt				diabase	ultramafic
ELEMENT	**A-21**	**A-22**	**A-23**	**A-24**	**A-25**	**A-26**
SiO_2	47.37	41.28	43.11	44.66	52.97	38.74
Al_2O_3	15.48	11.59	15.62	14.99	15.72	7.45
Fe_2O_3	13.18	12.11	11.95	9.67	11.32	13.07
MgO	5.40	9.13	8.46	4.74	5.14	23.66
CaO	5.05	12.61	6.59	12.63	2.60	4.17
Na_2O	3.37	2.99	3.39	3.94	4.30	.11
K_2O	.54	.06	.96	.29	.33	.09
TiO_2	3.65	3.78	1.70	1.53	1.53	.66
P_2O_5	.45	.67	.14	.14	.14	.05
MnO	.13	.10	.14	.11	.09	.15
Cr_2O_3	.017	.054	.034	.042	.018	.223
Ni	24	183	87	89	20	996
Sc	31	23	35	31	40	19
LOI	5.0	5.2	7.7	7.1	5.4	11.4
SUM	99.64	99.59	99.81	99.86	99.56	99.90
Ba	413.2	1879.3	74.6	74.1	439.8	18.8
Be	2	1	<1	1	1	1
Co	46.0	56.0	48.5	40.6	41.7	110.7
Cs	.6	.4	.3	.1	1.6	2.0
Ga	26.4	20.0	20.0	19.7	20.4	8.7
Hf	6.1	4.9	2.1	2.2	2.5	.8
Nb	31.9	63.8	12.2	11.8	1.9	4.9
Rb	15.2	1.6	8.7	3.4	12.5	5.5
Sn	2	2	<1	<1	1	<1
Sr	418.3	452.3	171.0	230.2	854.4	131.8
Ta	1.9	3.9	.7	.7	.1	.3
Th	2.8	2.8	.7	.9	.5	.2
U	.7	.9	.4	.2	.1	<.1
V	336	287	265	276	327	134
W	.4	.5	.1	.1	.2	<.1
Zr	236.5	182.4	80.1	75.0	82.5	25.8
Y	36.5	28.3	20.5	19.5	27.6	7.6
La	25.6	35.8	7.8	7.5	3.0	3.5
Ce	58.4	73.9	19.0	16.5	9.3	7.6
Pr	7.62	9.24	2.46	2.25	1.48	.99
Nd	36.1	40.6	11.6	10.6	9.7	4.4
Sm	8.6	9.8	3.8	3.1	3.1	1.2
Eu	2.87	3.17	1.21	1.19	1.19	.45
Gd	8.04	8.48	3.65	3.43	3.97	1.40
Tb	1.42	1.30	.64	.65	.80	.22
Dy	7.24	6.16	3.64	3.44	4.65	1.44
Ho	1.44	1.03	.82	.71	1.05	.27
Er	3.23	2.27	2.04	1.88	2.84	.71
Tm	.45	.27	.29	.28	.48	.12
Yb	2.68	1.59	1.81	1.50	2.85	.69
Lu	.42	.20	.23	.24	.44	.10

	Kadirler basalt					
ELEMENT	**K2B**	**K4A**	**K4C**	**K4D**	**K4E**	**K4F**
SiO_2	44.94	43.24	38.77	37.42	43.25	40.67
Al_2O_3	12.94	13.79	12.1	11.91	14.06	11.73
Fe_2O_3	10.36	10.88	8.77	9.54	7.56	9.25
MgO	6	5.31	4.07	3.6	3.62	3.92
CaO	7.74	10.82	16.25	16.2	11.4	15.17
Na_2O	3.91	3.39	2.95	3.22	4.64	4.27
K_2O	0.46	1.14	1.44	1.42	0.99	0.33
TiO_2	2.79	2.44	2.11	2.08	2.45	2.01
P_2O_5	0.51	0.36	0.33	0.32	0.37	0.31
MnO	0.07	0.11	0.11	0.1	0.14	0.08
Cr_2O_3	0.048	0.056	0.045	0.044	0.039	0.062
Ni	157	229	188	144	269	128
Sc	20	22	20	20	29	23
LOI	10.3	8.2	12.5	13.7	11.1	11.5
SUM	100.09	99.77	99.47	99.58	99.66	99.32
Ba	68.4	320.3	280.7	220.7	312.8	194.9
Be	6	< 1	5	< 1	< 1	5
Co	34.8	63.1	50	45.1	82.2	46.3
Cs	1.5	0.6	0.8	1.1	0.5	0.4
Ga	18.1	20.4	17.8	17.7	19.6	15.5
Hf	5	4.3	4	3.7	3.5	4.2
Nb	38.1	40.8	36.4	34.4	26.4	34.7
Rb	12.5	21.7	31	32.8	16.9	4
Sn	2	2	2	1	1	2
Sr	285.1	404.3	380.3	332.6	416.7	403.6
Ta	2.2	2.1	2.1	2	1.5	2
Th	4.1	4.5	4.2	2.9	2.6	3.4
U	1	0.9	1	1.1	1	0.7
V	212	225	197	197	291	220
W	1.2	1	0.3	0.1	0.1	0.7
Y	26.5	21.6	19.7	19.4	23.3	22
Zr	204.2	178.1	156.1	153.8	133.7	152
La	30.7	24.5	25.2	23.8	14.9	22.6
Ce	62.3	50.4	49.7	47.2	34.7	45
Pr	7.93	6.23	6.02	5.75	4.63	5.51
Nd	34.7	27.2	24.9	24.7	24	23.9
Sm	7.4	5.5	5.6	4.8	5.6	5.4
Eu	2.13	1.8	1.62	1.47	1.82	1.68
Gd	5.78	5.3	4.65	4.72	5.15	4.89
Tb	0.88	0.73	0.63	0.67	0.8	0.7
Dy	5.15	4.33	3.42	3.43	4.33	3.59
Ho	0.91	0.76	0.65	0.64	0.8	0.75
Er	2.18	1.76	1.61	1.67	2.01	1.68
Tm	0.33	0.24	0.24	0.22	0.27	0.25
Yb	1.91	1.57	1.64	1.28	1.85	1.58
Lu	0.3	0.23	0.23	0.18	0.24	0.24